The role of Chaperone Mediated Autophagy in the Central Nervous System

Doctoral Dissertation

Second Department of Neurology, Faculty of Medicine,
National and Kapodistrian University of Athens, Greece

Daphne Antoniou

Biologist

Performed in the Center for Basic Research Foundation of the Academy of Athens (BRFAA)

Dr. Panagiotis K. Politis
in collaboration with Prof. Leonidas Stefanis

Three - member advisory committee:

1. Leonidas Stefanis , MD, PhD
   Professor of Neurology (Medical School, National and Kapodistrian University of Athens, NKUA – BRFAA)
2. Panagiotis Politis, PhD
   Investigator C - Assistant Professor Level
3. Kostas Vekrellis,PhD
   Investigator B - Associate Professor Level

Seven – member Board of Examination:

1. **Leonidas Stefanis**, MD, PhD, Prof. of Neurology (Medical School, NKUA)
2. **Panagiotis Politis**, PhD, Principal Investigator C (BRFAA)
3. **Kostas Vekrellis**, PhD ,Principal Investigator B (BRFAA)
4. **Stavros Taraviras**, PhD, Prof. of Physiology (Medical School, University of Patras)
5. **Panagiota Papazafiri**. PhD, Assoc. Prof. of Physiology (Biology Depart., NKUA)
6. **Spiros Efthimiopoulos**, PhD, Assoc. Prof. of Physiology (Biology Depart., NKUA)
7. **Christina Dalla**, PhD, Assist. Prof. of Psychopharmacology (Medical School, NKUA)

ΕΚ ΤΟΥ ΙΠΠΟΚΡΑΤΕΙΟΥ ΟΡΚΟΥ

ΚΕΙΜΕΝΟ

« ΟΜΝΥΜΙ ΤΟΝ ΘΕΟΝ ΕΠΙΤΕΛΕΑ ΠΟΙΗΣΕΙΝ ΚΑΤΑ ΔΥΝΑΜΙΝ ΚΑΙ ΚΡΙΣΙΝ ΕΜΗΝ ΟΡΚΟΝ ΤΟΝΔΕ ΚΑΙ ΞΥΓΓΡΑΦΗΝ ΤΗΝΔΕ. ΗΓΗΣΕΣΘΑΙ ΜΕΝ ΤΟΝ ΔΙΔΑΞΑΝΤΑ ΜΕ ΤΗΝ ΤΕΧΝΗΝ ΤΑΥΤΗΝ ΙΣΑ ΓΕΝΕΤΗΣΙΝ ΕΜΟΙΣΙ. ΔΙΑΙΤΗΜΑΣΙ ΤΕ ΧΡΗΣΟΜΑΙ ΕΠ' ΩΦΕΛΕΙΗ ΚΑΜΝΟΝΤΩΝ ΚΑΤΑ ΔΥΝΑΜΙΝ ΚΑΙ ΚΡΙΣΙΝ ΕΜΗΝ, ΕΠΙ ΔΗΛΗΣΕΙ ΔΕ ΚΑΙ ΑΔΙΚΙΗ ΕΙΡΞΕΙΝ. ΟΥ ΔΩΣΩ ΔΕ ΟΥΔΕ ΦΑΡΜΑΚΟΝ ΟΥΔΕΝΙ ΑΙΤΗΘΕΙΣ ΘΑΝΑΣΙΜΟΝ. ΟΥΔΕ ΥΦΗΓΗΣΟΜΑΙ ΞΥΜΒΟΥΛΙΗΝ ΤΟΙΗΝΔΕ. ΟΜΟΙΩΣ ΔΕ ΟΥΔΕ ΓΥΝΑΙΚΙ ΠΕΣΣΟΝ ΦΘΟΡΙΟΝ ΔΩΣΩ. ΑΓΝΩΣ ΔΕ ΚΑΙ ΟΣΙΩΣ ΔΙΑΤΗΡΗΣΩ ΒΙΟΝ ΤΟΝ ΕΜΟΝ ΚΑΙ ΤΕΧΝΗΝ ΤΗΝ ΕΜΗΝ. ΕΣ ΟΙΚΙΑΣ ΔΕ ΟΚΟΣΑΣ ΑΝ ΕΣΙΩ, ΕΣΕΛΕΥΣΟΜΑΙ ΕΠ' ΩΦΕΛΕΙΗ ΚΑΜΝΟΝΤΩΝ, ΕΚΤΟΣ ΕΩΝ ΠΑΣΗΣ ΑΔΙΚΙΗΣ ΕΚΟΥΣΙΗΣ ΚΑΙ ΦΘΟΡΙΗΣ ΤΗΣ ΤΕ ΑΛΛΗΣ ΚΑΙ ΑΦΡΟΔΙΣΙΩΝ ΕΡΓΩΝ. Α Δ' ΑΝ ΕΝ ΘΕΡΑΠΕΙΗ, Η ΙΔΩ Η ΑΚΟΥΣΩ, Η ΚΑΙ ΑΝΕΥ ΘΕΡΑΠΕΙΗΣ ΚΑΤΑ ΒΙΟΝ ΑΝΘΡΩΠΩΝ, Α ΜΗ ΧΡΗ ΠΟΤΕ ΕΚΛΑΛΕΕΣΘΑΙ ΕΞΩ, ΣΙΓΗΣΟΜΑΙ, ΑΡΡΗΤΑ ΗΓΕΥΜΕΝΟΣ ΕΙΝΑΙ ΤΑ ΤΟΙΑΥΤΑ. ΟΡΚΟΝ ΜΕΝ ΟΥΝ ΜΟΙ ΤΟΝΔΕ ΕΠΙΤΕΛΕΑ ΠΟΙΕΟΝΤΙ ΚΑΙ ΜΗ ΞΥΓΧΕΟΝΤΙ ΕΙΗ ΕΠΑΥΡΑΣΘΑΙ ΚΑΙ ΒΙΟΥ ΚΑΙ ΤΕΧΝΗΣ, ΔΟΞΑΖΟΜΕΝΩ ΠΑΡΑ ΠΑΣΙΝ ΑΝΘΡΩΠΟΙΣ ΕΣ ΤΟΝ ΑΙΕΙ ΧΡΟΝΟΝ· ΠΑΡΑΒΑΙΝΟΝΤΙ ΔΕ ΚΑΙ ΕΠΙΟΡΚΕΟΝΤΙ, ΤΑΝΑΝΤΙΑ ΤΟΥΤΕΩΝ. ΤΑΥΤΗΝ ΤΗΝ ΕΠΑΓΓΕΛΙΑΝ ΕΠΙΤΕΛΟΥΝΤΙ ΕΙΗ ΜΟΙ ΤΟΝ ΘΕΟΝ ΑΡΩΓΟΝ ΚΤΗΣΑΣΘΑΙ ΕΝ ΤΩ ΒΙΩ ».

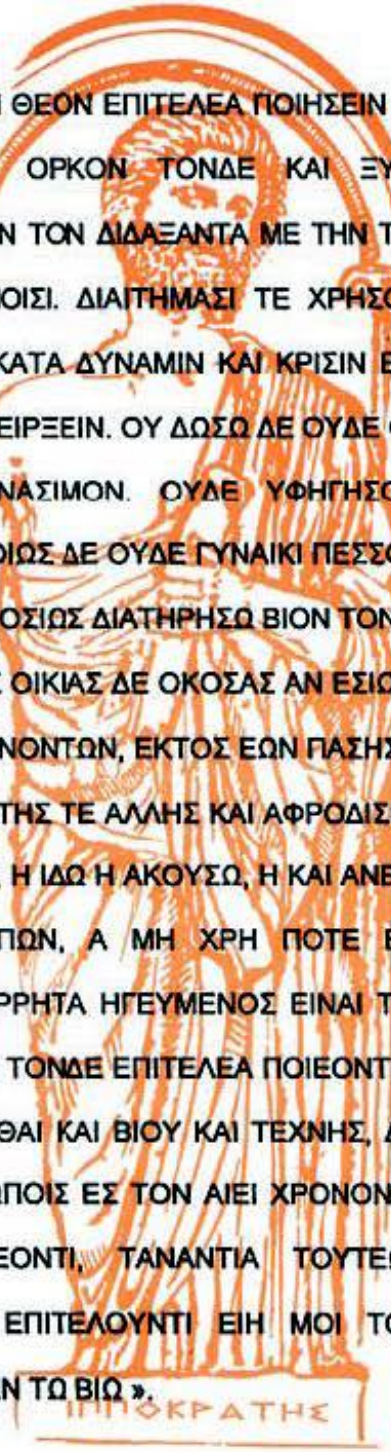

Table of contents

List of figures-themes-tables

Chaperone Mediated Autophagy regulates Notch signaling and modulates neural stem cell differentiation during development

Daphne Antoniou[1], Maria Xilouri[2], Nikos Malissovas[1], Elpinickie Ninou[1], Christina Kyrousi[4], Stavros Taraviras[4], Leonidas Stefanis[2,5*] and Panagiotis K. Politis[1*]

[1]*Center for Basic Research, Biomedical Research Foundation of the Academy of Athens, 4 Soranou Efesiou Str, 115 27, Athens, Greece*

[2]*Center of Clinical Research, Experimental Surgery and Translational Research, Biomedical Research Foundation of the Academy of Athens, Athens, Greece*

[4]*Department of Physiology, School of Medicine, University of Patras , Patras, Greece*

[5]*Second Department of Neurology, National and Kapodistrian University of Athens Medical School, Athens, Greece*

*****These authors are equal corresponding authors

Classification: Biological Sciences: Developmental Biology.

Correspondence to:

Panagiotis K. Politis,

Center for Basic Research, Biomedical Research Foundation of the Academy of Athens, 4 Soranou Efesiou Str, 115 27, Athens, Greece.

Tel: 0030-210-6597479;

Fax: 0030-210-6597545;

Email: ppolitis@bioacademy.gr

Stefanis Leonidas

Center of Clinical Research, Experimental Surgery and Translational Research, Biomedical Research Foundation of the Academy of Athens, Athens, Greece

[4]*Second Department of Neurology, National and Kapodistrian University of Athens Medical School, Athens, Greece*

Tel: 0030-210-6597214

Email: lstefanis@bioacademy.gr

Keywords: LAMP2A; neurogenesis; brain development; Hes5; lysosomal degradation; Notch1.

Abstract

Protein degradation systems have profound effects on signaling pathways and molecular networks that regulate organogenesis. Although autophagy-mediated protein degradation has been strongly associated with brain function and related diseases, its involvement in neural development remains unclear. Chaperone Mediated Autophagy (CMA), one of the main lysosomal degradation systems, has been linked to neurodegenerative diseases and neurodevelopmental disorders, however, nothing is known about its physiological role in mammalian brain development. Here we identify a novel regulatory role of CMA pathway in Neural Stem Cell (NSC) differentiation during development. In particular, we show that CMA is highly active in NSCs and that LAMP2A, the principal limiting component of CMA, together with HSC70 (HSPA8), another component of CMA, are strongly expressed in *ex vivo* cultured NSCs and embryonic rodent brain. Interestingly, LAMP2A expression pattern is associated with induction of neurogenesis. Most importantly, overexpression and loss of function experiments in NSCs, suggest an inductive role of CMA in neuronal differentiation. Mechanistically, we provide evidence that LAMP2A is involved in NSC fate decisions by interfering with Notch1 signaling pathway. Forced expression of LAMP2A reduces the protein levels of Notch1 Intracellular Domain (NICD) as well as expression of downstream effector genes, *Hes1* and *Hes5*. Consistently, a CMA recognition motif (KFERQ-like) on the NICD peptide sequence was identified with functional importance in the ability of NICD to activate downstream genes and CMA-mediated degradation. Collectively, our data

suggest a key role for LAMP2A and CMA in the regulation of neuronal fate acquisition via direct targeting of NICD activity.

Περίληψη

«Τα κυτταρικά συστήματα αποικοδόμησης πρωτεϊνών επηρεάζουν ουσιαστικά τα σηματοδοτικά μονοπάτια και μοριακά δίκτυα που ρυθμίζουν την οργανογένεση. Παρ'όλο που η αποικοδόμηση πρωτεϊνών μέσω αυτοφαγίας έχει συσχετιστεί πολύ ισχυρά με τη λειτουργία του εγκεφάλου και σχετικές ασθένειες, η συμμετοχή αυτής στην ανάπτυξη του νευρικού συστήματος παραμένει ασαφής. Η Αυτοφαγία Διαμεσολαβούμενη απο Σαπερόνες, ένα από τα κύρια λυσοσωμικά μονοπάτια, έχει συνδεθεί άμεσα με νευροεκφυλιστικές ασθένειες και ασθένειες σχετικές με την ανάπτυξη του εγκεφάλου, παρ'όλ'αυτά δεν υπάρχει κάτι γνωστό σχετικά με το φυσιολογικό ρόλο αυτής στην ανάπτυξη του εγκεφάλου των θηλαστικών. Με αυτή την εργασία παρουσιάζουμε ένα καινοτόμο ρυθμιστικό ρόλο της Αυτοφαγίας Διαμεσολαβούμενης απο Σαπερόνες, κατά τη διαφοροποίηση των Νευρικών Βλαστικών κυττάρων (NBK) κατά τη διάρκεια της ανάπτυξης. Συγκεκριμένα, παρουσιάζουμε πως αυτό το μονοπάτι αυτοφαγίας είναι σημαντικά ενεργό στα NBK και πως η LAMP2A, η βασικότερη πρωτεΐνη του μονοπατιού, μαζί με την HSC70 (HSPA8), ένα επιπλέον κομβικό μόριο για αυτό το αυτοφαγικό μονοπάτι, εκφράζονται σημαντικά και στα NBK και στο εμβρυονικό εγκέφαλο των τρωκτικών. Επιπλέον, η LAMP2A συσχετίζεται με την έναρξη της νευρογένεσης. Πιο σημαντικά ακόμα, παρατηρείται πως υπερέκφραση και αποσιώπηση της LAMP2A οδηγεί στην ενεργοποίηση της νευρογένεσης κατά την διαφοροποίηση των NBK. Σχετικά με τον μηχανισμό, στην μελέτη αυτή παρουσιάζεται πως η LAMP2A επηρεάζει την κυτταρική διαφοροποίηση των NBK παρεμβαίνοντας στο NOTCH1 σηματοδοτικό μονοπάτι. Η υπερέκφραση της LAMP2A καταστέλλει την έκφραση του NICD (του ενδοκυτταρικού τμήματος της NOTH1 πρωτεΐνης που λειτουργεί ως μεταγραφικός παράγοντας στον πυρήνα) όπως επίσης και την έκφραση των γονιδίων που επάγει το NICD, το HES5 και HES1. Επιπρόσθετα, το γνωστό και αναγνωρίσιμο μοτίβο των πρωτεϊνών-στόχων στην αμινοξική τους αλληλουχία(KFERQ-like motif) της Αυτοφαγίας Διαμεσολαβούμενης απο Σαπερόνες , αναγνωρίστηκε στο NICD και φαίνεται να καθορίζει την ενεργότητά του σχετικά με την μεταγραφή των γονιδίων-στόχων. Η ρύθμιση αυτή φαίνεται να συμβαίνει μέσω της αποικοδόμησης της πρωτεΐνης NICD από το μονοπάτι της Αυτοφαγίας . Εν κατακλείδι, τα δεδομένα που προκύπτουν από την παρούσα εργασία οδηγούν στο συμπέρασμα ενός νέου ουσιαστικού ρόλου της LAMP2A και της Αυτοφαγίας Διαμεσολαβούμενης απο Σαπερόνες στην ρύθμιση της νευρονικής μοίρας του κυττάρου μέσω στόχευσης του NICD, επομένως και της ενεργότητας του NOTCH1 σηματοδοτικού μονοπατιού.»

Significance Statement

This manuscript reports for the first time that one of the main lysosomal mechanisms for protein degradation, the Chaperone Mediated Autophagy, is associated to brain development. These findings are of great significance as they indicate a novel homeostatic function of this pathway in the determination of cellular fate during the early stages of neurogenesis. Chaperone Mediated Autophagy, known so far for its implication in neuronal diseases such as Parkinson's disease, affects neuronal differentiation through the regulation of Notch1 signaling pathway. This research is of high importance providing insights for a new regulatory role of Chaperone Mediated Autophagy in the brain by directly controlling the levels of active form of Notch1 protein, a key player in brain organogenesis and function.

Introduction

Neural differentiation during embryonic development

Understanding the molecular mechanisms of brain formation remains one of the most fascinating questions in biological sciences. In the last few decades, many signaling pathways and molecular networks have been associated with the ability of neural stem cells (NSCs) to generate the enormous complexity of mammalian brain (Martynoga et al., 2012). These NSCs form a pool of multipotent cells that proliferate intensely and divide symmetrically. During very early stages of development, these symmetric divisions result in two daughter stem cells, thus increasing the pool of stem cells. This intense proliferation of stem cells leads to the expansion of neural plate which is the first main developing step of Central Nervous System (CNS). Between embryonic day 9 (E9) and E10 of the mouse, asymmetric divisions of these cells give rise to the first progenitors that will have the neurogenic potential. These same progenitors can also give rise to radial glial cells that will later on divide, and, through intermediate lineages, will give rise to astrocytes and oligodentrocytes. Both neural induction and initiation of differentiation pathways, either neurogenic or gliogenic, appear to be connected to cell cycle control systems that regulate whether NSCs will maintain their proliferative ability or differentiate into the appropriate neural cell type. Some of the newly born progenitors continue the asymmetric division, generating one radial glial cell and one differentiated

daughter cell, which then migrates away from the apical progenitor domain and begins neuronal differentiation (Gotz and Huttner, 2005, Chevalier and Blow, 1996, Rowitch and Kriegstein, 2010, Guerout et al., 2014, Urban and Guillemot, 2014).

Specifically in the forebrain, many different cell lineages can be detected, contributing to the complexity of the progenitor stages between stem cells and postmitotic cells. These cells are called basal progenitors and are generated by the previously mentioned asymmetric divisions of radial glial cells. Basal progenitors are mostly observed in the telencephalon, where they outnumber the apically dividing neuron-generating neuroepithelial cells (Haubensak et al., 2004). Basal progenitors usually divide symmetrically once or a few times and are thought to generate most cortical progenitor neurons including early-born neurons of deep cortical layers, and late-born neurons of superficial cortical layers. Basal progenitors delaminate from the apical surface of the neuroepithelium, translocate their nucleus to the basal region of the ventricular zone to form the second germinal layer, the subventricular zone, and retract both their apical and basal process before mitosis. Most basal progenitor divisions are symmetric self-consuming, producing two neurons (Farkas and Huttner, 2008).

As neurogenesis progresses, there is an ever-increasing propensity for progenitors to undergo a symmetric terminal division, in which both daughters differentiate. Consequently the expansion of the progenitor pool gradually slows and then stops. Many studies over the last decade have shed light on specific signaling, transcriptional, and epigenetic mechanisms that are integrated to ensure a timely and coordinated switch in progenitor properties (Scheme 1).

Both radial glial and neuroepithelial cells can directly generate neurons. Moreover, both can self-renew while producing basal progenitors, neurons or

glia. These self-renewing cell types share a similar epithelial morphology (they span the neuroepithelium), both express the intermediate filament Nestin and have an apically located mitotic spindle, and both can be distinguished by an array of molecular markers. By contrast, most basal progenitors lack self-renewal potential and typically generate two postmitotic neurons. They do not span the neuroepithelium and undergo mitosis in a basal region termed the subventricular zone (Noctor et al., 2004).

Neuroepithelial and radial glial cells have a columnar epithelial morphology. Their apical process is exposed to the ventricular fluid, their basal process contacts the extracellular matrix, and they have lateral contacts with each other, including at the region of subapical adherens junctions. Thus, cues from apical, basal or lateral directions could modulate neuroepithelial/radial glial self-renewal. These cues may be correlated to many different signaling pathways such as Wnt, Notch and sonic hedgehog (Shh), which are known to contribute to the regulation of mammalian NSC self-renewal and consequently to neuronal differentiation (Doe, 2008).

A large number of molecules, such as transcription factors, non coding RNAs and signaling pathways participate during this differentiation procedure in order for the cells to maintain a neuronal, glial, or a stem cell fate. This regulatory network is essential for the generation of the appropriate number of neurons, neural subtypes and proper wiring of neuronal circuits in the CNS. One of the main effectors during this process is the evolutionary conserved Notch signaling pathway (Scheme.1). (Antoniou et al., 2014, Bally-Cuif and Hammerschmidt, 2003, Lathia et al., 2008, Louvi and Artavanis-Tsakonas, 2006, Corbin et al., 2008).

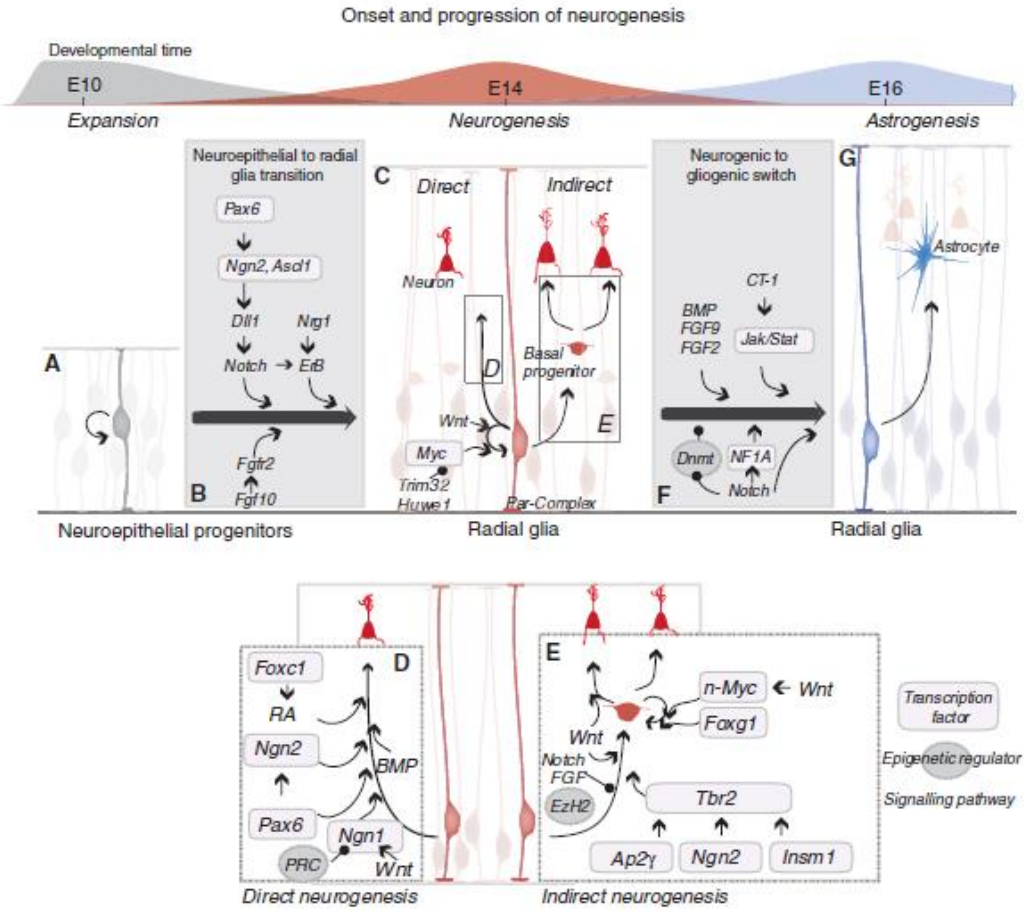

Introductory Scheme 1: *Molecular pathways regulating the onset, progression, and termination of neurogenesis in the rodent cerebral cortex. The onset of neurogenesis is concomitant with the transformation of neuroepithelial stem cells (A) into radial glial stem cells (C). Several signaling pathways, including the Dll1/Notch, Nrg1/ErB, and Fgf10/ Fgfr2 pathways have been implicated in this transformation. Radial glial cells then generate neurons directly (D) or via basal progenitors (E). Several transcription factors (Ap2g, Ngn2, Insm1, Tbr2) have been shown to promote the generation of basal progenitors from Radial glial cells, whereas the Notch and FGF pathways and the epigenetic regulator Ezh2 inhibit this step. Whether AP2g, Ngn2, and Insm1 act primarily by inducing Tbr2 expression or also via Tbr2- independent mechanisms is unclear. Other transcription factors and signaling molecules promote the self-renewal of RGs (Wnt,Myc) and the proliferation of basal progenitors (Foxg1, Wnt/n-Myc).Whether the same factors and pathways that promote the direct generation of neurons by Radial glial cells (Pax6, Ngn1/2, RA) also drive the generation of neurons by basal progenitors (data not shown)*

is unclear. The termination of neurogenesis results from the terminal differentiation of Radial Glial cells into astrocytes (G). Multiple signaling pathways (Jack/Stat, Notch, BMP, FGF) synergize to elicit the neurogenic-to-gliogenic switch. It is noteworthy that the same pathways frequently operate in different temporal contexts to exert contrasting cellular effects (Martynoga et al., 2012) .

Notch signaling pathway

- **A developmental key player**

As described above, the neuroepithelium generates mainly two general cell lineages, neurons and glia. Neurons occur from the stem cells of the ventricle earlier during neural development, and after their final mitotic division they migrate to the outer layer of the newly formed cortex in order to differentiate into one of the multiple neuronal subtypes. On the other hand, glial cells are generated from the progenitor cells later on during development and in the early postnatal stage. Notch signaling is one of the most significant players during these early fate decisions in brain development (Ahmed et al., 2009, Androutsellis-Theotokis et al., 2006, Artavanis-Tsakonas et al., 1999, Corbin et al., 2008).

The onset of neurogenesis and the transition from neuroepithelium to radial glial cells coincides with the onset of Notch signaling in the brain. Indicative data show that Notch targets such as *Hes1* and *Hes5* genes are mainly expressed, during the early developmental stages of the cortex, in the ventricular zone (VZ); the zone that progenitor cells are detected, pinpointing the topological activity of Notch signaling pathway (Mason et al., 2005, Yoon et al., 2004).

Secondly, gain - and loss – of - function studies support that activation of the pathway promotes the maintenance of progenitor fate, inhibiting at the same time neuronal differentiation (Hitoshi et al., 2002, Yoon et al., 2004, Gaiano et al., 2000)

In support of the idea that Notch signaling promotes the neuroepithelium-to-radial glia transition, Gaiano and Fishell showed that premature Notch pathway activation strongly induces radial glia markers and the cellular phenotype of dorsal telencephalon, as detected by the expression of the major Notch ligand Delta-like 1 (Dll1) and the downstream transcription factors Hes1 and Hes5 (Martynoga et al., 2012, Hatakeyama et al., 2004, Gaiano et al., 2000). Notch signaling components are expressed in embryonic neuroepithelial/radial glial stem cells, as well as in adult NSCs. Mutations in the genes encoding Dll1 (a Notch ligand), Notch1 (a Notch receptor), RBPJk (Rbpj – Mouse Genome Informatics; a Notch transcriptional effector), Hes1, Hes3 or Hes5 (RBPJk-induced transcription factors) all lead to the depletion of radial glia stem cells and to precocious neuronal differentiation in the mouse embryo, and to NSC loss in the adult (Gaiano et al., 2000) Conversely, misexpression of Hes1, Hes3 or of activated Notch in the embryonic cortex blocks neuronal differentiation. Radial glia stem cells from Dll1, Notch1, Rbpj, Hes1 and Hes5 mouse mutants all have a reduced neurosphere-forming ability, indicating that they have a reduced ability to self-renew. Furthermore, radial glial cells that express a Notch-induced GFP reporter can be sorted by flow cytometry into Notch-high (GFP+) and Notch-low (GFP–) populations; the Notch-high cells are more potent at generating primary and secondary neurospheres, and can be transplanted *in vivo* to generate all three neural lineages – neurons, astrocytes and oligodendrocytes. Thus, Notch signaling correlates with, and is required for, the maintenance of embryonic and

postnatal NSCs. In other words, Notch pathway activation promotes the survival of NSCs and thus the maintenance of pluripotent state. Notch signals block neuronal fate resulting in the inhibition of neuronal differentiation (Louvi and Artavanis-Tsakonas, 2006, Yoon and Gaiano, 2005, Shimojo et al., 2011, Mizutani et al., 2007) (Scheme 2).

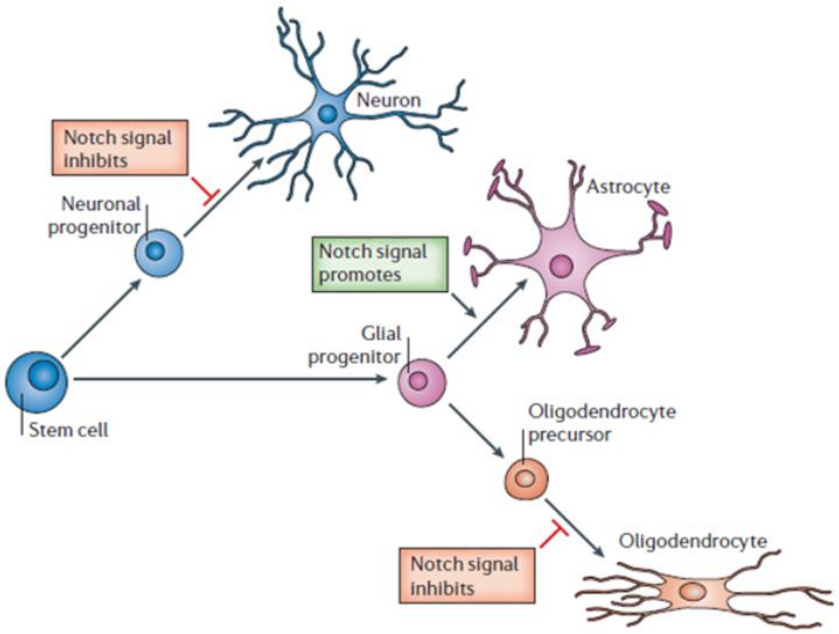

Introductory Scheme 2: *Schematic representation of Notch signaling activation on cell fate decisions during neural differentiation (Louvi and Artavanis-Tsakonas, 2006).*

Such a distinctive role of Notch pathway was firstly associated with stem cell phenotype when loss of Notch signaling and disruption of the Notch cascade led to massive neuronal generation in *Drosophila melanogaster*. Complete deletion of *Notch* in *Drosophila melanogaster* resulted in failure of the early neurogenic ectoderm segregation. Instead, all cells became neuroblasts, which led to hypertrophy of the neural tissue at the expense of epidermal structures, giving rise to a ‘neurogenic’ phenotype and leading to hypertrophy of both CNS

and PNS (Louvi and Artavanis-Tsakonas, 2006). The role of Notch signaling during vertebrate neural development concerns mainly the maintenance of the proliferative population, thus regulating the pool of progenitor cells (Yoon and Gaiano, 2005, Yoon et al., 2004).

Knowing that Notch plays a critical role in many fundamental processes and in a wide range of tissues, it is not surprising that aberrant gain or loss of Notch signaling components have been directly linked to multiple human disorders, ranging from developmental syndromes (e.g., Alagille, Teratology of Fallot, Syndactyly, Spondylocostal dysostosis, Familial Aortic Valve Disease) (Garg et al., 2005, Gridley, 2003) to adult onset diseases (e.g., Cancer, Alzheimer's disease, CADASIL) (Louvi and Artavanis-Tsakonas, 2006). In addition, any therapeutic manipulation of embryonic or adult stem cells will require development of receptor-specific antagonists and agonists of Notch signaling.

It is not clear what initiates Notch signaling in the cortex, although the induction of Dll1 coincides with the appearance of the pro-neural proteins Ngn2 and Ascl1, which are major transcriptional regulators of neurogenesis and have been shown to directly regulate Dll1. Notch can instruct acquisition of radial glia identity, but strong perturbation of the pathway via deletion of *Hes1*, *Hes5*, or of the Notch effect did not block the appearance of radial glia, although Notch-deficient radial glial cells commenced neurogenesis prematurely and lost their apico–basal polarity. Thus Notch is important, if not essential, for the instigation of radial glia development and to maintain neurogenic radial glia in an undifferentiated state (Scheme 1) (Martynoga et al., 2012). As a consequence, research into the finer mechanistic detail of Notch activation and nuclear activity is of growing clinical and commercial relevance. (Kopan and Ilagan, 2009).

- **Structure and cleavage**

The fly genome contains only one Notch receptor (dNotch) (Scheme 3A), whereas worms have two that act redundantly. In contrast, mammals have four Notch paralogs that act both redundantly and uniquely (mNotch1-mNotch4) (Scheme 3A). The extracellular domain of all Notch proteins contains 29-36 tandem Epidermal Growth Factor (EGF)-like repeats, some of which mediate interactions with ligand. Some of the repeats bind calcium, which is necessary for the determination of Notch structure and affinity to its ligands. The EGF repeats are followed by a unique negative regulatory region (NRR), a region critical for preventing receptor activation in the absence of ligand. This region is composed of three cysteine-rich Lin12-Notch repeats (LNR) and a heterdimerization domain (HD) (Scheme 3A).

A Notch receptors

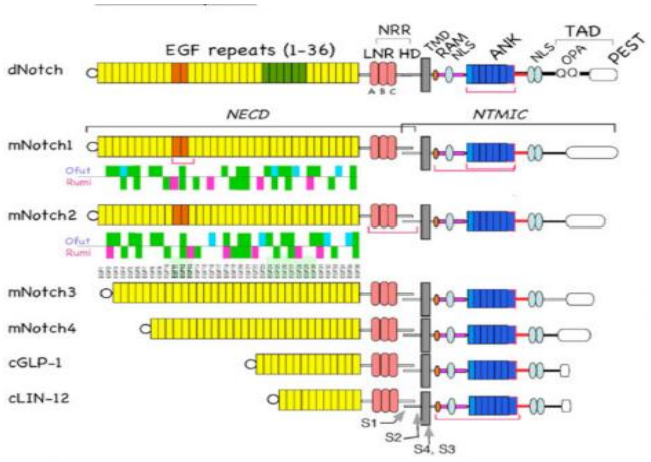

B TMD domain of mouse Notch1

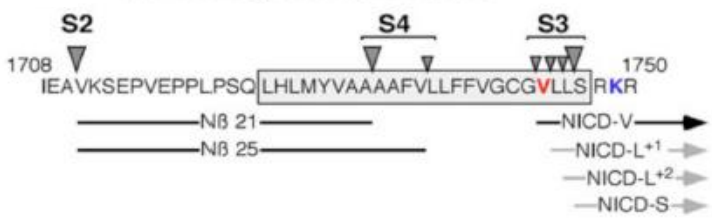

Introductory Scheme *3: Schematic representation of Notch receptors' structural domains (A).Schematic representation of Single Transmembrane Protein (TMD) cleavage sites and corresponding products. on mouse Notch1(B). Notch1 is cleaved at S2 by metalloproteases. γ-secretase can cleave multiple scissile bonds at S3 but only NICD molecules initiating at Val (V1744) evade N-end rule degradation (NICD-V).Cleavage then proceeds towards S4 until the short Nβ peptides can escape the lipid bilayer; most Nβ peptides are 21 amino acids long. The V1744G and K1749R amino acid substitutions (colorized) shift the S3 cleavage site NICD-V, NICD-L, NICD-S are variants with diverse N-termini(Kopan and Ilagan, 2009)*

The cleavage of Notch protein is one of the most critical steps concerning the ability of the protein to translocate into the cytoplasm and the nucleus. Most surface Notch proteins are cleaved by furin-like convertases at site 1 (S1) located within an unstructural loop protruding from the HD domain, thereby converting the Notch polypeptide into an NECD-NTMIC (Notch extracellular domain-Notch transmembrane and intracellular domain) heterodimer held together by non-covalent interactions between the N- and C-terminal halves of HD (Scheme 3A).

The single transmembrane domain (TMD) (Scheme 3B) is terminated by a 'stop translocation' signal comprised of 3–4 Arg/Lys residues. Intracellularly, the RAM (1RBPjκ association module) domain forms a high affinity binding module of 12–20 amino acids centered around a conserved WxP motif. A long, unstructured linker containing one nuclear localizing sequence (NLS) links RAM to seven ankyrin repeats (ANK domain). Following the ANK domain are an additional bipartite NLS and a loosely defined and evolutionarily divergent transactivation domain (TAD). The very C-terminus contains conserved proline/glutamic acid/ serine/threonine-rich motifs (PEST), containing degrons

that regulate the stability of NICD. Drosophila Notch also contains the glutamine-rich OPA repeat (Scheme 3A).

The mature receptor is produced after proteolytic cleavage by PC5/furin at S1 site and thereafter targeted to the cell surface as a heterodimer held together by noncovalent interactions (Scheme 3B). The Notch receptor is activated by binding to a ligand presented by a neighboring cell. Endocytosis and membrane trafficking regulate ligand and receptor availability at the cell surface. Ligand endocytosis is also thought to generate sufficient force to promote a conformational change that exposes Notch to cleavage at site S2 by ADAM metalloproteases (perhaps following heterodimer dissociation at S1). Juxtamembrane cleavage at S2 generates the membrane-anchored NEXT (Notch extracellular truncation) fragment, which is a substrate for the γ-secretase complex. γ-secretase cleaves the Notch TMD progressively to release NICD (Notch intracellular domain) and Nβ peptides. γ-secretase cleavage can occur at the cell surface or in endosomal compartments however cleavage at the membrane favors the production of more stable form of NICD (Kopan and Ilagan, 2009).

Nuclear translocation of Notch-IC, results in the formation of a complex with the CSL transcription factor family [CBF1/RBP-Jk/KBF2 in mammals, Su(H) in Drosophila and Xenopus, and Lag2 in Caenorhabditis elegans].

In the absence of NICD, the DNA-binding protein CSL associates with ubiquitous co-repressor (Co- R) proteins and histone deacetylases (HDACs) to repress transcription of target genes. In particular, in the absence of Notch-IC, CSL interacts with the SKIP, SMRT, CoR and HDAC proteins, resulting in the formation of a transcriptional repressor complex (Lee et al., 2015). When NICD enters the nucleus, its binding to CSL triggers an allosteric change that facilitates

displacement of transcriptional repressors. Mastermind (MAM) then recognizes the NICD/ CSL interface, and this tri-protein complex recruits co-activators (Co-A) to activate transcription (Scheme 4). Notch-IC dissociates the co-repressors, and then interacts with co-activator complexes, including the Lag-3/mastermind, p300/CBP and P/CAF/GCN5, to form a transcriptional active complex and activates CSL-dependent transcription. The RAM domain of Notch1, which mediates the interaction of RBP-Jk/Su(H) with the Notch1-IC, induces the activation of target gene transcription. In addition to the enhancer of split [E(spl)] complex genes, and the mammalian homologues of the Hairy and E(spl) genes, *Hes1*, *Hes5*, *Hes7*, *Hey1*, *Hey2* and *Heyl* are the downstream target genes of Notch signaling (Lee et al., 2015).

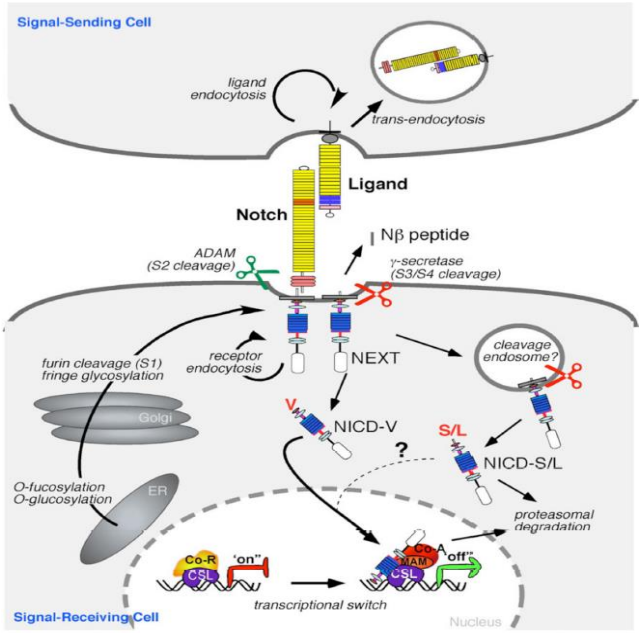

Introductory Scheme 4*: Schematic representation of Notch signaling pathway (Kopan and Ilagan, 2009).*

- **Regulation of NICD**

Activation of Notch signaling is normally tightly controlled by direct interactions with ligand-expressing cells, and dysregulated Notch signaling is associated with developmental abnormalities and cancer. Ligand activity can also be indirectly regulated by other signaling pathways at the level of ligand expression, serving to spatiotemporally compartmentalize Notch signaling activity. This regulatory complex results in the orchestration of Notch signaling during developmental events. Activation of Notch receptors triggers the initiation of signal in the form of NICD.

Most Notch-mediated processes require a transient pulse of activity for instance, in developmental contexts where iterative activation of the Notch pathway is required. In some tissues, this could last a fraction of the cell cycle. Even the few processes that require prolonged activation still seem to be sensitive to the activation “strength”, a yet to be defined aspect of Notch signaling. Given what we know about Notch biology, sustained Notch activation can be catastrophic for cell homeostasis. Thus, in addition to the above mentioned mechanisms that regulate NICD production, optimal signal strength is regulated in most cells by ensuring that NICD half-life is short. What is known so far about the removal of NICD molecules, is that during the transcriptional activation process, NICD is phosphorylated on its PEST domain by the CDK8 kinase and targeted for proteasomal degradation by the E3 ubiquitin ligase Sel10/Fbw7. This results in the deactivation of NICD and resets the cell for the next round of signaling (Kopan and Ilagan, 2009).

Taken together, Notch signaling is one of the main key players for the determination of progenitor cell identity during mammalian brain development.

Notch signaling induced by canonical Notch ligands is critical for normal embryonic development and tissue homeostasis through the regulation of a variety of cell fate decisions and cellular processes. Highlighting the importance of NICD turnover, equally crucial is the regulation of deactivation of this signaling pathway. It is already known that mutations or domain deletions of the C-terminal of NICD, which result in stabilizing the molecule can cause T cell acute lymphoblastic leukemia (T-ALL) in humans (Weng et al., 2004). Further studies are necessary to unravel the physiological elimination of NICD, with possible involvement of degradation pathways that could keep the equilibrium of NICD at the desirable levels in the cell.

Studies have focused on the impact of autophagic pathways on the regulation of Notch1 by its spaciotemporal degradation. Protein degradation pathways are already known to have a fundamental influence on cell fate during developmental differentiation, by removing signaling proteins and thus interfering contextually with the regulation of signaling pathways. Recently, it was revealed that one significant cellular mechanism of lysosome degradation, macroautophagy, plays a significant role in the equilibrium of total protein of Notch1 by degrading it, thus modulating stem cell maintenance during brain development (Wu et al., 2016).

Together all these studies raise the question of a possible direct synergy between the NICD levels, that acts as a transcription factor, and the lysosome degradation pathways, in order to control self-maintenance, proliferation and differentiation of NSCs during neural development.

Lysosomal degradation pathways

There are two major, fundamentally different mechanisms by which mammalian cells degrade proteins: the proteasome and the lysosome. The first one is a cylindrical protein complex found in the cytosol which cleaves up proteins tagged with ubiquitin. There is a huge variety of different ubiquitin ligases, reflecting the many different regulatory pathways by which the cell selects and recognizes proteins aimed for degradation. The proteasome consists of two subunits. The smaller one recognizes and binds ubiquitinated proteins, powered by ATP – unlike the lysosome, the proteasome is an energy-consuming operation. Once recognized, these proteins must be de-ubiquitinated and unfolded in order to pass through the narrow channel of the subunit and enter the bigger one, a cylindrical complex which does the actual chopping up of proteins. Unlike the lysosome, where proteases shear proteins up into individual amino acids, the proteasome just chops proteins into small peptides, usually of 7 – 9 amino acids each. These are later broken into amino acids by cytosolic proteases (Reinstein and Ciechanover, 2006).

The lysosome is another organelle of equal significance for protein degradation. This cellular compartment is responsible for autophagy. Autophagy is defined as the natural, regulated, destructive mechanism of the cells, enabling them to systematically recycle unnecessary or malfunctioned components in response to increased metabolic demands or stresses. Autophagy is a physiological and highly conserved intracellular degradation pathway, essential for the maintenance of cellular homeostasis (Mizushima and Levine, 2010). The selectivity of the response to removal of selected organelles or molecules may vary according to each cell type (Zhang et al., 2016). The main autophagic systems are macroautophagy, microautophagy and **C**haperone

Mediated **A**utophagy (CMA) (Scheme 5). The last one occurs only in mammalian cells.

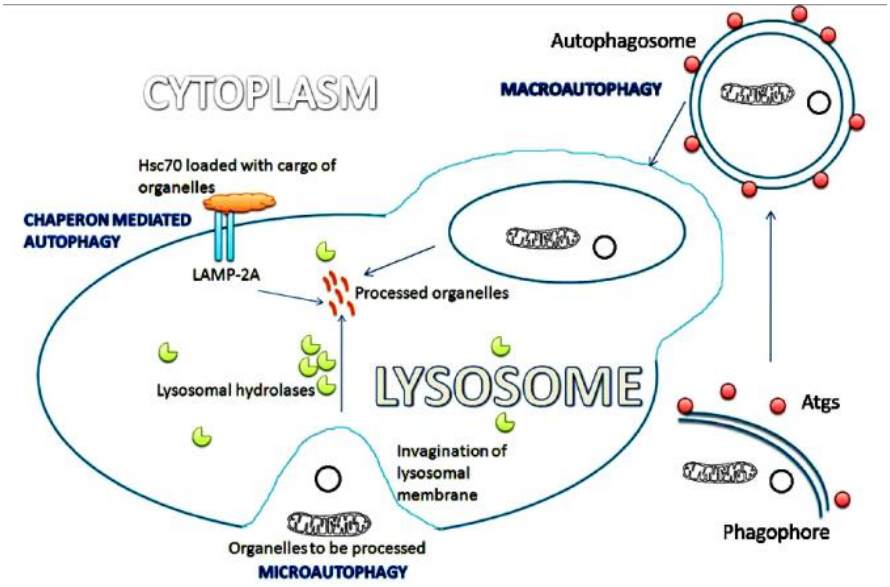

Introductory scheme 5*: Schematic representation of the lysosome indicating the three main classes of autophagy (Jacob et al., 2017).*

- **Macroautophagy**

Macroautophagy is a highly conserved, non-selective, predominant pathway for removal of damaged organelles or unused proteins through the formation of a cytosolic double membrane around the organelle marked for destruction called autophagosome (Jacob et al., 2017). These autophagosomes later fuse with the lysosome and result in breakdown of the unwanted organelles or proteins. The resultant products are then released back into the cytosol for recycling of energy during stress conditions (Feng et al., 2014, Jacob et al., 2017). The substrates of macroautophagy include superfluous and damaged organelles, cytosolic proteins and invasive microbes (Scheme 6).

Macroautophagy is highly conserved from yeast to mammals, both morphologically and with regard to the proteins that make up the core autophagy machinery (Feng et al., 2014).

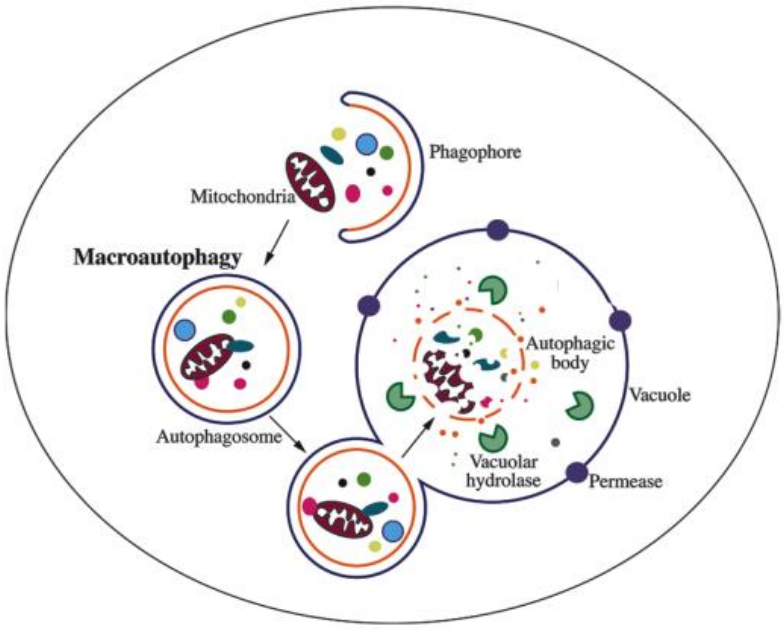

Introductory scheme 6*: Schematic depiction of macroautophagy in yeast. Parts of cytoplasm and targeted organelles are sequestered by the phagophore resulting in the formation of autophagosome. Subsequently, the autophagosome fuses with the vacuole membrane, releasing the autophagic body into the vacuole. Eventually, the cargo is degraded by hydrolases (Feng et al., 2014).*

In more details, macroautophagy is a well-coordinated multi-step process. The steps describing this process are the initiation, nucleation, elongation-closure, maturation and degradation (Zhang et al., 2016). For a successful completion of degradation, various signaling pathways take place along with the activation of about 30 autophagy-related genes (*Atg-)*. During the initiation process, mTOR pathway is inhibited (under stressful conditions), thus allowing the formation of the isolation membrane, called “phagophore”. Once triggered, the phagophore enters the nucleation process. This process includes the

activation of PI3K class III phosphatidylinositol 3-kinase (PI3KCIII) complex that stimulates the production of phosphatidylinositol 3-phosphate (PI3P). Sequentially, PI3P binds to a family of proteins located to the surface of the isolated membranes (WIPI proteins) leading to their nucleation. Many studies have shown that 3-methyladenine (3MA) (used in this study), can block the specific autophagic pathway by inhibiting the PI3KC3 complex leading to the prevention of the formation of mature autophagosomes (Patel and Cuervo, 2015, Seglen and Gordon, 1982). The next step is about the elongation and closure of phagophore. This process involves two ubiquitin-like reactions. The first one is the conjugation of two molecules, Atg12 and Atg5, catalyzed by two other Atg, Atg7 and Atg10. The second reaction is about the formation of a tetrameric complex, the already formed Atg5/12 structure and the homo-oligomerized form of Atg16L. During the second reaction, microtubule-associated protein 1 light chain (LC3) is hydrolyzed to LC3-I (cytosolic form) and then the previously formed structure (Atg12/Atg5/Atg16L) mediates the conjugations of LC3-I with phosphatidyl-ethanolamine (PE) to produce the lipidated form, LC3-II. The latter promotes the elongation and closure of the inner and outer bilayers of phagophore, leading to formation of the autophagosomes (Scheme 7A) (Zhang et al., 2016). In addition to proteins, macroautophagy targets include damaged or oxidized organelles such as mitochondria (mitophagy, endoplasmic reticulum (ERphagy), peroxisomes (pexophagy), lipid droplets (lipophagy), ferritin (ferritinophagy) and zymogen granules (zympohagy) (Alfaro et al., 2018).

A. B.

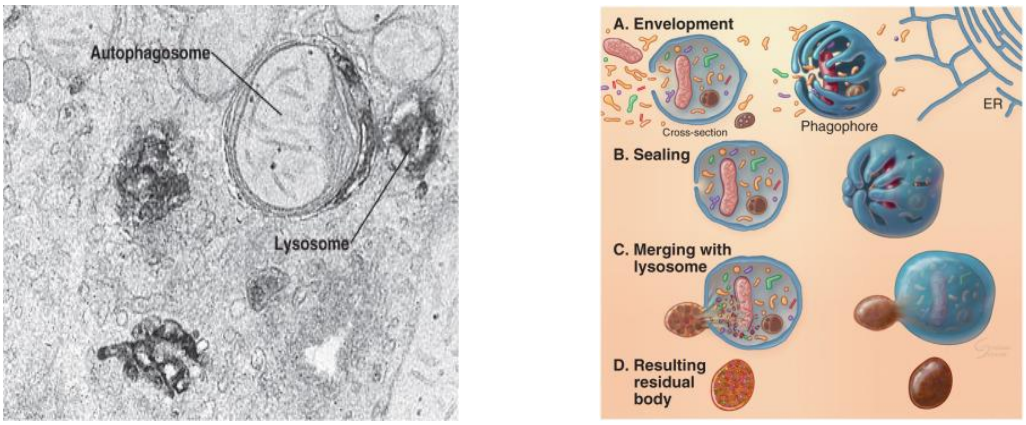

Introductory scheme 7*: Electron micrograph of an autophagosome. From starved rat liver, the photo depicts an autophagosome containing a mitochondrion in the process of fusing with a secondary lysosome (**A**) A phagophore membrane forms, enveloping a region of cytoplasm containing target proteins and organelles. **B,** Membrane fusion results in formation of a nascent autophagosome. **C,** The nascent autophagosome fuses with a primary or secondary lysosome, which delivers hydrolytic enzymes that degrade the autophagosome contents. **D,** Undigested material remains in residual bodies(**B**). (Dunn, 1990) . Cell Biology (Third Edition) 2017, Pages 393-405 Chapter 23 - Processing and Degradation of Cellular Components https://doi.org/10.1016/B978-0-323-34126-4.00023-2*

Next, the maturation step occurs when this autophagosome is transported towards a microtubule organizing center, enriched with lysosomes (Scheme 7B). During this process, the autophagosome is fused with the lysosome. This fusion allows the digestion of the autophagosome contents by the lysosomal hydrolases, completing multiple steps of macroautophagy (Scheme 7B).

Fusion of a nascent autophagic vacuole with late endosomes and lysosomes involves a specialized SNARE (soluble *N*-ethylmaleimide-sensitive factor [NSF] attachment protein receptor) protein and forms an autolysosome with acid hydrolases in the lumen. These degrade the contents, including the internalized membrane, releasing amino acids, lipids, sugars, and nucleotides back to the cytoplasm. The end stage of an autolysosome is a residual body with

a dense core of undegraded material (Scheme 7B). The process of formation and degradation of autophagic vacuoles in the liver requires less than 15 minutes.

Some organisms like yeast, use the autophagy-machinery as a compensatory pathway for cell apoptosis. For example budding yeast uses macroautophagy for cell death when a cell receives a lethal insult under conditions in which apoptotic pathways are not functional. Macroautophagy has also been implicated in the developmental programs of a number of higher organisms and in the destruction of intracellular protein aggregates. Protein aggregates and damaged organelles, such as mitochondria are tagged with ubiquitin and recognized by one of two autophagy receptors that bind both ubiquitin and Atg8-containing vesicles. This results in their envelopment by growing phagophore membranes, and delivery to autolysosomes via macroautophagy. . Cell Biology (Third Edition) 2017, Pages 393-405 Chapter 23 -Processing and Degradation of Cellular Components https://doi.org/10.1016/B978-0-323-34126-4.00023-2

The past two decades studies regarding macroautophagy have been very intense, bringing light to many new players and molecular machineries. This great interest is mainly due to the correlation of macroautophagy with a wide range of human pathophysiologies including cancer, myopathies, diabetes and neurodegenerative disease.

- **Microautophagy**

The second type of lysosomal degradation pathways is called microautophagy. Little is known about microautphagy, a non-selective lysosomal degradation pathway where the vacuole directly invaginates and internalizes the

cytosolic components without the prior formation of the double membrane phagophore. This results in the degradation of the vesicle into the vacuole lumen. The engulfment of macroautophagy can also involve cell organelles. Microautophagy can be further subcategorized, depending on the particles that are invaginated, into micromitophagy (for mitochondrial parts), micronucleophagy (for nuclear parts) and micropexophagy (for peroxisomes). The limiting/sequestering membrane is the lysosomal membrane, which invaginates to form tubules that pinch off into the lysosomal lumen. Microautophagy of soluble components, as in macroautophagy, is induced by nitrogen starvation and rapamycin. Microautophagy is controlled by the TOR and EGO signaling complexes, resulting in direct uptake and degradation of the vacuolar boundary membrane (Uttenweiler et al., 2007). Hence, this process could compensate for the enormous influx of membrane caused by autophagy. It seems that microautophagy is required for the maintenance of organelle size and membrane composition rather than for cell survival under nutrient restriction. Uttenweiler et al. (2007) have identified the vacuolar transporter chaperone, VTC complex, required for microautophagy. This complex is present on the ER and vacuoles and at the cell periphery and deletion of the VTC complex blocks micrautophagic uptake into vacuoles.

- **Chaperone Mediated Autophagy (CMA)**

The third type of autophagy is the chaperone mediated autophagy (CMA). CMA is a specific, lysosomal-dependent protein degradation pathway (Isenman and Dice, 1989). There are some basic characteristics that define this mechanism as one of the main and significant lysosomal pathways, and of equal importance

to the most known and studied macroautophagy (Alfaro et al., 2018). Firstly, the main characteristic that discriminates this pathway from the other two is that it does not involve the formation of autophagosomes and autolysosomes. Secondly, the targets of CMA are strictly cellular proteins and not organelles, a property of the pathway which defines it as an exclusively selective protein degradation pathway. The third difference is that the protein cargo is directly delivered into the lysosomal lumen through the interaction with HSC70 (HSPA8) and LAMP2A. CMA is highly selective towards a group of cytosolic proteins and the mechanism of delivery of the substrate proteins to the lysosomes is exclusive to this type of autophagy, which differentiates them from the other two types of autophagy (Scheme 8).

HSC70 belongs to the Hsp70 protein family and it has a constitutive expression, participating principally in the CMA pathway but also in macroautophagy (Tekirdag and Cuervo, 2018). LAMP2A protein is the A isoform of Lamp-2 (lysosome associated-membrane protein type 2) and restricts the CMA degradation process. The lysosome-associated membrane glycoprotein 2 (LAMP-2) is able to generate three variants through its pre-mRNA alternative splicing, (*LAMP2A*, *LAMP2B*, and *LAMP2C*) but, to date, it is well established that only the variant A is responsible for the CMA activity (Cuervo and Dice, 2000). Compared to variants B and C, LAMP2A has four positively charged residues in its C-terminal domain that specifically allow its interaction with target proteins. Characterization of LAMP2A showed that multimerization of this variant (and not the others) in the lysosomal membrane is directly correlated with CMA activity (Cuervo and Dice, 2000, Rout et al., 2014).

Importantly, in CMA, selectivity resides in the fact that all CMA substrate proteins contain at least one amino acidic motif biochemically related to

the penta-peptide KFERQ (Dice, 1990, Wing et al., 1991). The mechanism by which CMA is activated is when HSC70 recognizes the KFERQ-like sequence in target proteins to form the complex HSC70-substrate. Dice et al in 1985 found a pentapeptide in the Ribonuclease A which was necessary for its degradation by lysosomes in fibroblasts. After the analysis of different proteins, it was found that the optimal aminoacidic sequence to be present in a protein in order to be degraded through CMA, corresponds to the pentapeptide KFERQ. It is now well-established that HSC70 specifically recognizes the KFERQ-like motif in cytosolic proteins to target them for lysosomal degradation through CMA (Chiang et al., 1989, Dice, 1990). Although the temporal sequence of events that drive this process is not well known, the complex HSC70-substrate interacts with the cytosolic tail of LAMP2A that, in turns, drives the translocation of the target protein into the lysosome lumen.

In detail, the substrate up-take by the lysosome is a step that depends on LAMP2A. LAMP2A organizes in dynamic, defined protein complexes at the lysosomal membrane and the contribution of LAMP2A to each complex changes with changes in CMA activity. CMA substrates bind preferentially to LAMP2A monomers, while the efficient translocation of substrate proteins across the lysosomal membrane requires the formation of a particular LAMP2A-containing complex. HSC70 plays distinctive role in the stepwise assembly of LAMP2A into protein complexes at the lysosomal membrane. HSC70 promotes the organization of LAMP2A into monomers or smaller complexes. The dynamic character of LAMP2A at the lysosomal membrane forces this protein to adopt transitory conformations until the proper assembly or complete disassembly is attained (Bandyopadhyay and Cuervo, 2008, Bandyopadhyay et al., 2008). Further evidence showed that LAMP2A

arranges in a stable homotrimer, with helical transmembrane domains bound by a coiled-coil conformation, and with the cytosolic tails interacting with the complex HSC70-substrate protein. In addition, LAMP2A oligomerization was shown to be regulated by different proteins. Glial fibrillary acidic protein (GFAP) helps to stabilize the translocation complex in an EF1a dependent manner. The stabilizing effect of GFAP is disrupted by the association of EF1a to GTP, which in turn is released from the translocation complex and allows the self-association between GFAP molecules. The self-interaction between GFAP molecules has a negative impact on the stabilization of the translocation complex. Thus, GTP acts as an inhibitor of CMA activity (Bandyopadhyay et al., 2008).

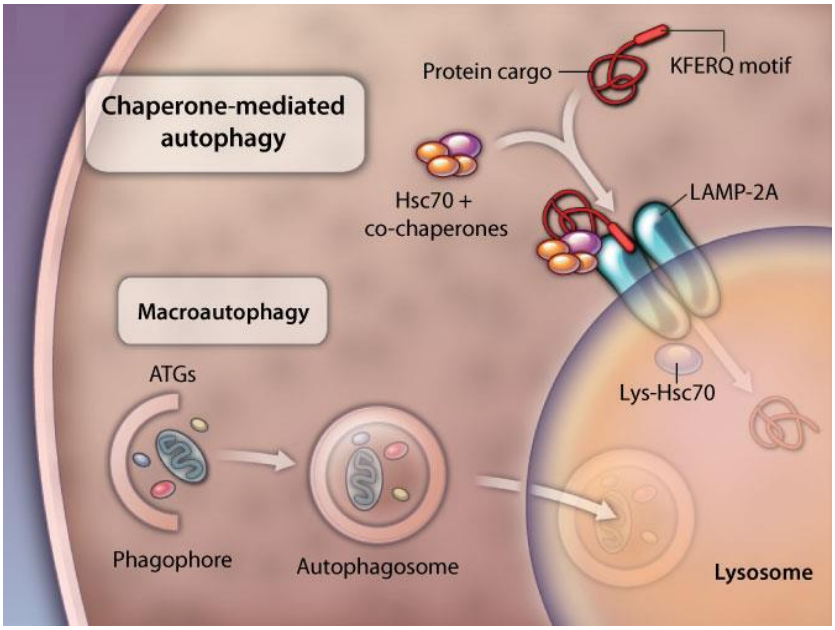

Introductory scheme 8*: The two best-characterized routes for the degradation of unwanted proteins by autophagy in mammalian cells are macroautophagy and chaperone-mediated autophagy (CMA). During CMA, soluble cytosolic proteins containing the pentapeptide motif KFERQ are selectively recognized by the Hsc70 chaperone complex. The chaperone complex*

then targets the protein cargo for binding to the lysosomal receptor LAMP2A. A second chaperone, Lys-Hsc70, facilitates complete translocation of the substrate protein into the lumen of the lysosome, where it is degraded by lysosomal proteases. In macroautophagy, cytoplasmic proteins and organelles are sequestered into double-membraned autophagosomes, which subsequently fuse with the lysosome, resulting in bulk degradation of the autophagosome's cytosolic contents. (Thorburn and Debnath, 2011).

- **KFERQ-like motif**

The pentapeptide KFERQ-like sequence, the CMA targeting motif, can be located in the C-terminus, N-terminus or in central regions of the protein, the only requirement being that it becomes exposed or accessible for chaperone binding. Scenarios that could promote exposure of the CMA-targeting motif include partial unfolding of the protein, dissociation of protein complexes in which interacting proteins mask the targeting motif, or protein release from intracellular membranes. As for the number of the pentapeptide motif in the aminoacid sequence, although several cytosolic proteins contain more than one targeting motif, experimental addition of tandem motifs does not make proteins better CMA substrates (one motif suffices for lysosomal targeting). In proteins with multiple targeting motifs, it is plausible that different motifs become available for chaperone recognition depending on the stimuli that induce the degradation of the protein (i.e. partial unfolding versus dissociation from a protein complex when still fully folded). In proteins that undergo physiological cleavage to release functional peptides, the presence of multiple motifs could guarantee selective removal of the resulting peptides by CMA. Concerning the motif's abundance, sequence analysis reveals that about 30% of soluble cytosolic proteins contain a putative CMA-targeting motif. However, the fact that post-

translational modifications may generate additional motifs increases the number of possible substrates. Motifs are only detected in soluble cytosolic proteins, or proteins inside organelles that may end in the cytosolic compartment under specific conditions. Membrane proteins cannot be translocated into lysosomes and subsequently this pool of proteins lacks CMA targeting motifs. The only known exceptions are specific membrane proteins in which the targeting motif is present in regions of the membrane protein that can be released in the cytosol upon cleavage (Kaushik and Cuervo, 2012).

- **CMA activation**

It has been reported that CMA is necessary for proper functioning of cellular homeostasis. All cells have a basal CMA activity which helps to maintain the homeostasis of many cellular proteins. However, under certain stimulus, like nutrient starvation, serum deprivation or cellular stress (e.g., protein aggregation), CMA activity increases. This up-regulation condition can be visualized by mRNA *LAMP2A* overexpression, HSC70 and LAMP2A co-localization and LAMP2A positive lysosomes with increased perinuclear distribution. Koga et al. showed that basal CMA activity is present in a variety of cell types. However, an up-regulation in this pathway can be observed under different stimuli or conditions (Koga et al., 2011b).

The most common stimulus for CMA activation is nutrient deprivation (or starvation). Starvation activates CMA both *in vitro* and *in vivo* and, although the exact mechanism has not been described yet, at least *in vivo*, it has been proposed that it depends on the circulating ketone bodies (Finn and Dice, 2005).

CMA over-activation has also been observed under DNA damage. Under this condition, CMA activity is up-regulated with the purpose to degrade the checkpoint protein kinase 1 (Chk1). The accelerated degradation of Chk1 by CMA reduces its nuclear entrance and consequently decreases the phosphorylation and destabilization of the MRN (Mre11–Rad50–Nbs1), a complex that participates in the early steps of particular DNA repair pathways (Park et al., 2015). Moreover, for unknown reasons so far, oxidative stress also activates CMA constitutively. Both *LAMP2A* mRNA and the recruitment of LAMP2A to the lysosomal membrane were augmented under oxidative stress (Kiffin et al., 2004).

Another stressor that up-regulates CMA activity is hypoxia. Over-activation of CMA was directly correlated with the survival of neuronal cells exposed to different hypoxic conditions and, on the contrary, the down-regulation of this pathway sensitized the cells to the stress. On the other hand, it was reported that HIF-1a, a protein that activates HIF-1 (Hypoxia-inducible factor-1) and mediates an adaptive response to hypoxia, is degraded by CMA in cells exposed to hypoxic conditions (Dohi et al., 2012, Hubbi et al., 2013).

Finally, alterations of CMA have been observed in different models of neurodegenerative diseases like Huntington's and Parkinson's disease.

- **CMA and neurodegenerative diseases**

LAMP2A is the rate-limiting factor for the neuronal uptake and degradation of aggregation-prone proteins via CMA such as α-synuclein (α-syn)

(Cuervo et al., 2004, Xilouri et al., 2013) and huntingtin (Htt) that are neurotoxic when aggregated (Rothaug et al., 2015).

Interestingly, human mutations in the LAMP2 gene have been linked to specific cases of Danon disease (Majer et al., 2014, Rothaug et al., 2015). Danon disease is defined as an X-linked "lysosomal glycogen storage disease with normal acid maltase". Danon disease patients suffer from severe skeletal and cardiac myopathy as well as intellectual dysfunction. The pathological hallmark of Danon disease is the presence of accumulated glycogen and autophagic vacuoles within liver and muscle of patients as well as a mouse model for this disease. Rothaug et al. suggest that LAMP-2 plays an important role in the clearance of glycogen and maturation of autophagic vacuoles within hippocampal neurons (Rothaug et al., 2015).

Moreover, evidence indicates that a dysregulation in CMA could impact on the onset or progression of Parkinson's Disease. The main protein associated with this neurogenerative disorder, alpha-synuclein protein (a-syn), has been identified as a CMA substrate (Cuervo et al., 2004). More specifically, reduced a-syn degradation was observed when its KFERQ motif was mutated or the expression of LAMP2A was knocked down. The involvement of CMA in a-syn degradation was confirmed in different neuronal cell lines (PC12 and SH-SY5Y) and primary cultures of cortical and midbrain neurons (Vogiatzi et al., 2008). One of the hallmarks of PD is the neurotoxicity caused by the abnormal aggregation of a-syn. In this context, mutations in the protein impair its degradation through a CMA pathway, causing the accumulation of a-syn oligomers that are unable to be degraded by the lysosome. This event blocks the entire CMA pathway, enhancing oligomer formation and compromising the degradation of other CMA substrates (Martinez-Vicente et al., 2008, Xilouri et

al., 2009). Additionally, LAMP2A and HSC70 were observed to be up-regulated when a-syn was over-expressed *in vivo* (Mak et al., 2010). In line with these results, it was shown that the down-regulation of LAMP2A in adult rat substantia nigra, via an adeno-associated virus, induced intracellular accumulation of a-syn puncta. In addition, LAMP2A down-regulation was also correlated with a progressive loss of dopaminergic neurons, severe reduction in striatal dopamine levels/terminals, increased astro- and microgliosis and relevant motor deficits (Xilouri et al., 2009). Additionally, studies using Drosophila melanogaster model have shown that by simultaneous overexpression of human LAMP2A and neuronal expression of a human pathological form of a-syn that causes progressive locomotor and oxidative defects, flies were protected from the pathological phenotype (Issa et al., 2018).

Except a-syn, other proteins related to PD are also correlated to CMA degradation. One example is PARK7/DJ-1. PARK7/DJ-1 is an autosomal recessive familial PD gene. PARK7 plays a critical role in anti-oxidative response and its dysfunction leads to mitochondrial defects. It has been proposed that PARK7 lysosome-dependent degradation is mediated through CMA. Specifically, CMA preferentially removes the oxidatively damaged non functional PARK7 protein, contributing to the protection of the cell. Wang et al. also showed that this protective effect is lost under PARK7-deficieny conditions (Wang et al., 2016). Another recent study correlating the PD protein, PARK7, and CMA activity, showed that controlled manipulation of CMA activity, through suppression or overexpression of LAMP2A protein, could significantly alter the levels of PARK7 protein (Brekk et al., 2019). These interventions to LAMP2A expression, previously reported to cause functional alterations of CMA activity (Xilouri et al., 2013, Vogiatzi et al., 2008, Massey et al., 2006), led to

phenotypical modifications that could be rescued by restoring the levels of PARK7 protein, indicating the relevance of known to CNS-disorders-molecules to CMA activity. These studies suggest that alterations in the abundance of neuronal proteins involved in neuropsychiatric disorders, upon CMA manipulation, may in part be responsible for the neurodegeneration observed upon CMA impairment *in vivo.*

Another example of a PD related protein and its regulation by CMA activity is MEF2D. Myocyte enhancer factor 2D (MEF2D) is a transcription factor required for neuronal survival. MEF2D is a cytosolic protein found to interact with HSC70 and undergo degradation. MEF2D is accumulated in the cytoplasm under inhibition of CMA activity. Furthermore, MEF2D levels were increased in the brains of α-synuclein transgenic mice and patients with Parkinson's disease, correlating this transcription factor to PD pathology. Wild-type α-synuclein and a Parkinson's disease–associated mutant disrupted the MEF2D-Hsc70 binding and led to neuronal death. (Yang et al., 2009).

It has also been shown by the group of Orenstein et al, that LRRK2 (leucin-rich repeat kinase 2) a protein known from its correlation to PD, is also linked with CMA activity (Orenstein et al., 2013). There is a mutant form of this protein that is targeted as one of the most common causes of familial PD. This group has shown that the wild type LRRK2 can be degraded in lysosomes by CMA whereas its mutant pathogenic form can barely be degraded in the same way. Additionally, there is evidence that the mutant pathogenic forms of LRRK2, as well as high concentrations of wilt-type, inhibit the CMA machinery. This blockage of CMA by LRRK2 drives the cells to increase the amount of LAMP2A, thus also affecting the levels of a-syn (Orenstein et al., 2013).

Another neurodegenerative disease potentially correlated to the activity of CMA is Alzheimer's disease (AD). CMA and AD could be connected by the degradation of the RCAN1 protein (Regulator of calcineurin 1) through this pathway. RCAN1 expression was shown to be increased in AD brains. *In vitro* studies showed that disruption of CMA increased RCAN1 expression. Additionally, two CMA recognition motifs were identified in RCAN1, concluding that its degradation is also mediated through a CMA-lysosome pathway (in addition to the already known degradation through the ubiquitin proteasome pathway) (Liu et al., 2009). On the other hand, the Tau protein, one of the principal factors associated with AD, was also shown to be a CMA substrate. The Tau protein is degraded by the autophagy–lysosomal system producing different fragments that, in turn, bind to HSC70 and become CMA substrates. Although these fragments are able to reach the lysosomes, they remain bound to the lysosomal membrane, causing the formation of pathological Tau aggregates that cause lysosomal damage and block the degradation of other CMA targets (Wang et al., 2009b, Wang et al., 2010). Finally, another protein correlated with AD is amyloid precursor protein (APP). APP is a transmembrane protein that affects b-catenin, anchoring the protein to the actin cytoskeleton and plays an important role in cell-cell adhesion as well as in Wnt signaling. Upon cleavage of APP through g-secretase-mediated processes by PSEN1 and PSEN2, the neurotoxic peptide amyloid-b (Ab) is formed. Abnormal levels of extracellular Ab-peptides are found as plaques in patients diagnosed with AD (Ghavami et al., 2014). APP contains a KFERQ-like motif in its aminoacid sequence; deletions of this motif do not affect its binding to HSC70, but prevent its lysosomal degradation, causing its accumulation (Park et al., 2016).

Another neurodegenerative disease that has been correlated to CMA impairment is Huntington Disease (HD). HD is caused by an abnormal expansion of polyQ tract in the protein named huntingtin (Htt). HD pathology is characterized by accumulation and aggregation of mutant Htt in striatal and cortical neurons. Aberrant Htt degradation is implicated in HD pathogenesis. A constitutive activation of CMA has been observed in cell lines and mouse models of HD. In a mouse model for this disease, a strong co-localization between LAMP2A and HSC70 was correlated with augmented lysosomal degradation of the native and aberrant huntingtin protein (Htt). Furthermore, additional studies performed *in vivo* also showed that Htt aggregates could be forced to be degraded through CMA, by targeting them with a polyQ binding protein (QBP1) including a KFERQ domain in its amino acidic sequence. The data indicated that modulation of the CMA pathway can be a plausible strategy for HD treatment (Bauer et al., 2010, Koga et al., 2011a, Qi et al., 2012).

Finally, there is a correlation of the protein TPD-43 which is a ribonuclear protein that associates CMA with two significant neurodegenerative diseases, Amyotrophic Lateral Sclerosis (ALS) and Frontotemporal Lobar Degeneration (FTLD). Huang et al. described a KFERQ-like domain in TDP-43 that was responsible for the interaction of this protein with HSC70 under ubiquitination conditions. Mutation of the KFERQ-like domain disrupted the ubiquitin-dependent binding of TDP-43 with HSC70. In addition, down-regulation of *LAMP2A* by siRNA treatment, seems to increase the level of the pathologically related 25-KDa and 35-KDa TDP-43 C-terminal fragments, but not the full-length protein (Huang et al., 2014). Studies indicate that CMA targeted degradation of TDP-43 can be used as a strategy to ameliorate neurodegenerative diseases associated with this protein (Tamaki et al., 2018).

Aim of the Thesis

In general, although CMA malfunction is correlated to many brain-related diseases, including neurodevelopmental disorders (Xilouri and Stefanis, 2011), nothing is known about its physiological role in brain development.

The starting point for this thesis is the fact that the levels of LAMP2A were found to be regulated during normal rodent brain development (Vogiatzi et al., 2008), suggesting the intriguing hypothesis that CMA could be involved in central nervous system developmental processes. It is already known by Dr. Stefanis research group that LAMP2A's protein expression is increased during the latest embryonic stage and the beginning of the fetal period. Additionally, increased LAMP2A was detected in *in vitro* primary cortical cultures from E18 rat embryos. High levels of CMA activity were also observed during neuronal differentiation, suggesting the pathway's implication during embryonic cortical formation. While macroautophagy has been shown to directly affect differentiation of NSCs and mammalian brain development (Wu et al., 2016, Fimia et al., 2007), CMA had not been studied in this context. Consistent with this hypothesis, here, we show that LAMP2A is expressed in the mammalian brain during early development, and is associated with neuronal differentiation, while the CMA pathway is highly active in NSCs. Most importantly, gain- and loss-of-function studies in NSCs suggest an inductive role of CMA in neurogenesis. Mechanistically, we provide functional evidence indicating that the CMA degradation pathway is a negative regulator of Notch1 signaling activity in NSCs. Collectively we describe here a novel mechanism in the regulation of

neurogenesis via a direct effect of the CMA pathway on the Notch1 signaling pathway.

Materials and Methods

Ethics statement. The study protocol was approved by the local ethics committee (Athens Prefecture Veterinarian Service; K3237/11-05-2012) and took place in the animal facilities of the Center for Experimental Surgery of the Biomedical Research Foundation of the Academy of Athens. All animals were handled in strict accordance with good animal practice as defined by the relevant European and Greek animal welfare bodies.

RNA extraction and real-time RT-qPCR analysis. Total RNA was isolated by TRI reagent solution (AM9738, Ambion/RNA, Life Technologies) according to manufacturer's instructions followed by treatment with RQ1 DNase (Promega, Madison, WI, USA). RNA concentration and purity was measured by Nanodrop 2000c (Thermo), and 1.5 μg was used for cDNA synthesis using the SuperScript First-Strand Synthesis System (Invitrogen, Carlsbad, USA) together with random hexamer primers. Quantitative Real time RT-PCR analysis was performed in a LightCycler 96 Instrument (Roche). Measured values were normalized using *Gapdh* mRNA levels as internal references.

Primer sets used in RT-qPCR assays:

Lamp2a For: 5' CAACCTGACTCCTGTCGTTC 3'

Lamp2a Rev: 5' TCATAGGGATAGCCCGCATA 3'

Hspa8 (*Hsc70*) For: 5' GAACCAGACTGCGGAGAAGAAGG 3'

Hspa8 (*Hsc70*) Rev: 5' GCACTCTGGTACAGCTTGGT 3'

Gapdh For: 5' TGCCACTCAGAAGACTGTGG 3'

Gapdh Rev: 5' TTCAGCTCTGGGATGACCTT 3'

Foxg1 For: 5' GCCAAGCTAGCCTTTAAGCG 3'

Foxg1 Rev: 5’ CGTGGTCCCGTTGTAACTCA 3’

Ngn2 For: 5’ GTCCCCATACAGCTGCACTT 3’

Ngn2 Rev: 5’ CAGGTGAGGTGCATAACGGT 3’

NeuN (*Rbfox3*) For: 5’ GGCAAATGTTCGGGCAATTCG 3’

NeuN (*Rbfox3*) Rev: 5’ TCAATTTTCCGTCCCTCTACGAT 3’

Sox2 For: 5’ ATGGAGACGGAGCTGAAGCC 3’

Sox2 Rev: 5’ GGACCACACCATGAAGGCAT 3’

NeuroD1 For: 5’ TTGAAGCCATGAATGCAGAG 3’

NeuroD1 Rev: 5’TCTTGGGCTTTTGATCATCC 3’

Hes5 For: 5’ CCCAACTCCAAACTGGAGAA 3’

Hes5 Rev: 5’ TAGTCCTGGTGCAGGTCTT 3’

Pax6 For: 5’ CCGAATTCTGCAGGTGTCCA 3’

Pax6 Rev: 5’ AGTCGCCACTCTTGGCTTAC 3’

Tbr2 For: 5’ TTCCGGGACAACTACGATTCA 3’

Tbr2 Rev: 5’ ACGCCGTACCGACCTCC 3’

Notch1 For: 5’ GCCGCAAGAGGCTTGAGAT 3’

Notch1 Rev: 5’ GGAGTCCTGGCATCGTTGG 3’

Immunofluorescence. Rodent embryonic brains were washed in 4% PFA for 4 hours and left o/n in 30% sucrose in PBS. The tissue then was embedded in OCT, sectioned transversely at 12μm and collected on super-frost slides. LAMP2A was detected using a rabbit polyclonal antibody (1:100 dilution), kindly provided by Judith Blanz, as previously reported (Rothaug et al., 2015). The specificity of the anti-LAMP2A antibody was further confirmed with shRNA-mediated down-regulation of *Lamp2A* transcript isoform (Scheme 4A). Anti-GFP (1:2.500 dilution) was purchased from Molecular Probes (Invitrogen),

mouse monoclonal anti- TUBB3 (βIII-TUBULIN) from Covance USA (Tuj1, MMS-435P, 1:1.500 dilution), mouse monoclonal anti-GFAP (1:1000 dilution) from Sigma, mouse monoclonal anti-Nestin from Developmental Studies Hybridoma bank (the University of Iowa, Iowa city, 1:100 dilution). Goat polyclonal anti-SOX2 (Y-17; sc-17320, 1:200 dilution) and anti-LAMP1 (sc65236, 1:1000 dilution) were purchased from Santa Cruz, RIP from Hybridoma Bank (1:100 dilution) and rabbit polyclonal HSPA8 (1427, 1:1000 dilution) from Abcam. The anti-cleaved CASPASE 3 was purchased from Cell Signaling (#9661, 1:200 dilution) and rabbit anti-myc tag from Millipore (06-549, 1:100 dilution). Rabbit polyclonal anti-activated NOTCH1 that corresponds only to the intracellular activated NOTCH1 (NICD) (ab8925, 1:100 dilution) was purchased from Abcam. Secondary antibodies conjugated with AlexaFluor 488, 568 (red) and 647 (far red) were from Molecular Probes (1:500 dilution). Cell nuclei were labeled with DAPI (1:2.000 dilution, Molecular Probes). Specimens were viewed and analyzed with a Leica confocal microscope (Politis et al., 2007). Statistical analysis was performed with the two-tailed Student's *t* test.

Quantification of co-localization of NICD with HSPA8 and NICD with LAMP1. Stacked images of NSCs immunostained with NICD and HSPA8 acquired with confocal microscopy were used for co-localization. These images were imported in Fiji (ImageJ) software where specific regions of interest (ROI) were selected. For the quantification of co-localization, Pearson Correlation Coefficiency method was used (Dunn et al., 2011) and automatically performed in Coloc2 plug-in. The same procedure was followed to quantify the colocalization of NICD with LAMP1 in NSCs.

Western Blot analysis. Total protein was isolated from cultured NSCs, HEK293A, N2A or embryonic tissues with lysis buffer RIPA plus protease inhibitor cocktail. The homogenates were centrifuged at 17.000 *g* for 15 min at 4^0 C. The supernatants were collected, and protein concentration was measured with Bradford protein assay (Bio-Rad protein assay). 35μg of protein samples were loaded each time into SDS-PAGE gels, and transferred to nitrocellulose membranes (Whatman) using the semi-dry transfer system (Bio-Rad). The membranes were blocked with 5% dry milk dissolved in Tris-buffered Saline (1x) containing 0.1% Tween-20 for 1 hour at room temperature (RT). The membranes were incubated with primary antibodies at 4° C overnight followed by secondary antibodies for 1.30 hours at RT. The primary antibodies in the Western blot were rabbit anti-LAMP2A, kindly provided by Judith Blanz, exactly as previously described (Rothaug et al., 2015), rabbit anti-HSPA8 (1:1.000 dilution), rabbit anti-TUBB (1:8.000 dilution) and rabbit anti-LC3II (1:1.000 dilution) (MBL Life Science, PM036). Goat polyclonal anti-NOTCH1 that detects the NOTCH1-intracellular domain (NICD) (1:1.000 dilution) (C20;sc-6014) and goat anti-SOX2 (1:200 dilution) were purchased from SantaCruz. Anti-RFP (1:1.000 dilution) (detects DsRed) and anti-myc tag (1:100) were from Chromotek and Sigma, respectively. Moreover, chicken anti-GFP (1:1.000 dilution). The secondary antibodies were donkey anti-mouse (1:20.000 dilution), anti-rabbit (1:10.000 dilution), anti-goat (1:30.000 dilution) IgGs.

Culture of NSCs, knockdown and overexpression studies. Neurosphere cultures from E16.5 rat cortical tissue were prepared as described previously (Kaltezioti et al., 2010, Kaltezioti et al., 2014, Politis et al., 2008). Proliferation of differentiation assays were performed after dissociation of NSCs

to single cells, plating onto poly-L-lysine (Sigma) coated coverslips in 24-well plates at a density of 10^5 and further *ex vivo* culture for 2 or 3 days with or without GFs, respectively, in a 37° C humidified incubator with 5% CO2. The cells were maintained in suspension in full medium +growth factors as follows: 1:1 mixture of Dulbecco's modified Eagle's medium (1 g/liter d-glucose, l-glutamine, pyruvate; Sigma), F-12 nutrient mixture (Sigma) plus 20 ng/ml human epidermal growth factor (EGF; R&D Systems) and 20 ng/ml human basic fibroblast growth factor (R&D Systems), 20 μg/ml insulin (Sigma), 1× B27 supplement (Gibco), 0.25 mm l-glutamine, and 1% penicillin/streptomycin to promote the production of the neurospheres. The neurospheres were passaged 2–3 times before the assays. Differentiated neurosphere cultures were maintained in −growth factors conditions, the same as the full medium +growth factors without human EGF and basic FGF, in order to promote differentiation.

For shRNA knockdown studies, the small hairpin RNAs (shRNAs) against Lamp2a (two targets) and scrambled were cloned into the TRC2-pLKO.1 vector (Sigma) containing the U6 promoter, the selection marker puromycin, the woodchuck hepatitis post-transcriptional regulatory element and the EGFP sequence (kindly provided by Dr. Dermentzaki G.).

The sense/antisense primers that were used for each shRNA were as follows:

- pLKO LAMP2A (LV1) sense:

5’TGCAGTTGTGGCGATGATAATCAAGAGTTATCATCGCCACAACTGC TTTTTTC -3’

- pLKO LAMP2A (LV1) antisense:

5’TCGAGAAAAAAGCAGTTGTGGCGATGATAACTCTTGATTATCATCG CCACAACTGCA -3’

- pLKO LAMP2A (LV2) sense:

5’TGCGCCATCATACTGGATATTCAAGAGATATCCAGTATGATGGCGC TTTTTTC -3’

- pLKO LAMP2A (LV2) antisense:

5’TCGAGAAAAAAGCGCCATCATACTGGATATCTCTTGAATATCCAGT ATGATGGCGCA -3’

- pLKO scrambled sense:

5’TGCTGATTCCGCCTAAAGATTCAAGAGATCTTTAGGCGGAATCAGC -3’

- pLKO scrambled antisense:

5’TCGAGAAAAAAGCTGATTCCGCCTAAAGATCTCTTGAATCTTTAGG CGGAATCAGCA -3’

Viral transductions with lentiviruses expressing shSCRs, and shLAMP2A-LV1 and shLAMP2A-LV2 were performed overnight at a MOI of 10 in NSCs. Construction of the recombinant control (Ad-GFP) and LAMP2A (Ad-LAMP2A) overexpressing adenoviruses was performed using the pAd/PL-DEST Gateway vector (ViraPower Adenoviral Expression System, Invitrogen Life Technologies) as previously described (Stergiopoulos and Politis, 2016), using LAMP2A expressing vector (Xilouri et al., 2013). The generated adenoviral supernatants were used to infect primary NSCs for 6 hours at a multiplicity of infection (Klionsky et al.) of 10. For the overexpression of LAMP2A with AMAXA electroporations and transient transfection experiments, the coding sequence of rat LAMP2A was amplified with RT-PCR from the rat

adult brain (Xilouri et al., 2013) and then cloned into pCAGGs-IRES-GFP expression vector. The primers used for the RT-PCR are:

- For 5' GAGA-GAGCTC-AAG-ATGCGCCTCCTCTCTCCGGTTACGG 3'
- Rev 5' GAGA-GAGCTC-CTAAAATTGCTCATATCCAGTATGAT 3'

Empty pCAGGs-IRES-GFP vector was used as a control for the overexpression experiments. NSCs were transfected using an AMAXA electroporator (Lonza) with 6μg of plasmid DNA per electroporation, according to manufacturer's instructions (Kaltezioti et al., 2010, Kaltezioti et al., 2014). For the overexpression of NICD, NICD-myc (pCDNA3.1 vector) was used, kindly donated by Dr. T. Kadesch, the University of Pennsylvania, Philadelphia,PA). Transient transfections were performed with $CaCl_2$ with HEPES from Fluka as previously described (Foskolou et al., 2013).

Silencing of *Atg5* was performed using specific siRNAs purchased by IDT, (si*Atg5* #1, si*Atg5* #2, si*Atg5* #3). We have utilized 3 predesigned DsiRNAs against rat *Atg5* and a nontargeting scramble DsiRNA (Negative Control DsiRNA, scr) that has no known targets in human, mouse, or rat is used as control (Scr). All 3 *Atg5* DsiRNAs were mixed at a final concentration of 10nM and were transiently transfected in neurosphere cultures using AMAXA electroporation system. Cells were collected after 48 hrs. Silencing efficiency was assessed by immunoblotting.

- si*Atg5* #1*:* 5'- UUGUUUGCAUACCAAUAGACUGACUGU -3'
- si*Atg5* #2*:* 5'- UUGGUAAUGAUAAGGAAAAGCUACUGC -3'
- si*Atg5* #3: 5'- UAUCUCAUCCUAGAUAGAGAUAAAGCA -3'

Luciferase assays. Luciferase-reporter assays were performed with luciferase/β galactosidase kits (Promega) (Foskolou et al., 2013, Kaltezioti et al., 2014, Kaltezioti et al., 2010, Politis et al., 2008). For *Hes5*-Luc construct we have used 0.5 μg per transfection per well (cells plated in 12 well-plate at a density of 2 x10^5) and 1.5 μg of NICD-myc or LAMP2A-IRES-GFP or NICD mutant-myc and 0.15 μg of a b-galactosidase expression plasmid to normalize for transfection efficiency. All luciferase experiments were done in quadruplicate at least three times, and statistical analysis was performed by the paired two-sample Student's *t* test.

Intracellular protein degradation. Total protein degradation was measured by labeling the cells with 3H-leucine (2 mCi/ml) (Leucine, L-3,4,5, NEN-Perkin Elmer Life Sciences) using pulse-chase experiments as described previously (Vogiatzi et al., 2008). To discriminate the contribution of each type of autophagy to the degradation of the long-lived proteins, blockers of lysosomal proteolysis were used. In particular, the general lysosomal inhibitor NH_4Cl (20 mM) was used to assess total lysosomal proteolysis in NSCs. The inhibitor of phosphatidylinositol-3-kinase (PI3K) 3-methyladenine (10 mM, 3-methyladenine) was used to separate the percentage of total lysosomal degradation (NH_4Cl-sensitive) that occurs via macroautophagy (3-methyladenine-sensitive). The remaining lysosomal degradation (insensitive to 3-methyladenine) can be attributed to microautophagy and CMA. Because the contribution of microautophagy in total lysosomal proteolysis is considered minor and the chase is performed in serum-free conditions where CMA is induced, the proteolysis calculated by subtracting the 3-methyladenine-sensitive

from the NH_4Cl-sensitive proteolysis is considered relative CMA degradation (Kaushik and Cuervo, 2009, Patel and Cuervo, 2015). Moreover, we have shown that LAMP2A downregulation in neuronal systems results in a commensurate reduction of 3-methyladenine-insensitive degradation measured by this assay, indicating that the above represents mainly CMA-dependent degradation (Vogiatzi et al., 2008). Total radioactivity incorporated in cellular proteins was measured in a liquid scintillation counter (Wallac T414, Perkin Elmer) in triplicate samples per condition.

***In Situ* Hybridization on Cryosections.** Non-radioactive *in situ* hybridization on cryosections were carried out as previously described (Kaltezioti et al., 2014, Kaltezioti et al., 2010). The plasmid containing the sequence of mouse Hes5 mRNA for the preparation of the probe was kindly donated by Dr. A. Louvi. The RNA probe complementary to Hes5 mRNA was prepared and labeled with digoxinenin.

***In utero* electroporation (IUE).** IUE was performed in mouse embryos E14.5 as previously described (Kyrousi et al., 2015, Lv et al., 2014). Briefly**,** pregnant mice were deeply anesthetized with isoflurane. Then, 1-1.5μg of plasmids (1-2μg/μl), either empty pCAGGs-IRES-GFP for control or pCAGGs-IRES-LAMP2A for overexpression of LAMP2A, mixed with 0.01% Fast Green (Sigma), were microinjected into the lateral ventricle of the forebrain of E14.5 mouse embryos. Embryonic brains were electroporated using an electroporator (BTX ECM830) with five 40-V pulses (50 milliseconds duration; 950 milliseconds interval). After electroporation, the brain from the embryos was obtained at E16.5 and fixed for 5 hours in 4%PFA at 4° C. After dehydration

with 30% sucrose for 24 hours at 4° C, the brains were embedded in OCT compound and frozen. The tissues were cut coronally at 12 μm thickness and were used either for *in situ* or immunostaining experiments.

PCR-directed mutagenesis assay. To mutate the residues within the predicted motif to Ala, we used the Quikchange Lightning site-directed mutagenesis kit (Agilent Technologies) as per the manufacturer's instructions. The primers were as follows:

- FOR: 5'-gggaaccagagctggccatgcgccgccgcggccgcccccatggctcgagtctagag-3'
- REV: 5'-ctctagactcgagccatgggggcggccgcggcggcgcatggccagctctggttccc-3'

To ensure that errors were not introduced, the cDNA was fully sequenced.

Purification of Flag-tagged NICD protein. HEK293T cells were transiently transfected with plasmids encoding Flag-tagged NICD overexpression vector (Addgene, plasmid catalog #20183). Forty-eight hours following transfection, the cells were washed in cold PBS, and lysed for 20 min on ice in lysis buffer (20 mM Tris, ph 7.5; 150 mM NaCl; 1 mM EGTA, 10% glycerol, 1% Triton X-100) including protease and phosphatase inhibitor cocktails. Following lysis, one mg of clarified extract was incubated with 50 □l of anti-Flag resin (A-2220; clone M2, Sigma-Aldrich), previously equilibrated with lysis buffer, overnight at 4˚C under rotation. The following day, the beads were washed four times with lysis buffer, and eluted in three separate fractions of buffer containing an excess of 3X Flag peptide (125 □l each containing 200 □g/ml peptide diluted in 20 mM Tris, pH 7.4; 200 mM NaCl; 5 mM MgCl2;

0.02% Triton X-100; 1 mM DTT). The individual fractions were pooled and buffer exchanged to 10 mM Tris, pH 8, using 50 kDa MWCO microspin filters.

Isolation of lysosomes. Male Sprague Dawley rats (200-250 g) were fasted for 24 hours before sacrifice for lysosomal isolation. Brains were homogenized in 0.25 M Sucrose and isolation of lysosomes from a light mitochondrial - lysosomal fraction was performed with a discontinuous density gradient, as described (Storrie and Madden, 1990, Cuervo et al., 1997), using nycodenz, a non-ionic derivative of metrizoic acid, instead of metrizamide. Following isolation, lysosomal integrity was verified by measuring the activity of β-hexosaminidase and preparations with more than 10% broken lysosomes after isolation or more than 20% at the end of the incubation were discarded.

***In vitro* reconstitution of CMA.** Transport of human cell-produced NICD into isolated rat brain lysosomes was analyzed using an *in vitro* reconstituted system, as previously described (Cuervo et al., 2004, Xilouri et al., 2016a). Briefly, 2 μg of flag-tagged cell-produced NICD were incubated with freshly isolated whole brain lysosomes in MOPS buffer (10 mM 3-(N-morpholino) propanesulfonic acid (MOPS) pH 7.3, 0.3 M sucrose), in the presence of 0.6 μg recombinant HSPA8, for 20 min at 37°C. Where indicated, lysosomes were pre-incubated with a cocktail of proteinase inhibitors (PI) for 10 min at 0°C (Cuervo et al., 1997). block NICD uptake by CMA-active lysosomes, an excess amount (6 μg) of human recombinant alpha-synuclein (SNCA), a bona-fide CMA substrate, was added in the reaction mixture, in the absence of proteinase inhibitors. At the end of the incubation, lysosomes were collected by

centrifugation, washed and subjected to SDS-PAGE gel electrophoresis and immunoblotted for flag (tag for NICD), CATHEPSIN D, SNCA and TUBB.

Multimodal bioinformatics analysis for identifying KFERQ-like motifs. In an effort to identify a KFERQ-like motif in NICD as well as to investigate and determine the molecular, structural and physicochemical KFERQ likeness of the identified KRRRQ motif, we initiated a machine learning pipeline. Our approach was trained by establishing the physicochemical profiles of KFERQ and all known and established KFERQ-like motifs using the QSAR descriptor module of MOE (available from: https://www.chemcomp.com/Research-Citing_MOE.htm) (2013.08). Thus a decision support system (an algorithm) was calibrated that was capable of evaluating the KFERQ likeness of new candidate motifs, by including them in the analysis of the training dataset and determining whether the candidate motif, fall within the spectrum of physicochemical descriptors of the KFERQ and KFERQ-like motifs. Our pipeline is based on convolutional neural networks (deep learning) and data fusion as we included a total of 435 different physicochemical descriptors (dimensions) to be able to confidently quantify the KFERQ likeness of KRRRQ, while providing spatial and temporal analysis and data mining functionalities. The included motifs from literature are shown below:

KFERQ, RKVEQ, QEKRV, QDLKF, QRFFE, DRIKQ, IRDLQ, QDIRR, QEFVR, QKIIE, DLLRQ, QKDFR, DFRKQ, KDLLQ

At the last step all physicochemical profiles are converted into normalized percentages against the original KFERQ motif. This results in zeroing the KFERQ physicochemical profile on the plot and then the motifs appear as percentage of KFERQ-likeness with the ones closer to zero on the y-

axis (i.e. KFERQ) asserting a more KFERQ-like nature. KRRRQ is by far more KFERQ-like than most of the known and established KFERQ-like motifs.

Experimental design and statistical analysis

All experimental design are explained in each part of the section " materials and methods", respectively. The normal distribution of values was verified with the Shapiro–Wilk normality test using IBM SPSS Statistics for Windows, Version 20.0. To ensure the reproducibility of results, all experiments were performed independently three to four times as indicated in each figure legend. For statistical analysis all measurements and experimental values from independent experiments were estimated with two-tailed Student's t-test. All the results are shown as mean ± SD. The exact P values are described in each figure legend. P values < 0.05 are considered statistically significant. All analyses were done using Microsoft Excel 2013.

Results

LAMP2A expression is correlated to neuronal lineage in the developing cortex.

To examine the involvement of CMA in neural development, we initially investigated the expression pattern of LAMP2A in the embryonic cortex of mouse and rat brain (Fig. 1). For this purpose, we used an anti-LAMP2A antibody against a unique epitope of LAMP2A isoform that specifically recognizes this protein (Rothaug et al., 2015). Interestingly, higher expression levels of LAMP2A were observed in the mouse outer cortical layers (marginal zone, MZ) (i.e arrowhead in Fig. 1B), as compared to inner layers (ventricular zone, VZ) (i.e arrow in Fig. 1B). In particular, LAMP2A was mainly detected in TUBB3+ (βIII-TUBULIN+) neurons of the MZ (i.e brackets in Fig. 1C) and to a lesser extent in NESTIN+ neural stem/progenitor cells (NSCs) of the VZ (Fig. 2A-C). These data suggest that LAMP2A expression is associated with the induction of neuronal differentiation. Consistently, the expression domain of LAMP2A is gradually expanded as embryonic development proceeds from E12.5 to E17.5 and newly produced TUBB3+ neurons are generated and migrated towards the cortical plate (Fig. 1A-G). Similar expression pattern was observed in the rat cortex during embryonic development (Fig. 1H-L and Fig. 2C). Moreover, higher magnification analyses of the anti-LAMP2A immunostaining indicate typical punctuated lysosomal distribution of LAMP2A signal (i.e. inlets in Fig. 1E and Fig. 2D).

Next, we asked whether the CMA pathway is active in NSCs during embryonic development. To this end, we employed an *ex vivo* culture system

using NSCs derived from rat developing cortex, which have the ability to self-renew and proliferate, as well as to differentiate into neurons and astrocytes upon withdrawal of growth factors (GFs) (Kaltezioti et al., 2014, Kaltezioti et al., 2010, Politis et al., 2008). We first studied the expression of the two basic components of CMA, LAMP2A and HSPA8. Both components were highly expressed at the mRNA level as compared to the *Nestin* gene, a neural stem cell marker (Fig. 3A-B). We were also able to detect expression at the related proteins (Fig. 3C and Supplementary Fig. 1C, D), although at a lower expression level as compared to the adult cortex, a brain region previously reported to exhibit enhanced CMA activity (Brekk et al., 2018, Xilouri et al., 2016a, Xilouri and Stefanis, 2015, Orenstein et al., 2013). These data raise the possibility that the CMA pathway is also active in NSCs. Indeed, by measuring the lysosomal-dependent proteolysis with a pulse-chase assay, we showed that CMA is active in NSCs, at levels almost as high as macroautophagy (Fig. 3D). Interestingly, although it is well-established that macroautophagy critically regulates neural differentiation (Fimia et al., 2007, Lv et al., 2014, Wu et al., 2016), the involvement of CMA in the differentiation of NSCs is unknown. The observation that CMA is highly active in NSCs and the *in vivo* immunostaining data (Fig. 1), implied a regulatory action in neuronal differentiation. To initially address this, we examined the expression pattern of LAMP2A in neural cell types, derived from *ex vivo* cultured NSCs. In agreement with the *in vivo* results, these experiments displayed higher expression of LAMP2A in TUBB3+ neurons, compared to GFAP+ astrocytes (Fig. 3G, H, I), and lower expression in NESTIN+ or SOX2+ proliferating NSCs (Fig. 3E, F, I). Collectively, these data suggest a regulatory role of the CMA machinery in NSC differentiation towards neuronal fate. Moreover, co-stainings with the LAMP1 lysosomal marker

showed extended co-localization with the signal from the anti-LAMP2A antibody in ex vivo cultured NSCs (Supplementary Fig. 1B-C), further confirming our antibody specificity. Collectively, these data suggest a regulatory role of the CMA machinery in NSC differentiation towards neuronal fate.

LAMP2A is necessary and sufficient to induce differentiation of NSCs towards TUBB3+ neurons.

To test this hypothesis, we performed lentiviral-mediated shRNA knockdown of LAMP2A with two different target sequences targeting the rat *Lamp2a* mRNA (Fig. 4A-C). Remarkably, under differentiation conditions of *ex vivo*-cultured NSCs [3 days in vitro (DIV) in a conditional medium without growth factors], shRNA-mediated knockdown of LAMP2A (LV1) caused a significant reduction in the number of TUBB3+ neurons, which indicates that LAMP2A deficiency impairs neuronal differentiation (Fig. 4D, E). The same effect of LAMP2A knockdown on neuronal differentiation was observed with the second shRNA construct (LV2) (shSCR 10.18 ±1.2, shLV2 6.86 ±2.2, $P<0.001$). Conversely, the numbers of GFAP+ astrocytes were slightly increased, whereas no differences in NESTIN+ NSCs and RIP+ oligodendrocytes were observed (Fig. 4F-K). In addition, to test whether the reduction in TUBB3+ cells was due to shRNA-induced apoptosis, we investigated its effect on the activated CASPASE 3 marker for cell death as well as on Ethidium Homodimer (EthD-1) fluorescence marker for dead cells. No significant changes were noticed in these cell death indices (Fig. 4L-O). We further examined the correlation between the reduction of TUBB3+ neurons and apoptosis each day during the differentiation

protocol after lentiviral infection. Neuronal cells were significantly decreased only 3 days after lentiviral infection, whereas activated CASPASE 3 was slightly increased during the second day of the time-course experiment (Fig. 4P, Q). In this time interval, double TUBB3/activated CASPASE 3 immunostainings indicated that this increase was not due to the death of TUBB3+ neurons (Fig. 4R). Taken together, these results demonstrate that LAMP2A is required for neuronal differentiation of NSCs.

We next addressed whether LAMP2A overexpression is sufficient to affect differentiation towards the neuronal phenotype. AMAXA electroporation in *ex vivo*-cultured NSCs using a LAMP2A expression plasmid, revealed a significant induction in the number of TUBB3+ neurons, as well as a slight decrease in astrogliogenesis (Fig. 5A-C), in agreement with the shRNA data. Similarly, adenoviral-mediated overexpression of LAMP2A, previously shown to induce CMA activity (Han et al., 2017, Issa et al., 2018, Saha, 2012, Xilouri et al., 2013) was adequate to enhance neuronal differentiation of NSCs (Fig. 5D-I). Overall, these data suggest that LAMP2A and consequently CMA pathway are sufficient and necessary for the induction of neuronal differentiation of NSCs.

LAMP2A suppresses NOTCH1 signaling pathway to induce neuronal differentiation.

To explore the possible mechanism of CMA action on the induction of neuronal lineage progression, we examined the effect of LAMP2A overexpression on various molecular markers, characteristic for the transition of NSCs from progenitor cell stage to post-mitotic neuron. Interestingly, adenoviral-mediated overexpression of LAMP2A induced *NeuroD1* and *Rbfox3* (*NeuN*)

neuronal markers, and down-regulated *Foxg1*, *Pax6*, *Tbr2* and *Ngn2* intermediate neuronal progenitor markers (Fig. 5J). A subset of these genes was also affected by the shRNA-mediated knockdown of the *Lamp2a* gene (Supplementary Fig. 2). Most importantly, a major reduction was observed on the mRNA levels of *Sox2* and *Hes5* genes, which are markers for self-renewing NSCs. These observations indicate the involvement of LAMP2A and by extension of CMA in the suppression of NSC identity and consequently induction of their neuronal differentiation. Since down-regulation of *Sox2* and *Hes5* genes is one of the earliest events marking the initiation of neurogenesis (Amador-Arjona et al., 2015, Packard et al., 2016), we hypothesized that LAMP2A may directly affect the expression of these genes to induce neuronal differentiation.

To explore this scenario, we first tested whether CMA degradation pathway directly affects the stability of SOX2 protein. It has been previously shown that SOX2 transcription factor is able to bind and activate the transcription of its own gene by a positive feedback loop (Boyer et al., 2005, Kim et al., 2008). Therefore, we wanted to examine whether CMA directly targets SOX2 protein and consequently disrupts its feedback loop, which could also explain the observed reduction of *Sox2* mRNA levels (Fig. 5J). Such a hypothesis would predict that down-regulation of protein expression will precede the reduction of mRNA levels. However, we were not able to observe such discrimination during the time-course of adeno-viral mediated LAMP2A infection experiment (Fig. 6A). Both mRNA and protein levels were similarly reduced as early as 24 hours after initiation of the experiment. Furthermore, LAMP2A overexpression was not sufficient to target exogenously expressed SOX2 protein by a CMV promoter-driven construct (Fig. 6B). These data

suggest that SOX2 protein is not directly targeted for degradation by the CMA pathway.

Next, we investigated whether NOTCH1 signaling pathway is regulated by LAMP2A modulation, since *Sox2* is directly regulated at the transcriptional level by NOTCH1, and *Hes5* is a downstream effector of this pathway (Yan et al., 2009, Yoon and Gaiano, 2005). Consistent with this scenario, LAMP2A overexpression was sufficient to impair the well-established ability of constitutively active NOTCH1 isoform [Notch1-intracellular domain (NICD)] to transactivate the *Hes5* promoter (Fig. 6C, D). Moreover, adenoviral-mediated LAMP2A overexpression significantly reduced the endogenous NICD protein levels in NSCs (Fig. 6E, F), suggesting that CMA pathway targets NICD at the protein level. In agreement, *Notch1* mRNA levels were not decreased but were significantly increased, possibly due to a feedback cellular response to the reduced NICD protein levels (Fig. 6G).

To further investigate this effect of LAMP2A on NICD protein, we tested whether the CMA pathway significantly contributes to NICD protein degradation. To this end, we applied selective inhibitors of lysosomal and proteasomal pathways in *ex vivo* cultured NSCs. First, we showed that inhibition of total lysosomal activity by NH_4Cl caused dramatic accumulation of endogenous NICD protein as compared to control conditions (ctr), whereas inhibition of proteasomal activity by epoxomicin did not have any effect (Fig. 6H, I). These data suggest the involvement of lysosomal-dependent pathways in NICD degradation. However, taking into consideration that macroautophagy and CMA are the two main lysosomal degradation systems, we next applied on NSCs the selective inhibitor for macroautophagy 3 methyl-adenine (3MA) to discriminate between these two pathways. Conversely to the outcome of the

NH_4Cl inhibitor, in 3MA-treated cells NICD protein was not increased, suggesting a role of CMA pathway in the degradation of NICD (Fig. 6H, I). Furthermore, under the same experimental conditions, there were no CMA-dependent differences on Sox2 protein levels (Supplementary Fig. 3), confirming our previous findings on the indirect effect of LAMP2A on *Sox2* gene expression. In agreement with the observations about NICD, molecular inhibition of macroautophagy accompanied by significant reduction of LC3 II levels via siRNA-mediated knock-down of *Atg5*, had no effect on the protein levels of NICD (Fig. 6J).

Given that CMA substrates are recognized and bound by the HSPA8, the LAMP2A interacting partner in CMA protein machinery, we wanted to examine whether endogenous NICD is co-localized with HSPA8 and/or LAMP1 lysosomal marker. Accordingly, immunostainings in NSCs indicate that NICD with HSPA8 or LAMP1 proteins are distributed in the same sub-cellular compartments with a high degree of co-localization (Pearson correlation coefficiency value for HSPA8 and LAMP1 are 0.685±0.033 and 0.545±0.07, respectively) (Fig. 7A). To confirm that NICD is a CMA substrate, we proceeded with the gold standard method used for in vitro reconstitution of CMA activity (Juste and Cuervo, 2019, Klionsky et al., 2016). To that end, cell produced human flag-NICD (overexpression in human HEK293T cells) was first purified and then incubated, in the presence of recombinant HSPA8, with lysosomes isolated from adult rat brain, in the presence (+) or absence (-) of protease inhibitors. Immunoblot analysis indicates that flag-NICD was efficiently bound to and uptaken into the lysosomes through the CMA degradation pathway (Fig. 7B). In the presence of protease inhibitors reduced ability of degradation of NICD was observed, further suggesting that NICD is a CMA substrate. By this

well-established method we clearly show that NICD can be translocated and degraded into lysosomes via a CMA-dependent mechanism (Vogiatzi et al., 2008).

Next, we asked whether NOTCH1 protein contains a KFERQ-like motif in its amino acid sequence, which is recognized by the HSPA8 and mediates the localization of the targeted proteins to the lysosomal membrane (Cuervo, 2010, Kaushik and Cuervo, 2012, Park et al., 2016, Catarino et al., 2017). This motif is characterized by one or two positively charged residues (K, R), one or two hydrophobic residues (I, L, V, F), one of the negatively charged residues D or E, and one glutamine (Q) on either side of the pentapeptide (Cuervo, 2010, Kaushik and Cuervo, 2012, Park et al., 2016, Catarino et al., 2017). To this end, we thoroughly searched the amino acid sequence of the full length human NOTCH1 protein for a possible KFERQ-like motif. However, we were not able to identify a typical KFERQ-like motif based on these criteria. Nevertheless, based on the in vitro reconstitution lysosomal activity assay (Fig. 7B), we examined whether we could find an atypical CMA recognition motif, bearing similar physicochemical properties to KFERQ-like motifs. Our methodology for identifying the existence of this potential motif(s) was based on a multidimensional convolutional neural network that is capable of analyzing more than 435 physicochemical properties. This algorithm has been custom-developed for this study (see Materials and Methods) and was used to analyze all available pentapeptide combinations on the full length NOTCH1 using a sliding window approach. Consistent with a direct effect of CMA on NICD, we bioinformatically located a single atypical motif specifically at the beginning of the NICD protein with the sequence KRRRQ (Fig. 7C). In particular, our newly identified motif is distributed close to the original KFERQ motif in a KFERQ likeness plot (Fig. 7D), indicating highly

similar molecular, physicochemical and structural properties. In most cases, it is also distributed closer to the KFERQ motif than 10 (out of 13) other motifs that have been previously reported to function as KFERQ-like motifs and targeted by the CMA pathway (Fig. 7D). In agreement with this analysis, the KRRRQ motif is highly conserved among different vertebrate species, indicating its evolutionary importance and a possible conservation in the regulation of NOTCH1 at the protein degradation level (Fig. 7C).

We subsequently mutated this motif by replacing all five CMA-related amino acids with alanine, a residue with no charge (mutated NICD) and confirmed the ability of this construct to function as a constitutively active form of NOTCH1 on *Hes5* promoter (Fig. 8A). Interestingly, the mutated NICD was more efficient in *Hes5* promoter transactivation assay as compared to WT NICD, implying the involvement of this motif in NOTCH1 signaling activation, probably due to avoidance of CMA-dependent degradation system. Consistently, LAMP2A was not sufficient to impair the *Hes5* promoter transactivation by NICD bearing the mutated motif as compared to NICD with the WT motif (Fig. 8B). In agreement, by applying the autophagic inhibitors in exogenously supplied NICD with either WT or mutated CMA-targeting motif, we showed that KRRRQ motif is responsible for the lysosomal-mediated degradation of NICD via the CMA pathway (Fig. 8C, D). We initially confirmed that accumulation of exogenously applied WT NICD is induced by inhibiting total lysosomal activity with NH_4Cl but not by inhibiting macroautophagy with the specific inhibitor 3MA (Fig. 8C), in a manner similar to the endogenous NICD (Fig. 6H, I). In agreement, the NICD version with mutated KRRRQ motif did not follow the same CMA-dependent pattern of accumulation upon application of autophagic

inhibitors (Fig. 8D), indicating that this motif is required for NICD degradation through the CMA pathway.

In addition, to evaluate whether the observed LAMP2A effect on inducing neuronal differentiation is mediated by its regulatory action on NICD degradation, we performed overexpression experiments with both factors in NSCs. The aim of these experiments was to test whether overexpression of WT NICD is able to rescue the effect of LAMP2A on neuronal differentiation. We initially confirmed that under our experimental conditions (ratio of NICD vs LAMP2A vectors = 2/1) all LAMP2A-IRES-GFP positive cells were also positive for exogenously supplied NICD-myc (Fig. 9A). More importantly, overexpression of NICD together with LAMP2A was sufficient to totally rescue the effect of LAMP2A on neuronal differentiation (Fig. 9B, C).

To elucidate the *in vivo* role of LAMP2A in cell fate decisions and NOTCH1 signaling during embryonic development, we performed *in utero* electroporation experiments (IUE). To this end, we injected LAMP2A-overexpressing or control plasmids in the developing cortex of E14.5 mouse embryos (Fig. 10A-C). Both plasmids expressed GFP reporter gene and therefore we could specifically monitor the electroporated cells during the migration from the VZ towards the outer cortical layers (two days later, E16.5) (Fig. 10B, C). Interestingly, and in accordance to our previous *ex vivo* results (Fig. 6A), there was a significant decrease of Sox2 protein levels in the LAMP2A overexpressing cells as compared to the control embryos (Fig. 10D, E). In our previous analysis we showed that LAMP2A mediated reduction of SOX2 expression is probably due to impaired NOTCH1 signaling. To confirm this in an *in vivo* setting, we performed *in situ* hybridization stainings for *Hes5* mRNA to address whether LAMP2A is sufficient to counteract NOTCH1 pathway. In agreement, *Hes5*

mRNA levels, which were specifically expressed in the VZ at E16.5 stage of the embryonic cortex (Ohtsuka et al., 1999, Zhang et al., 2009), were strongly decreased upon LAMP2A overexpression (Fig. 10F, G). These results further validate our suggested mechanism of LAMP2A action, as its *in vivo* overexpression significantly decreases the downstream effectors of NOTCH1 signaling pathway, *Hes5* and *Sox2*.

Discussion

During cortical development an intricate network of interactions between protein molecules, complexes and pathways regulates the acquisition of neural cell fates. Autophagic pathways play significant roles in these regulatory cascades through the degradation of unwanted proteins to maintain cellular homeostasis and differentiation potential (Cecconi and Levine, 2008). For many of these proteins post-translational availability is essential to be controlled in a spatiotemporal manner, especially during cell differentiation and/or embryonic development. Regarding the autophagic pathways in brain development, it has been recently shown that macroautophagy is critically involved in cortical neurogenesis. Knockdown experiments of *Atg5*, a gene encoding an essential protein for the formation of autophagosomes, led to an increase in the number of neural progenitor cells and inhibition of differentiation during cortical development. Additionally, suppression of *Atg5* resulted in dendritic and axonal morphological impairments (Lv et al., 2014, Wu et al., 2016). Consistently, Fimia G. M. et al. showed that genomic ablation of macroautophagy-related genes resulted in the aberrant formation of the nervous system and unbalanced cell proliferation during development of the mouse embryo (Cecconi and Levine, 2008, Fimia et al., 2007, Srivastava et al., 2012, Nimchinsky et al., 2001, Lee et al., 2013). In addition, macroautophagy is strictly connected to apoptosis during the early stages of brain morphogenesis (Chung and Yu, 2013, Biebl et al., 2000). In contrast to the wealth of information on the role of macroautophagy in neural development, prior to our study, the involvement of CMA remained unclear.

In this thesis, we provide functional evidence that the CMA protein degradation pathway is essential for the determination of NSC's fate. In particular, we first showed that the CMA pathway is highly active in NSCs. Moreover, LAMP2A, which constitutes the principal limiting component of the CMA pathway (Kaushik et al., 2011, Jacob et al., 2017), is expressed in mouse and rat cortex during embryonic development and is mainly associated with the neuronal lineage. Most importantly, it is involved in the acquisition of early neuronal identity, indicating a significant role for this degradation system in cortical development. More specifically, we demonstrate that LAMP2A protein is required for differentiation of NSCs towards TUBB3+ neurons in *ex vivo* differentiation assays. These data indicate a functional role of the CMA pathway in neural differentiation and brain development.

Interestingly, the CMA pathway has not been previously correlated with brain development. It had only been studied in correlation to neurodegeneration. Specifically, a number of elegant studies support the idea that dysregulation of the CMA pathway plays a crucial role in neurodegeneration. In particular, recent evidence suggests that an impairment of CMA activity is detected in human neurodevelopmental diseases, and may contribute to their onset and progression. Most of the evidence is a result of studies on Parkinson's disease (Campbell et al., 2018). Accumulation of pathogenic CMA substrate proteins such as α-synuclein, in the form of insoluble inclusions, is a common hallmark underlying the degenerative process of many diseases, such as Parkinson's disease and certain tauopathies (Wang and Mao, 2014, Sala et al., 2016, Caballero et al., 2018). Although it is not clear whether CMA dysfunction may contribute to the initial formation of insoluble inclusions, it is quite possible that the "blockage effect" on CMA may exacerbate the formation of inclusion bodies by increasing

misfolded protein concentrations in the cytoplasm. This may result in a toxic effect on the cell, leading to neuronal death (Vogiatzi et al., 2008, Martinez-Vicente et al., 2008, Cuervo et al., 2004). It has also been reported that CMA activity is downregulated in Parkinson's disease and Alzheimer's disease, whereas the opposite is observed in Huntington's disease (Wang and Mao, 2014). This variation suggests the complicated role of this autophagic pathway in neuro-pathological conditions (Xilouri and Stefanis, 2016, Vogiatzi et al., 2008, Martinez-Vicente et al., 2008, Alvarez-Erviti et al., 2010, Xilouri et al., 2016b).

These pieces of evidence suggest that CMA activity may be deregulated in neurodegenerative diseases and could be associated with aged-related disorders. As aging is the main risk factor associated with PD and other neurodegenerative age-related diseases, it would be very important to assess whether alterations in CMA activity are taking place in the aged brain and whether brain areas affected in PD, such as the substantia nigra, exhibit lower LAMP2A (and/or Hsc70) levels compared to others that are spared. Therefore, considering that CMA activity is reduced with age (Alfaro et al., 2018, Xilouri and Stefanis, 2016), it is tempting to argue that a decline in CMA activity during aging can be a risk factor for the development of neurodegenerative disorders associated with adult and senior people. These data indicate the importance of CMA on brain physiology over the course of time, further strengthening the novelty and importance of our findings regarding its role during the early stages of brain development. For example, it would be very interesting to investigate whether a developmental impairment of CMA pathway may contribute to neurological and other brain related diseases.

Interestingly, previous studies suggest that the LAMP2 gene is correlated with neuronal deficiencies and intellectual dysfunction in the human brain. It has

been reported that mutations on the *LAMP2* gene, mainly affecting mRNA splicing, can cause Danon disease, which is characterized by mental retardation and other symptoms (Majer et al., 2014, Yang et al., 2010). In addition, the *LAMP2* gene has been identified in a large scale human exome sequencing as one of the genes associated with X-linked intellectual disabilities (Piton et al., 2013). These reports are consistent with our findings in rodent embryonic cortex, concerning the necessity of LAMP2A for neural differentiation. To further elucidate the neuropathology of neurodevelopmental disorders such as Danon disease, previous studies used as a model LAMP2-deficient mice. Histological and behavioral analyses of the adult mice revealed wide spread astrogliogenesis in the CNS as well as behavioral anomalies (Rothaug et al., 2015). Taken together, these data are in good agreement with our observations and further support our hypothesis that the LAMP2A receptor and consequently CMA is critically implicated in the early stages of neurodevelopment.

In this study, we identified LAMP2A as a critical regulator of *Sox2* expression and NOTCH1 signaling, two major suppressors for the initiation of neurogenesis in NSCs (Androutsellis-Theotokis et al., 2006, Ahmed et al., 2009, Artavanis-Tsakonas et al., 1999, Wang et al., 2009a, Corbin et al., 2008, Favaro et al., 2009). NOTCH1 activity is strongly associated with the control of proliferation, differentiation and apoptosis thus affecting morphogenesis of different organs, including the nervous system. Concerning neural development, NOTCH1 is a master regulator of the balance between stemness and neuronal differentiation. Due to its vital role in neural cell fate acquisition, NOTCH1 activation is a highly regulated process at multiple levels and consists in an extremely conserved molecular mechanism. The functions of NOTCH signaling during embryonic brain development have been extensively investigated

(Shimojo et al., 2008, Kageyama et al., 2008, Imayoshi and Kageyama, 2011). Loss of the essential NOTCH signaling components in the developing brain results in proliferation defects and premature neuronal differentiation of embryonic NSCs. Similarly, loss of NOTCH ligand Jagged1 during hippocampal development leads to defects in proliferation and stem cell maintenance (Lavado and Oliver, 2014, Breunig et al., 2007). Therefore, the main function of the NOTCH pathway in embryonic NSCs is to maintain their proliferative and undifferentiated state.

Up to now, there have been many studies reporting and investigating the effect of macroautophagy on NOTCH signaling pathway, with interesting findings about the impact of the first on the degradation of NOTCH1 protein. These studies reveal a dynamic effect of autophagy on cell fate during different developmental stages (Wu et al., 2016, Barth and Kohler, 2014). Despite the known so far regulation of NOTCH signaling by macroautophagy, the possible implication of CMA on this spatiotemporal expression balance remained elusive.

Here, we propose that CMA modulates the equilibrium of NICD protein levels in NSCs to relieve the negative action of NOTCH1 signaling on the initiation of neuronal differentiation. In particular, we show that induction of the activity of the CMA pathway by LAMP2A overexpression is sufficient to strongly reduce *Sox2* expression and NOTCH1 signaling activity in *ex vivo* cultured NSCs as well as *in vivo,* in the mouse developing cortex. By a series of biochemical experiments and transcriptional assays, we first excluded a direct effect of CMA on SOX2 protein and consequently demonstrated that CMA directly targets the activated form of NOTCH1, e.g. NOTCH1 intracellular domain. Thus, the observed alteration in Sox2 expression could be due to the suppression of NSC identity by the direct action of CMA pathway on NICD.

Next, we investigated whether NOTCH1 protein is a direct target of CMA pathway. It is now well-established, that proteins degraded by CMA need to be specifically recognized by HSPA8 protein through their KFERQ domain, thus CMA can be considered a selective protein degradation process (Kaushik and Cuervo, 2012). An initial analysis indicated that at least 30% of cytosolic proteins contain CMA KFERQ-like motifs, a group of mainly long-lived proteins that are degraded upon serum starvation or amino acid withdrawal (Cuervo et al., 1995). In addition, the selective pool of proteins degraded by CMA would also be associated with certain functions capable of overcoming metabolic changes in response to starvation. This has been observed in the regulation of glycolytic flux, through the degradation of glycolytic enzymes by CMA, in order to protect cells from apoptosis. On the other hand, proteins that do not contain KFERQ-like regions would most likely be protected against CMA-degradation, to sustain the critical functions of cells under nutritional stress. Additionally, one cannot exclude the possibility that post translational modifications may intervene with the quaternary structure of the protein, thus modifying the exposed or hidden possible KFERQ-like motifs of the sequence (Martinez-Vicente et al., 2008). Therefore, the protein of interest can be differentially degraded depending on the spatiotemporal structural modifications that it has undergone.

Taking this information into consideration and based on our results, we wanted to examine the possible direct effect of the CMA degradation pathway on NICD regulation. Interestingly, we identified a KFERQ-like motif in the NICD amino acid sequence. To confirm that NICD is a direct CMA substrate, firstly we showed that NICD is co-localized at the same cellular compartments with HSPA8, the mediator of the CMA target binding, and secondly that it can be degraded by an *in vitro* system of isolated lysosomes, in a CMA-dependent

manner. Mutation of the KFERQ-like motif sequence by substituting its amino acids with five alanines resulted in significant impairment in the ability of the CMA pathway to degrade NICD, further indicating a direct effect of CMA on NICD. In agreement, we also showed that LAMP2A is able to exert a negative effect on NOTCH1 signaling *in vivo* during mouse cortical development. We therefore suggest that CMA affects neuronal differentiation through the regulation of NOTCH1 signaling. In support of this mechanism, overexpression of constitutively active NOTCH1 was sufficient to rescue the action of LAMP2A on neuronal differentiation. Taken together, our results unveil a novel regulatory role of the CMA pathway in NSC differentiation during neurodevelopment. For the first time, we suggest how CMA is implicated in the degradation of such a multifunctional key player as NOTCH1 protein, thus affecting the balance of NSC fate and consequently brain physiology.

Moreover, recent reports have established a significant link between CMA and cancer. In particular, a proteomic analysis of isolated lysosomes in cancer cells during CMA-activated condition was performed, leading to the identification and categorization of proteins of multiple cellular pathways that were specifically targeted by CMA. These results along with integrated bioinformatics analyses showed that upon CMA activation multiple cellular pathways, which account for the most energy-consuming cellular mechanisms, were affected. This research resulted in the implication of CMA with metabolic pathways, targeting multiple proteins involved in cellular translation processes for degradation. In particular, several proteins of the translation initiation complex were identified as ”bona fide” CMA substrates in multiple cancer cell lines of distinct origin where CMA suppresses cellular translation. Additionally, the identified CMA substrates displayed high expression in multiple primary

cancers compared to their normal counterparts (Hao et al., 2019, Tang et al., 2017). Although whether activating or inhibiting CMA pathway would be the best strategy to treat cancer is still debated, targeting this pathway's substrate proteins provides a novel direction and a promising field for the development of a new anticancer therapeutic approach.

NOTCH signaling is also broadly correlated to cancer, with context-dependent functions in respect to its ability to promote or inhibit tumorigenesis. Remarkably, the positions, identities, and effects of NOTCH mutations are cancer-specific and reflect varied roles for NOTCH in different cancer contexts, possibly due to its effect on regulating multiple and complex cellular mechanisms (Aster et al., 2017). These findings together, indicate that there is a possible correlation of the CMA degradation pathway and the regulation of NOTCH signaling under disease conditions. Our data strengthen this possibility, unraveling for the first time how this selective degradation mechanism may affect such an abundant cellular signaling pathway. Conclusively, we would like to propose the possibility that part of the important roles of CMA in the physiology and/or homeostasis of other tissues and cancer may be mediated via its ability to intervene to NOTCH1 signaling.

To conclude, this thesis contributes to the perspective that, in the future, CMA could be a possible therapeutic target for neurodegenerative diseases and some types of cancer, while we show for the first time its important regulatory role in brain development, suggesting an additional link to neurodevelopmental disorders. As summarized above, increased or restored CMA activity could be protective in several pathological conditions. Combination of different types of approaches, including genetic methods and CMA-modulating drugs, should be useful to reveal additional mechanisms by which CMA dysfunction may trigger

pathogenesis and enable the dissection of the specific steps of CMA which are dysfunctional in the pathogenic process (Chaperone-mediated autophagy: roles in neurodegeneration) Thorough studies are needed to further evaluate and determine whether enhancing CMA activity or preventing CMA blockage thus improving CMA throughput, particularly in the brain, can provide substantial therapeutic benefits for neurodevelopmental and neurodegenerative diseases and have value in anticancer treatment.

Figures

Figure 1

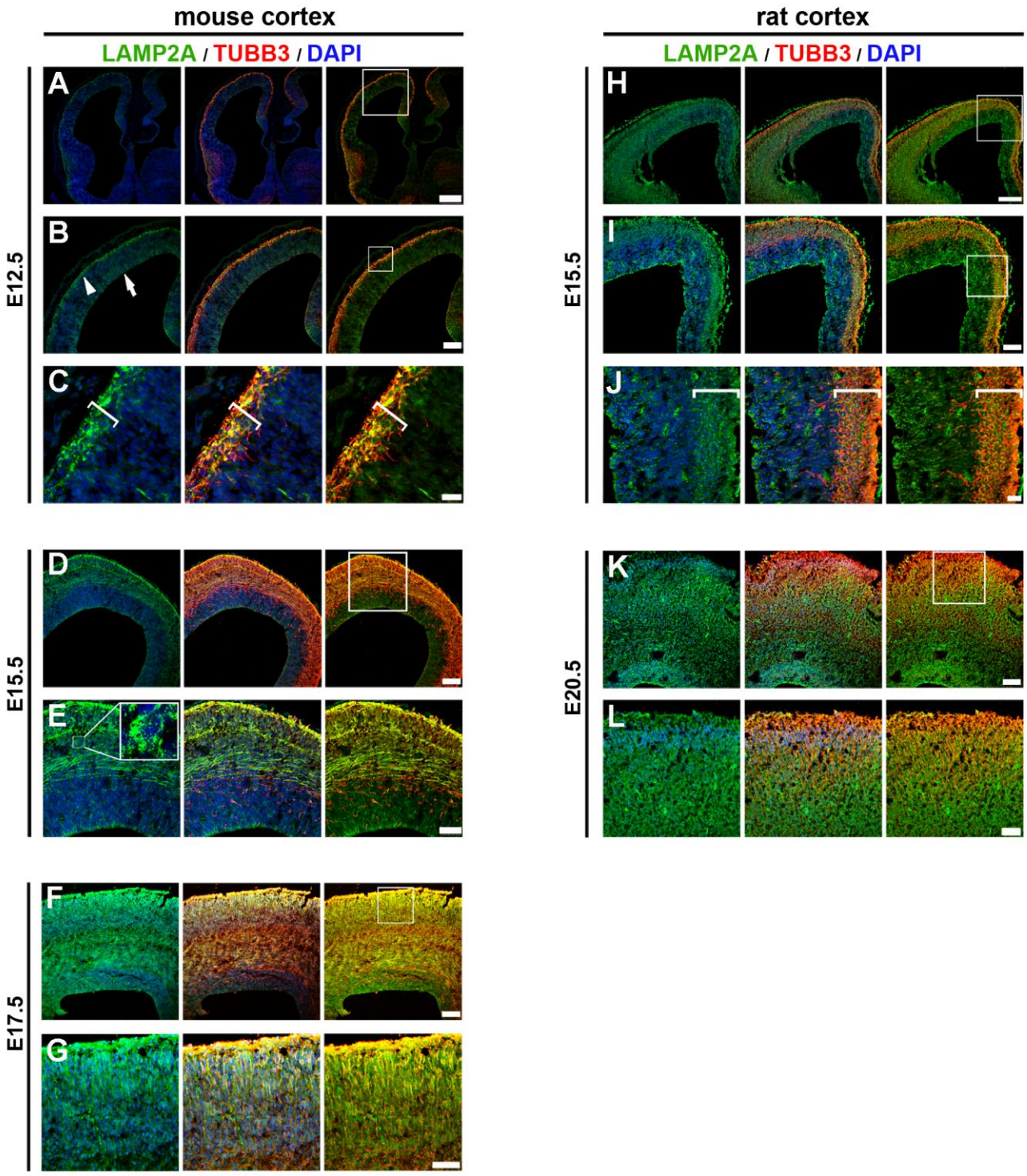
mouse cortex
rat cortex
LAMP2A / TUBB3 / DAPI
LAMP2A / TUBB3 / DAPI
E12.5
E15.5
E15.5
E20.5
E17.5
A
B
C
D
E
F
G
H
I
J
K
L

Figure 1. LAMP2A expression pattern is associated with the neuronal lineage during cortical development.

(**A-L**) Double immunostainings of LAMP2A and TUBB3 (βIII-TUBULIN, red) on cryosections from mouse embryonic cortex E12.5 (Klionsky et al.), E15.5 (**D, E**), E17.5 (**F, G**) and rat embryonic cortex E15.5 (**H-J**), or E20.5 (**K, L**), as indicated. Control immunostainings without primary antibody show no staining (Supplementary Fig. 1B). Boxed areas are represented underneath with higher magnification. Arrowhead in B indicates the expression of LAMP2A at the outer cortical layers of the marginal zone, while arrow in B indicates the lower expression levels of LAMP2A at the ventricular zone. Inlet of E represents higher magnification of the squared shape of the same image. Cell nuclei were visualized with DAPI.

Scale bars: (**A, H**) 250 μm; (**B, D, F, I, K**) 100 μm; (**C, J**) 25 μm; (**E, G, L**) 50 μm.

Figure 2

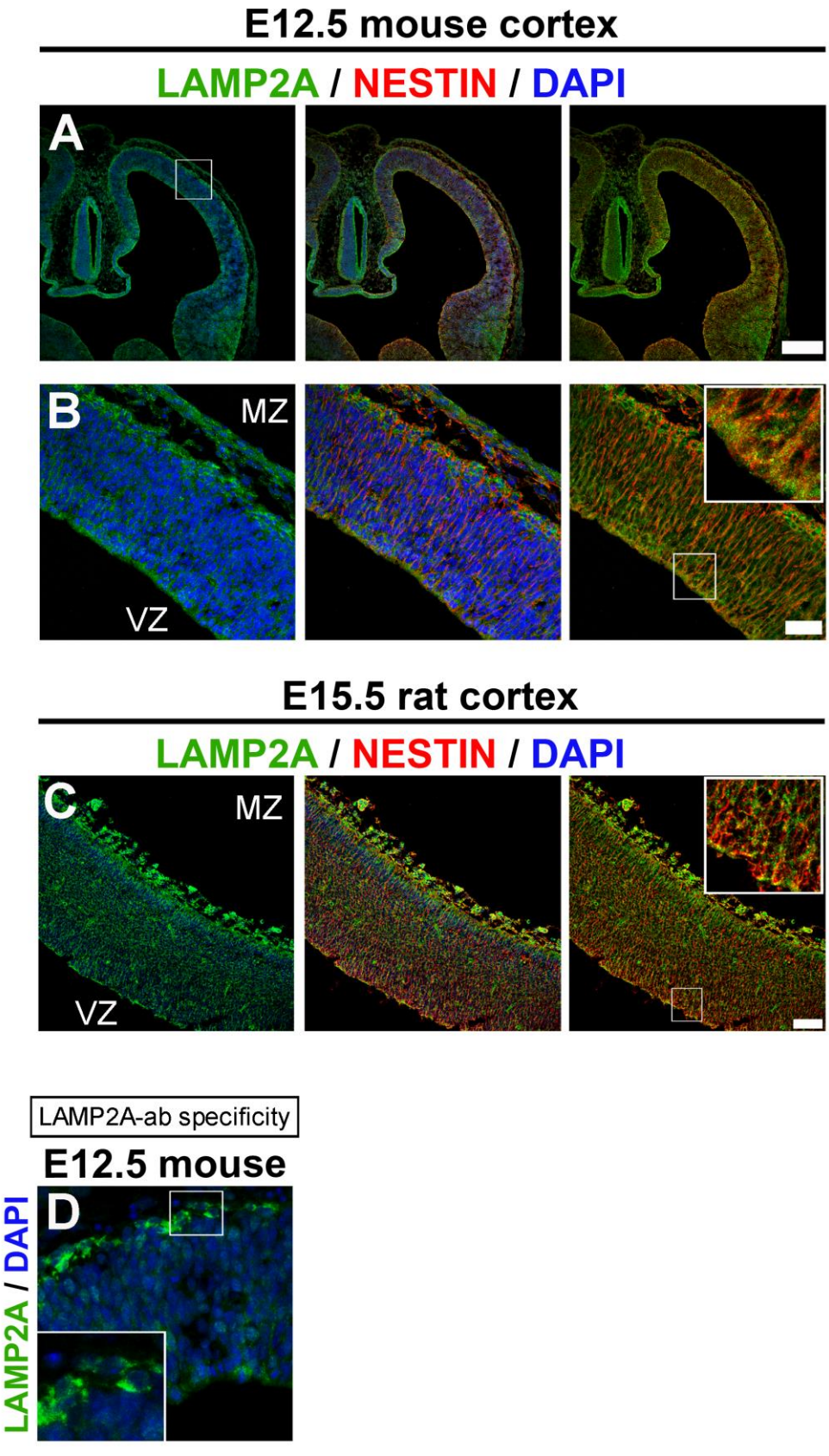
E12.5 mouse cortex
LAMP2A / NESTIN / DAPI
A
B
MZ
VZ
E15.5 rat cortex
LAMP2A / NESTIN / DAPI
C
MZ
VZ
LAMP2A-ab specificity
E12.5 mouse
D
LAMP2A / DAPI

Figure 2. LAMP2A expression pattern in mouse and rat embryonic cortex.

(**A-C**) Double immunostainings of LAMP2A and NESTIN (red) on cryosections from mouse embryonic cortex E12.5 (**A, B**) and rat embryonic cortex E15.5 (**C**). VZ, ventricular zone; MZ, marginal zone. Inlets of B and C represent higher magnification of the squared shapes.

(**D**) Larger magnification of the LAMP2A immunostaining micrograph presented in Fig. 1B (mouse E12.5 embryonic cortex). Inlet represent higher magnification of the squared shape to indicate the typical punctated lysosomal distribution of LAMP2A.

Scale bars: (**A**) 250 μm, (**B**) 50 μm, (**C**) 75 μm

Figure 3

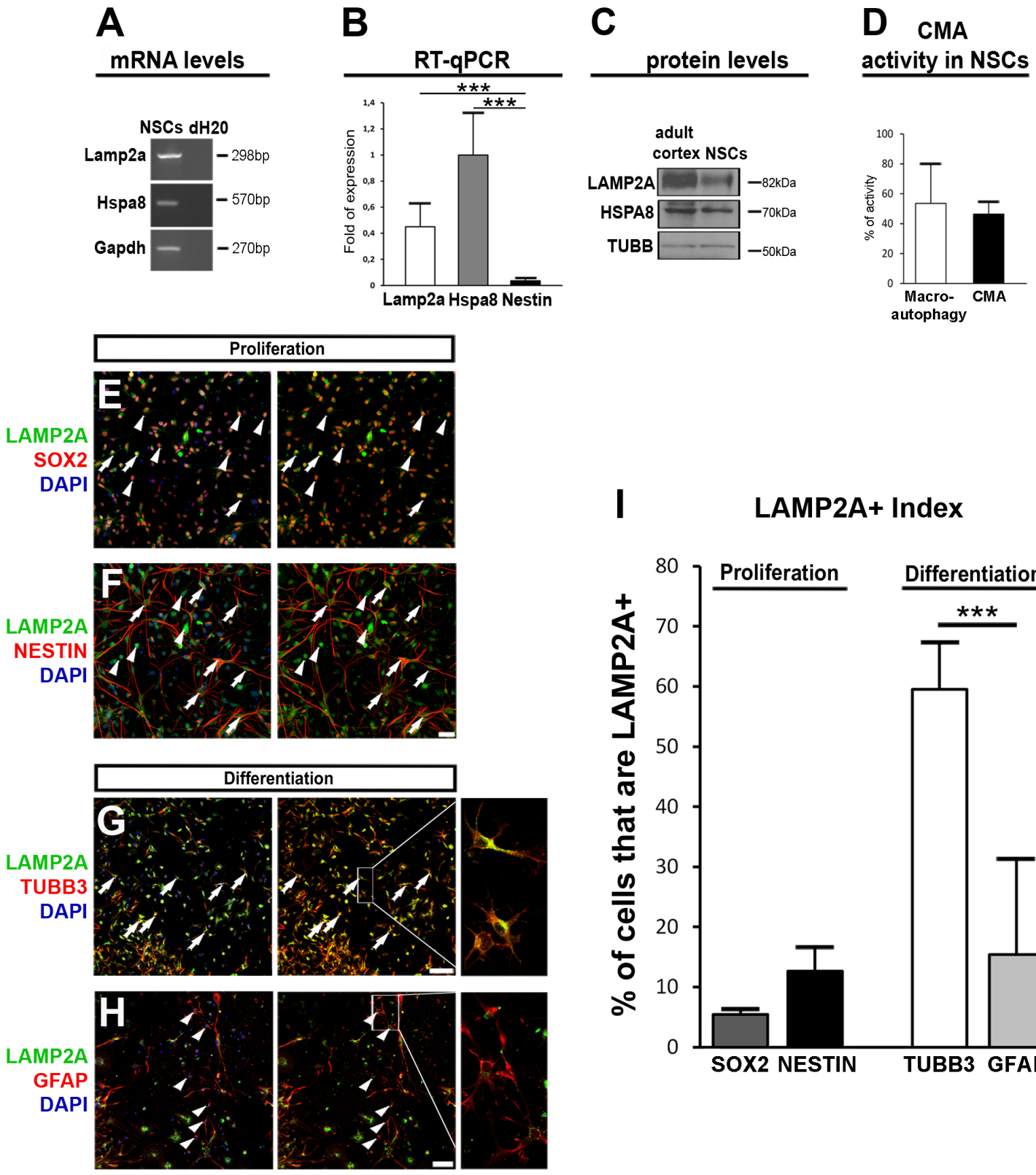
A
mRNA levels
NSCs dH20
Lamp2a
298bp
Hspa8
570bp
Gapdh
270bp
B
RT-qPCR
***
***
Fold of expression
Lamp2a Hspa8 Nestin
C
protein levels
adult
cortex NSCs
LAMP2A
82kDa
HSPA8
70kDa
TUBB
50kDa
D
CMA
activity in NSCs
% of activity
Macro-
autophagy
CMA
Proliferation
E
LAMP2A
SOX2
DAPI
F
LAMP2A
NESTIN
DAPI
Differentiation
G
LAMP2A
TUBB3
DAPI
H
LAMP2A
GFAP
DAPI
I
LAMP2A+ Index
% of cells that are LAMP2A+
Proliferation
Differentiation
***
SOX2 NESTIN
TUBB3 GFAP

Figure 3. CMA pathway is active in *ex vivo* cultured NSCs from rat embryonic telencephalon.

(**A-C**) Quantifications of endogenous expression at mRNA and protein levels of the basic components of CMA pathway, LAMP2A and HSPA8, in NSCs with conventional RT-PCR (**A**), real time RT-qPCR (**B**) and Western blot (**C**) analyses.

(**D**) Intracellular protein degradation assay indicating CMA versus macroautophagy activities in NSCs.

(**E-I**) Double immunostainings of LAMP2A and SOX2 (**E**), NESTIN (**F**), TUBB3 (**G**), GFAP (**H**) (all red) in NSCs in the presence (proliferation; +GFs) or in the absence of growth factors (differentiation; -GFs). Representative LAMP2A+ cells are indicated with arrows while LAMP2A negative cells with arrowheads. Inlets in G and H represent higher magnification of the squared shape of the same image. Control immunostainings without primary antibody show no staining (Supplementary Fig. 1D). (**I**) Quantification of cell populations that express LAMP2A (% of marker+, LAMP2A+ / total marker+).

The results are shown as mean ± SD, *** $P<0.001$ (Student's *t*-test). Cell nuclei were visualized with DAPI.

Scale bars: (**E, F**) 50 μm; (**G**) 100 μm; (**H**) 75 μm.

Figure 4

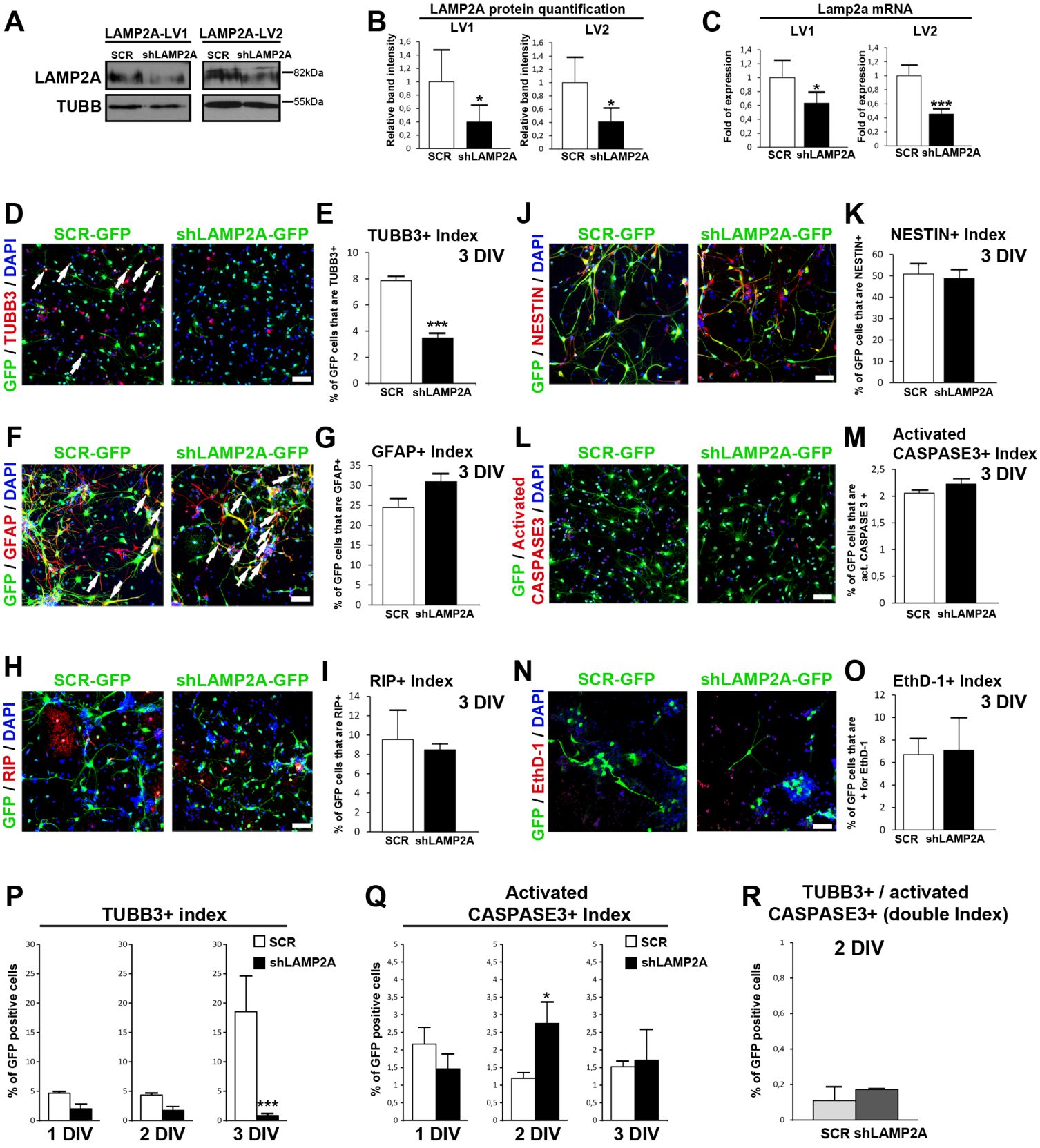
A
LAMP2A-LV1
LAMP2A-LV2
SCR shLAMP2A SCR shLAMP2A
LAMP2A
TUBB
82kDa
55kDa
B
LAMP2A protein quantification
LV1
LV2
Relative band intensity
SCR shLAMP2A
C
Lamp2a mRNA
LV1
LV2
Fold of expression
SCR shLAMP2A
D
SCR-GFP
shLAMP2A-GFP
GFP / TUBB3 / DAPI
E
TUBB3+ Index
3 DIV
% of GFP cells that are TUBB3+
SCR shLAMP2A
J
SCR-GFP
shLAMP2A-GFP
GFP / NESTIN / DAPI
K
NESTIN+ Index
3 DIV
% of GFP cells that are NESTIN+
SCR shLAMP2A
F
SCR-GFP
shLAMP2A-GFP
GFP / GFAP / DAPI
G
GFAP+ Index
3 DIV
% of GFP cells that are GFAP+
SCR shLAMP2A
L
SCR-GFP
shLAMP2A-GFP
GFP / Activated CASPASE3 / DAPI
M
Activated CASPASE3+ Index
3 DIV
% of GFP cells that are act. CASPASE 3 +
SCR shLAMP2A
H
SCR-GFP
shLAMP2A-GFP
GFP / RIP / DAPI
I
RIP+ Index
3 DIV
% of GFP cells that are RIP+
SCR shLAMP2A
N
SCR-GFP
shLAMP2A-GFP
GFP / EthD-1 / DAPI
O
EthD-1+ Index
3 DIV
% of GFP cells that are + for EthD-1
SCR shLAMP2A
P
TUBB3+ index
SCR
shLAMP2A
% of GFP positive cells
1 DIV
2 DIV
3 DIV
Q
Activated CASPASE3+ Index
SCR
shLAMP2A
% of GFP positive cells
1 DIV
2 DIV
3 DIV
R
TUBB3+ / activated CASPASE3+ (double Index)
2 DIV
% of GFP positive cells
SCR shLAMP2A

Figure 4. **shRNA-mediated knockdown of LAMP2A suppresses neuronal differentiation in NSCs without affecting neuronal cell death.**

(**A-C**) Expression levels of LAMP2A in *ex vivo* cultured NSCs, from rat E16.5 embryonic rat telencephalon, infected with two different lentiviruses encoding shRNAs targeting rat *Lamp2a* (LAMP2A-LV1, LAMP2A-LV2) or control-scrambled sequences (SCR). Quantification of LAMP2A protein levels with western blot analysis is depicted in A and B. Quantification of *Lamp2a* mRNA levels with real time RT-qPCR analysis is depicted in C.

(**D-M**) Double immunostainings of NSCs, infected with shSCR-GFP or shLAMP2A-GFP (LAMP2A-LV1) viruses, with GFP and TUBB3 (**D**), GFAP (**F**), RIP (**H**), NESTIN (**J**), and activated CASPASE 3 (**L**) (all red). NSCs were left to differentiate for 3 days in vitro (3 DIV) after the infection. All viral vectors co-express GFP from independent promoters. Quantifications of the specific indices are shown in E, G, I, K and M, respectively (% of GFP+; marker+/total GFP+). Arrowheads in D and F indicate the double positive cells.

(**N, O**) Triple stainings of NSCs, infected with shSCR-GFP or shLAMP2A-GFP (LAMP2A-LV1) viruses, with GFP, EthD-1 (Ethidium homodimer; used to test cell viability; red) and DAPI (**N**). NSCs were left to differentiate for 3 days in vitro (3 DIV) after the infection. All viral vectors co-express GFP from independent promoters. Quantification of the EthD-1 index is shown in O (% of GFP+; EthD-1+/total GFP+).

(**P, Q**) The quantification percentage of GFP and TUBB3 double positive cells (**P**), or GFP and activated CASPASE 3 double positive cells (**Q**) to total GFP positive cells during the 3-day (72 hours) differentiation assay after the lentiviral infection of NSCs, as indicated.

(**R**) The quantification percentage of GFP, TUBB3 and activated CASPASE 3 triple positive cells to total GFP positive cells only during the second day (DIV 2) of the lentiviral infection protocol of NSCs.

The results are shown as mean ± SD, * $P<0.05$, *** $P<0.001$ (Student's *t*-test). Cell nuclei were visualized with DAPI.

Scale bars: (**D, F, H, J, L, N**) 50 μm.

Figure 5

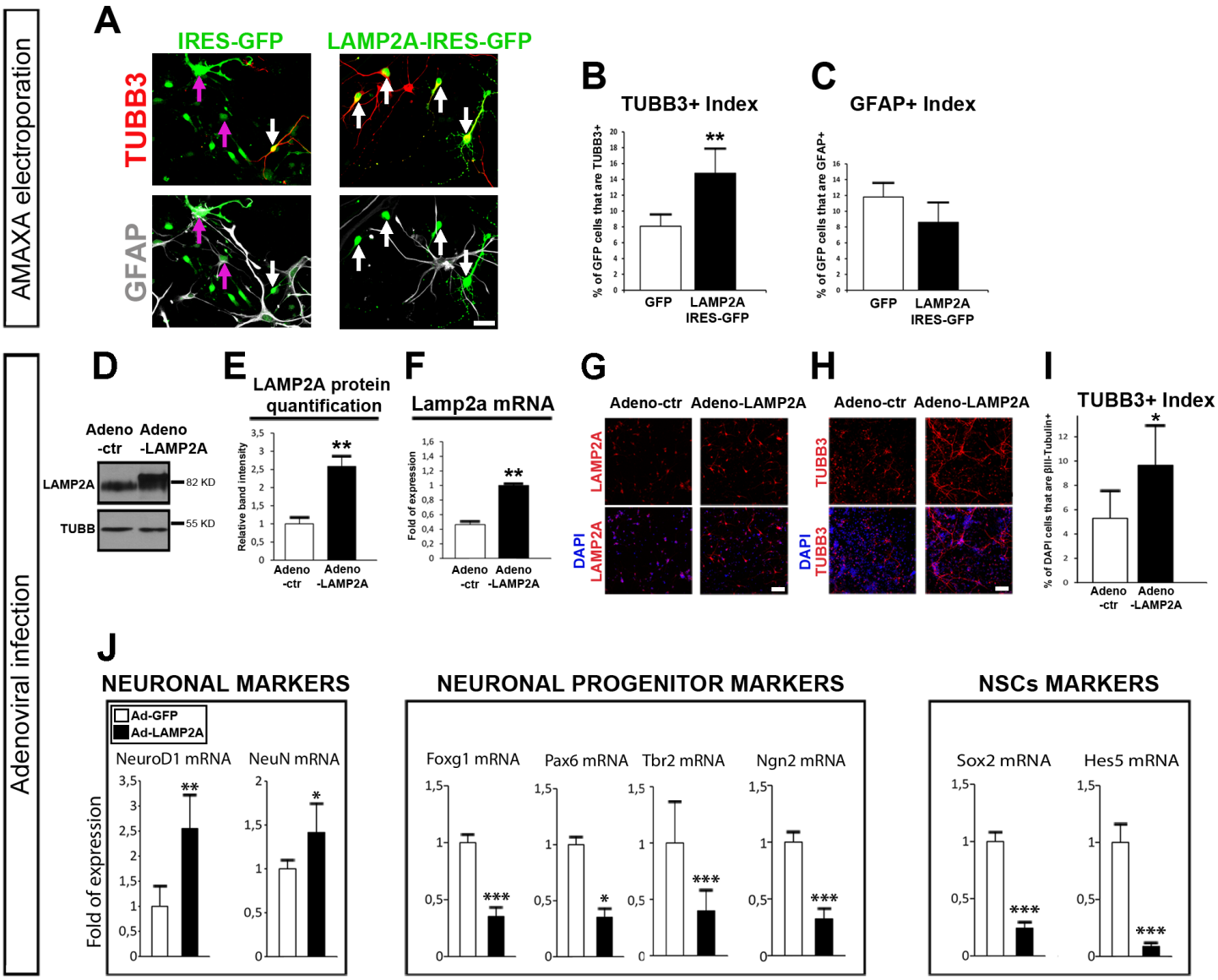
AMAXA electroporation
A
IRES-GFP
LAMP2A-IRES-GFP
TUBB3
GFAP
B
TUBB3+ Index
% of GFP cells that are TUBB3+
**
GFP
LAMP2A IRES-GFP
C
GFAP+ Index
% of GFP cells that are GFAP+
GFP
LAMP2A IRES-GFP
Adenoviral infection
D
Adeno -ctr
Adeno -LAMP2A
LAMP2A
TUBB
82 KD
55 KD
E
LAMP2A protein quantification
Relative band intensity
**
Adeno -ctr
Adeno -LAMP2A
F
Lamp2a mRNA
Fold of expression
**
Adeno -ctr
Adeno -LAMP2A
G
Adeno-ctr
Adeno-LAMP2A
LAMP2A
DAPI
LAMP2A
H
Adeno-ctr
Adeno-LAMP2A
TUBB3
DAPI
TUBB3
I
TUBB3+ Index
% of DAPI cells that are βIII-Tubulin+
*
Adeno -ctr
Adeno -LAMP2A
J
NEURONAL MARKERS
NEURONAL PROGENITOR MARKERS
NSCs MARKERS
Ad-GFP
Ad-LAMP2A
Fold of expression
NeuroD1 mRNA
NeuN mRNA
Foxg1 mRNA
Pax6 mRNA
Tbr2 mRNA
Ngn2 mRNA
Sox2 mRNA
Hes5 mRNA

Figure 5. **LAMP2A overexpression induces neuronal differentiation**.

(**A**) Triple immunostainings of AMAXA-electroporated NSCs with IRES-GFP (as a control) or LAMP2A-IRES-GFP, shown in green. TUBB3 is indicated in red and GFAP marker in grey. Purple arrows indicate GFP/GFAP double positive cells, whereas white arrows depict GFP/TUBB3.

(**B, C**) Quantification percentages of the two markers shown in A, TUBB3 (**B**) and GFAP (**C**) (% of GFP + cells; marker +/ total GFP +cells).

(**D-G**) Confirmation of adenoviral-mediated overexpression of LAMP2A in NSCs with western blot (**D, E**), real time RT-qPCR (**F**) and immunofluorescence (**G**) analyses.

(**H**) Immunostaining of NSCs with TUBB3 (red) after adenoviral infection with control (Adeno-ctr) or LAMP2A overexpressing virus (Adeno-Lamp2A).

(**I**) Quantification of the data presented in H, percentage of TUBB3 positive cells to total cell nuclei visualized with DAPI.

(**J**) Real time RT–qPCR analyses of expression levels of various genes (as indicated) after adenoviral-mediated overexpression of LAMP2A in *ex vivo* differentiated NSCs.

The results are shown as mean ± SD, * $P<0.05$, ** $P<0.01$, *** $P<0.001$ (Student's *t*-test).

Scale bars: (**A, G, H**) 100μm.

Figure 6

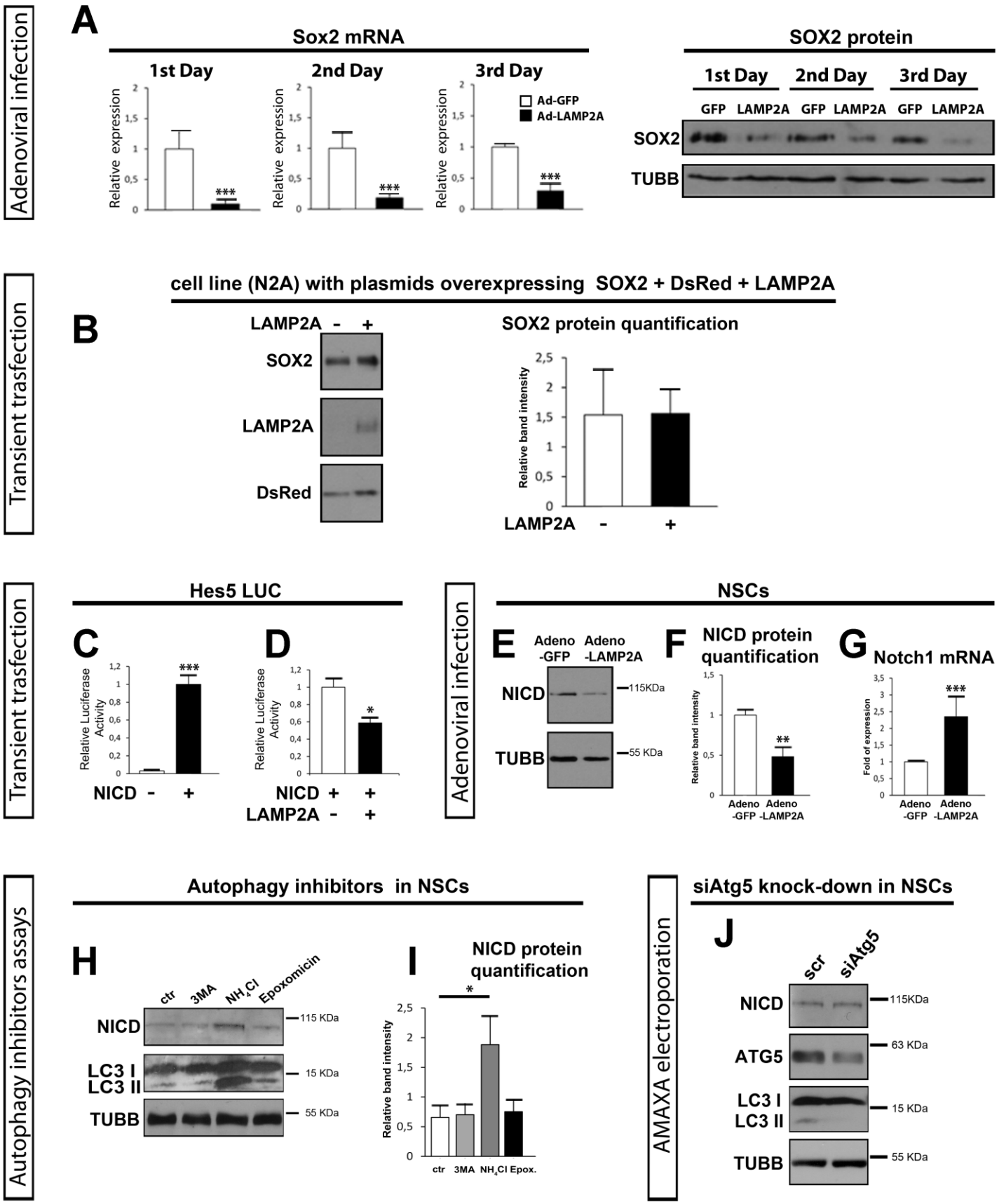
Adenoviral infection
A
Sox2 mRNA
1st Day
2nd Day
3rd Day
Relative expression
Ad-GFP
Ad-LAMP2A
***
SOX2 protein
GFP LAMP2A GFP LAMP2A GFP LAMP2A
SOX2
TUBB
Transient trasfection
cell line (N2A) with plasmids overexpressing SOX2 + DsRed + LAMP2A
B
LAMP2A - +
SOX2
LAMP2A
DsRed
SOX2 protein quantification
Relative band intensity
Transient trasfection
Hes5 LUC
C
D
Relative Luciferase Activity
NICD - +
NICD + +
LAMP2A - +
*
Adenoviral infection
NSCs
E
Adeno -GFP
Adeno -LAMP2A
NICD
TUBB
115KDa
55 KDa
F
NICD protein quantification
**
G
Notch1 mRNA
Fold of expression
Autophagy inhibitors assays
Autophagy inhibitors in NSCs
H
ctr
3MA
NH4Cl
Epoxomicin
NICD
LC3 I
LC3 II
TUBB
115 KDa
15 KDa
55 KDa
I
NICD protein quantification
ctr 3MA NH4Cl Epox.
AMAXA electroporation
siAtg5 knock-down in NSCs
J
scr
siAtg5
NICD
ATG5
LC3 I
LC3 II
TUBB
115KDa
63 KDa
15 KDa
55 KDa

Figure 6. **LAMP2A overexpression affects *Sox2* gene expression and NOTCH signaling activity**.

(**A**) Real time RT-qPCR (left panel) and western blot analyses (right panel) of *Sox2* gene expression at mRNA and protein levels, respectively, in NSCs infected with adenovirus overexpressing LAMP2A (Ad-LAMP2A) or control vector (Ad-GFP) during the 3-day differentiation protocol (72 hours after dissociation and plating).

(**B**) Transient co-trasfection of N2A cells with *Sox2* expression vector (1μg per well) and DsRed vector (0.5μg per well) in the presence or absence of LAMP2A vector (1.5μg per well). Western blot analysis indicates SOX2 protein levels in the presence or absence of exogenous LAMP2A, normalized to DsRed protein levels as loading control.

(**C, D**) Transcriptional assays in HEK293 cells with the luciferase reporter construct containing mouse *Hes5* promoter co-transfected with human *NICD* expression vector and compared to empty vector (**C**). The same experiment was repeated with the presence or absence of LAMP2A expression vector (LAMP2A-IRES-GFP) (**D**). In all luciferase assays in this figure, data are represented as mean ± SD of quadruplicate experiments.

(**E-G**) Assessment of expression levels of *Notch1* in NSCs infected with adenovirus overexpressing LAMP2A or control vector with western blot analysis (**E**, **F**) and real time RT-qPCR analysis (**G**).

(**H, I**) Western blot analysis of NSCs treated with 10 mM 3MA, 20mM NH_4Cl, 15nM Epoxomicin or control untreated NSCs (ctr) (**H**). Quantification of NICD protein levels relative to TUBB reference protein levels (**I**).

(**J**) Western blot analysis of NSCs electroporated with siRNAs against Atg5 (siAtg5) or control scrambled siRNAs (Klionsky et al.), as indicated.

The results are shown as mean ± SD, * $P<0.05$, ** $P<0.01$, *** $P<0.001$ (Student's *t*-test).

Figure 7

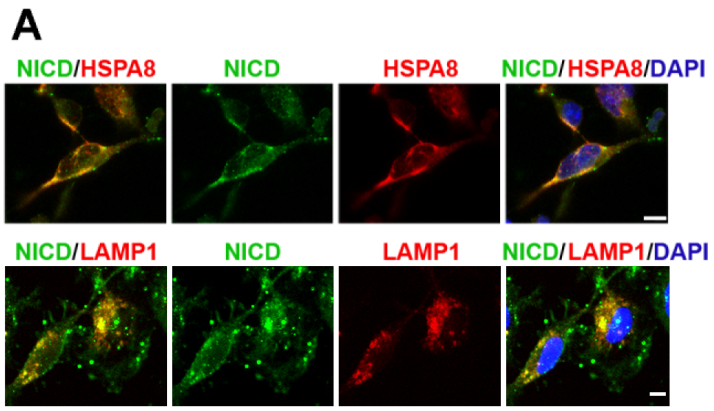
A
NICD/HSPA8
NICD
HSPA8
NICD/HSPA8/DAPI
NICD/LAMP1
NICD
LAMP1
NICD/LAMP1/DAPI

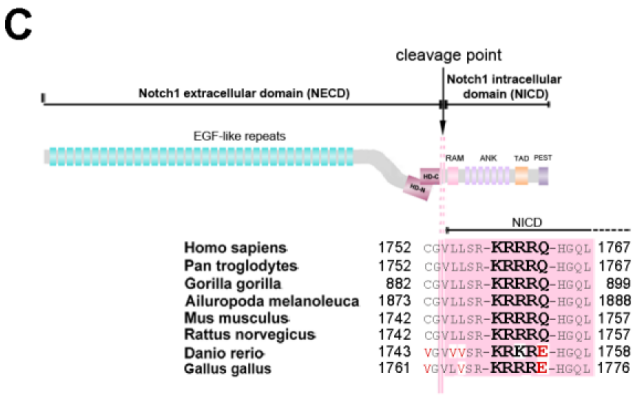
C
cleavage point
Notch1 extracellular domain (NECD)
Notch1 intracellular domain (NICD)
EGF-like repeats
RAM
ANK
TAD
PEST
NICD
Homo sapiens 1752 CGVLLSR-KRRRQ-HGQL 1767
Pan troglodytes 1752 CGVLLSR-KRRRQ-HGQL 1767
Gorilla gorilla 882 CGVLLSR-KRRRQ-HGQL 899
Ailuropoda melanoleuca 1873 CGVLLSR-KRRRQ-HGQL 1888
Mus musculus 1742 CGVLLSR-KRRRQ-HGQL 1757
Rattus norvegicus 1742 CGVLLSR-KRRRQ-HGQL 1757
Danio rerio 1743 VGVVSR-KRKRE-HGQL 1758
Gallus gallus 1761 VGVLVSR-KRRRE-HGQL 1776

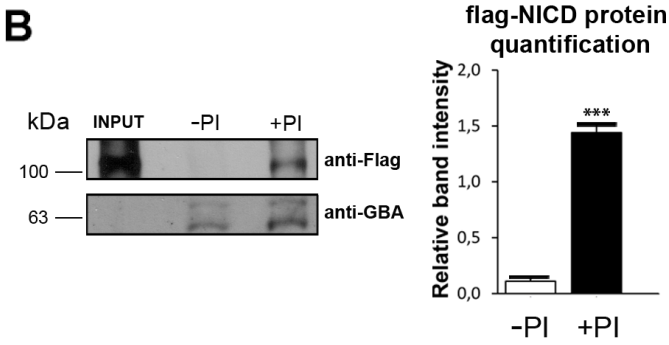
B
kDa
INPUT
-PI
+PI
100
63
anti-Flag
anti-GBA
flag-NICD protein quantification
Relative band intensity
2,0
1,5
1,0
0,5
0,0
***
-PI
+PI

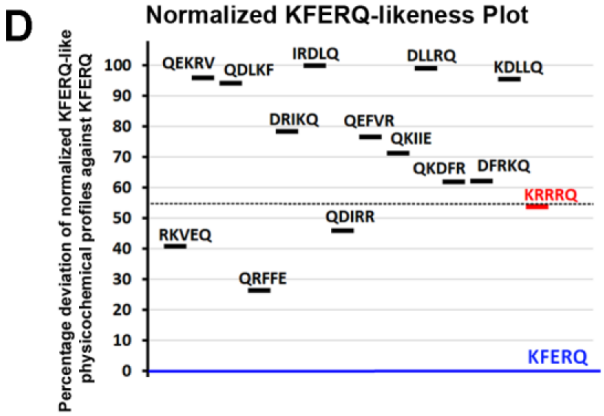
D
Normalized KFERQ-likeness Plot
Percentage deviation of normalized KFERQ-like physicochemical profiles against KFERQ
QEKRV
QDLKF
IRDLQ
DLLRQ
KDLLQ
DRIKQ
QEFVR
QKIIE
QKDFR
DFRKQ
KRRRQ
QDIRR
RKVEQ
QRFFE
KFERQ

Figure 7. **CMA degradation system targets NOTCH1 intracellular domain.**

(**A**) Double immunostainings of ex vivo cultured NSCs with NICD and either HSPA8 (upper panel, red) or LAMP1 lysosomal marker (lower panel, also red) (Pearson correlation coefficiency value for HSPA8 and LAMP1 are 0.685±0.033 and 0.545±0.07, respectively).

(**B**) Western blot of in vitro reconstitution of CMA activity. From left to right: Purified human flag-NICD (INPUT) (2μg), flag-NICD (INPUT) (2μg) in the absence (-) and in the presence (+) of protease inhibitors incubated with lysosomes. GBA antibody was used as a lysosomal marker and the relative quantification. The results arise from two independent experiments and are shown as mean ± SD, *** P<0.001 (Student's *t*-test).

(**C**) Schematic representation of the main NOTCH1 protein sequence divided by the cleavage site (arrow) into the extracellular (NECD) and intracellular (NICD) domains. The KRRRQ motif that was identified at the beginning of the NICD peptide sequence is indicated in bold. The conservation of this protein sequence between various species is also depicted in the figure (lower panel).

(**D**) Plot of the normalized fusion of 435 physicochemical properties that were used to train our model based on the existing known KFERQ-like motifs. It was concluded that when adding the KRRRQ motif using the trained model, it falls well within the range of physicochemical profiles of established KFERQ-like motifs. Thus, confirming that KRRRQ motif has similar physicochemical properties to the known KFERQ-like motifs. Closer to zero (where KFERQ profile lies) means more KFERQ-like in terms of physicochemical profiling.

Scale bars: (**A)** 10μm.

Figure 8

Luciferase assays

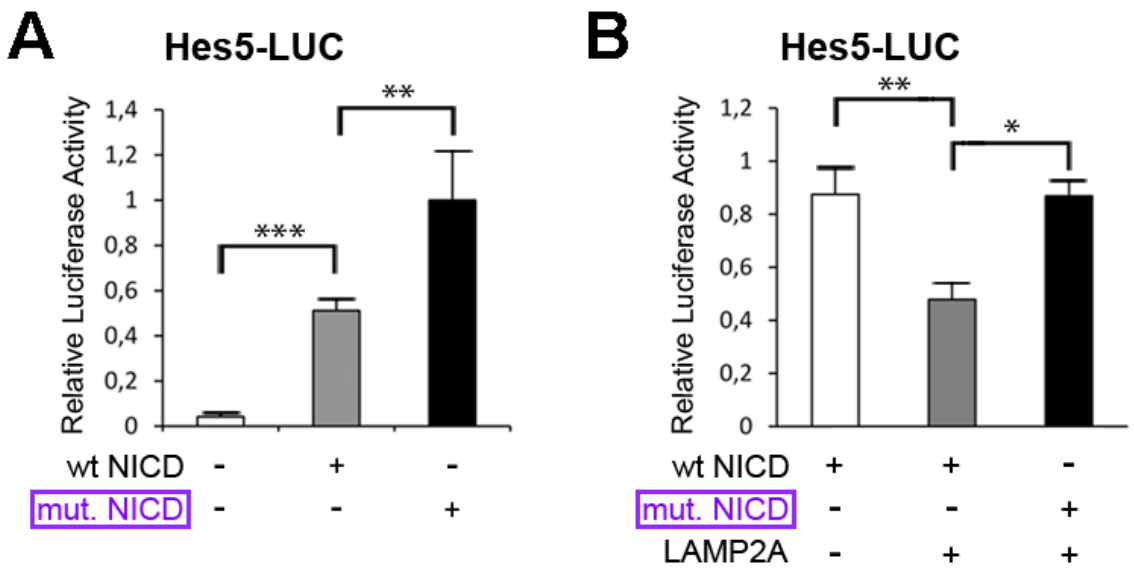

Autophagy inhibitors assays

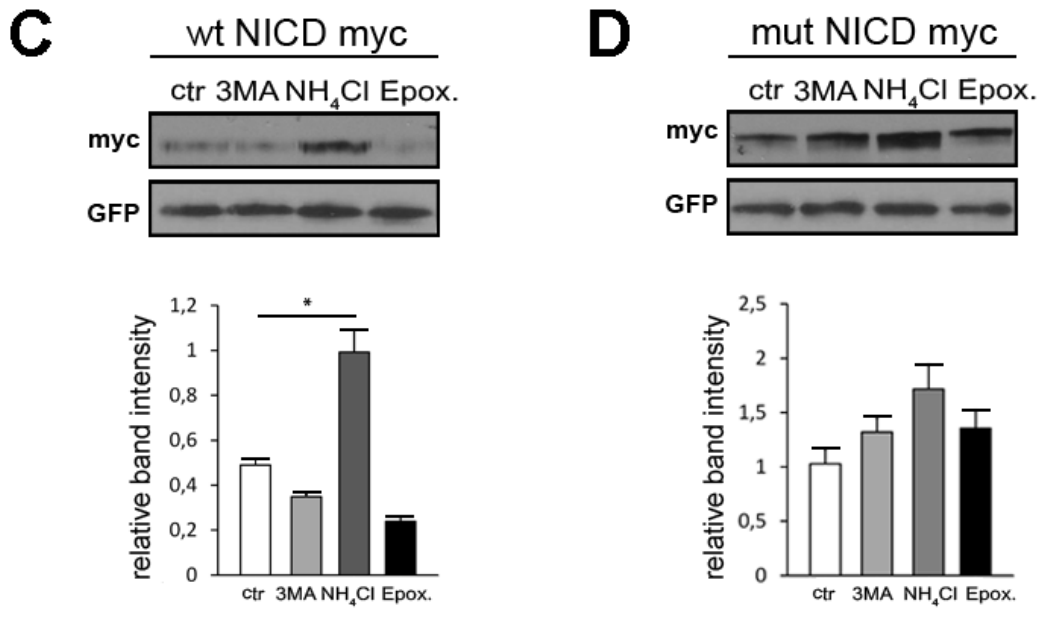

Figure 8. Mutated version of NICD (KRRRQ to AAAAA) is not affected by LAMP2A in *Hes5* promoter transactivation assays and is not degraded by the CMA pathway.

(**A**) Transcriptional assays in HEK293 cells with the luciferase reporter construct containing mouse *Hes5* promoter co-transfected with wild type human *NICD* expression vector (NICD) or *NICD* vector mutated for the KFERQ-like motif (NICD mut), or empty vector (IRES-GFP).

(**B**) The same experiment was repeated in the presence or absence of LAMP2A expression vector (LAMP2A-IRES-GFP). In all luciferase assays in this figure, data are represented as mean ± SD of quadruplicate experiments.

(**C, D**) Western blot analysis and quantification of myc protein levels relative to GFP levels in HEK293 cells transiently transfected with WT (**C**) or mutated (**D**) NICD (myc tagged) expression vectors and LAMP2A-IRES-GFP. Cells were treated with 10 mM 3MA, 20 mM NH_4Cl, or 15 nM Epoxomicin.

The results are shown as mean ± SD, * $P<0.05$, ** $P<0.01$, *** $P<0.001$ (Student's *t*-test).

Figure 9

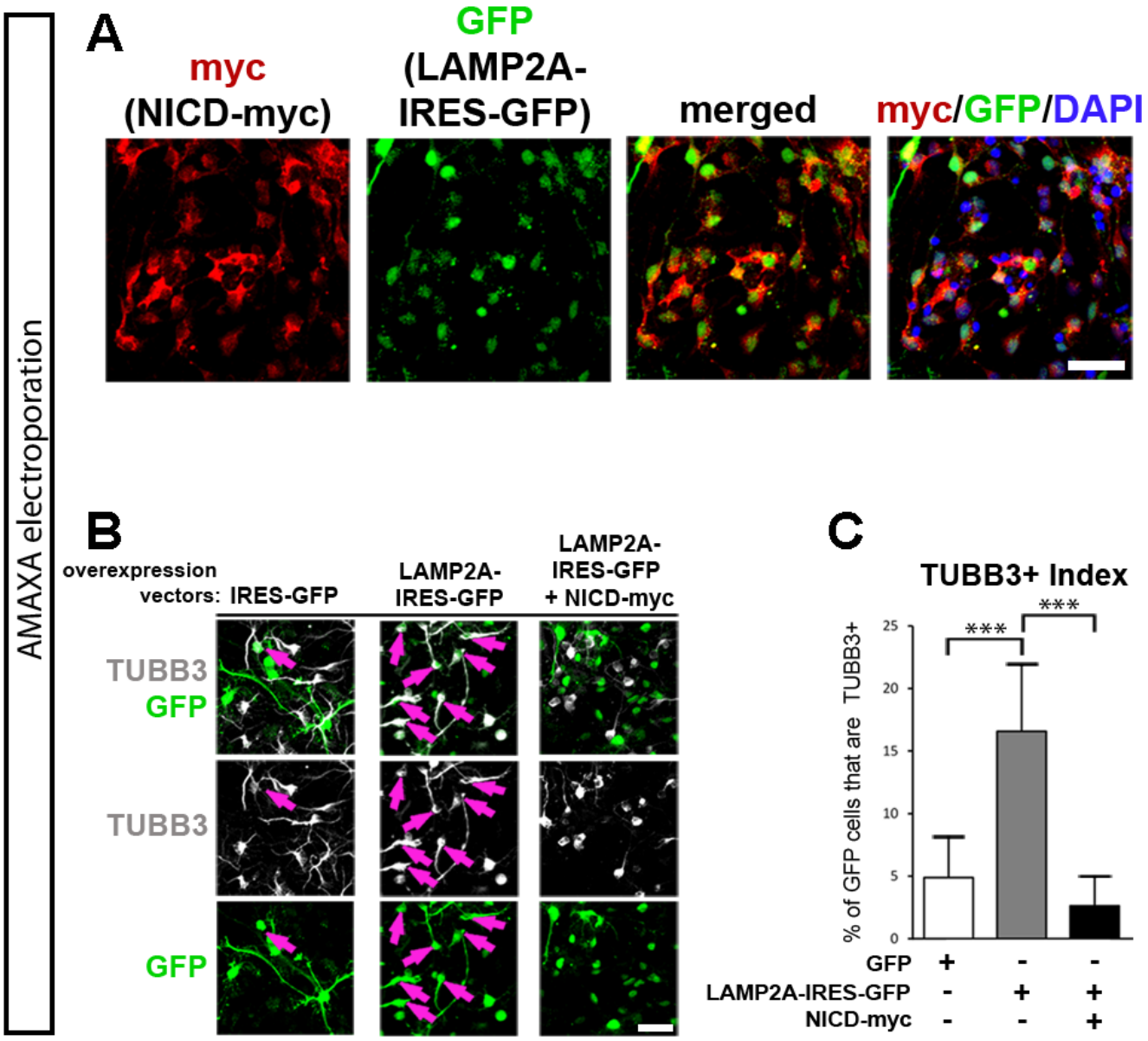
AMAXA electroporation
A
myc
(NICD-myc)
GFP
(LAMP2A-
IRES-GFP)
merged
myc/GFP/DAPI
B
overexpression
vectors:
IRES-GFP
LAMP2A-
IRES-GFP
LAMP2A-
IRES-GFP
+ NICD-myc
TUBB3
GFP
TUBB3
GFP
C
TUBB3+ Index
% of GFP cells that are TUBB3+
***
***
GFP + - -
LAMP2A-IRES-GFP - + +
NICD-myc - - +

Figure 9. NICD overexpression is sufficient to rescue the effect of LAMP2A on neuronal differentiation of NSCs.

(**A**) Double immunostainings of co-electroporated (AMAXA) NSCs in the absence of GFs, with LAMP2A-IRES-GFP and NICD-myc (red) with plasmid ratio 1:2. Cell nuclei were visualized with DAPI. Note that all myc (NICD) positive cells co-express GFP due to the co-electroporation of the two plasmids.

(**B, C**) Double immunostainings of GFP or LAMP2A with TUBB3 (grey) and triple immunostaining of LAMP2A, TUBB3 (grey) and myc (red) in NSCs electroporated (AMAXA) with IRES-GFP or LAMP2A-IRES-GFP, or co-electroporated (AMAXA) with LAMP2A-IRES-GFP and NICD-myc (ratio 1:2) respectively, in the absence of GFs (**B**). Quantification of TUBB3 index in all cases (**C**).

The results are shown as mean ± SD, *** $P<0.001$ (Student's *t*-test).

Scale bars: (**A**) 100 μm, (**B**) 100 μm.

Figure 10

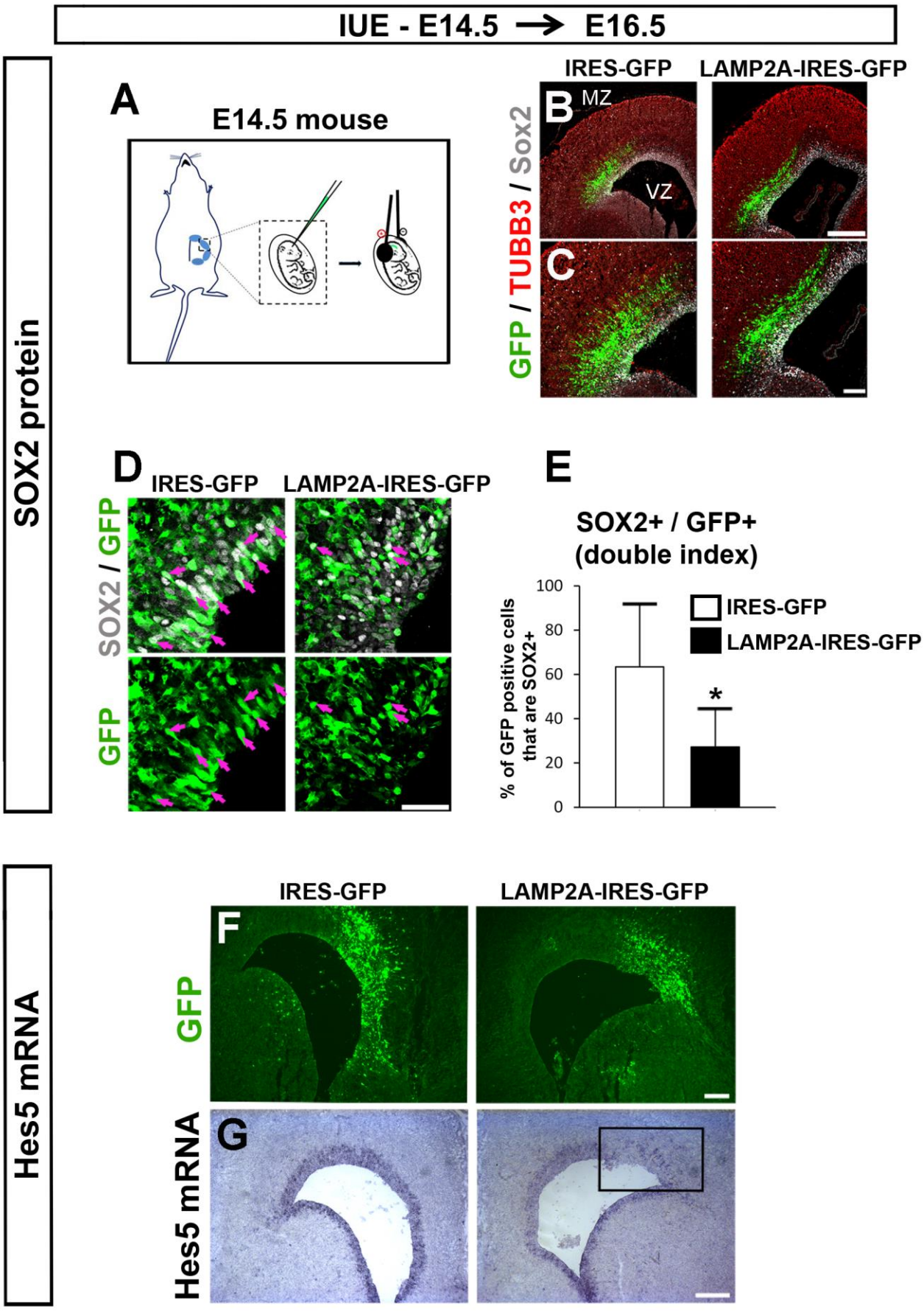
IUE - E14.5 → E16.5
SOX2 protein
A
E14.5 mouse
IRES-GFP
LAMP2A-IRES-GFP
B
MZ
VZ
C
GFP / TUBB3 / Sox2
D
IRES-GFP
LAMP2A-IRES-GFP
SOX2 / GFP
GFP
E
SOX2+ / GFP+
(double index)
% of GFP positive cells that are SOX2+
100
80
60
40
20
0
IRES-GFP
LAMP2A-IRES-GFP
*
Hes5 mRNA
IRES-GFP
LAMP2A-IRES-GFP
F
GFP
G
Hes5 mRNA

Figure 10. ***In vivo*** **LAMP2A overexpression suppresses NOTCH1 signaling pathway.**

(**A-C**) Schematic representation of IUE procedure in E14.5 mice (**A**). Triple immunostainings of E16.5 brains that were *in utero* electroporated, indicating the distribution of the electroporated cells either with IRES-GFP or LAMP2A-IRES-GFP plasmids at E14.5. SOX2 (grey) and TUBB3 (red) mark the boundaries for VZ layer (**B**). The lower panel of micrographs corresponds to higher magnification of the same image (**C**).

(**D, E**) Double immunostainings of SOX2 (grey) and GFP on cryosections of electroporated mouse cortex of E16.5 embryos (**D**). Quantification of cell populations that express both SOX2 and GFP at the VZ (**E**).

(**F, G**) Micrographs capturing GFP expression and indicating the electroporated areas with IRES-GFP or LAMP2A-IRES-GFP cells from the IUE E16.5 cortices (**F**). *In situ* hybridization stainings for *Hes5* mRNA riboprobe in the same cryosections, as above (**G**).

The results are shown as mean ± SD, * $P<0.05$, (Student's *t*-test).

Scale bars: (**B**) 250 μm, (**C, D**) 100 μm, (**F, G**) 200 μm

Supplementary Figures

Supplementary Figure 1

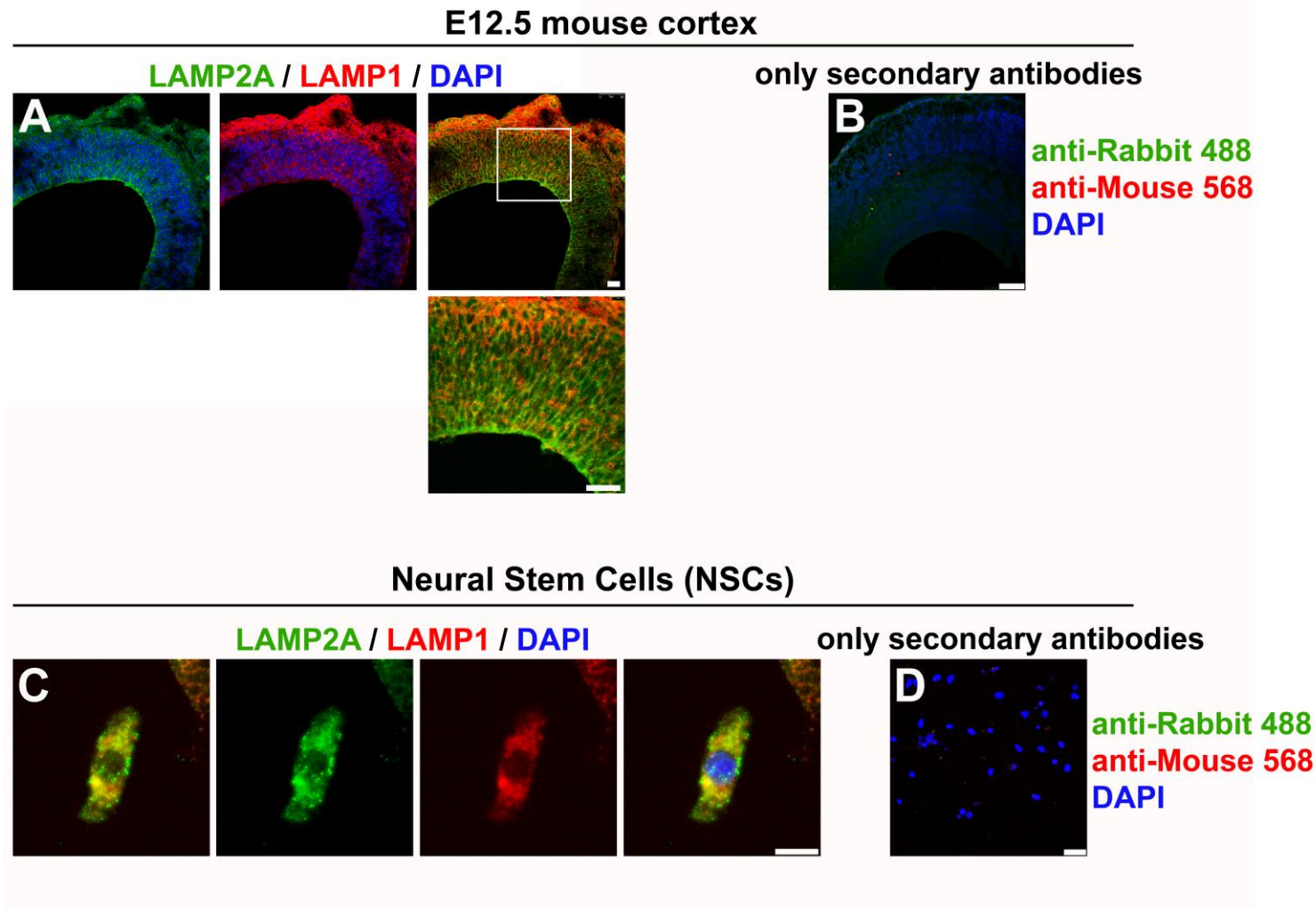

Supplementary Figure 1. **Immunofluorescence analysis with the anti-LAMP2A antibody reveals a lysosomal localization pattern.**

(**A**) Double immunostaining of LAMP2A and lysosomal marker LAMP1 (red) in cryosections from mouse embryonic cortex E12.5, as indicated. Boxed areas are represented underneath with higher magnification. Cell nuclei were visualized with DAPI.

(**B**) Control immunostaining without primary antibody show no signal under the same experimental and image acquisition settings as in A. Cell nuclei were visualized with DAPI.

(**C**) Double immunostaining of LAMP2A and and lysosomal marker LAMP1 (red) in ex vivo cultured NSCs as described in Figure 3. Cell nucleus is visualized with DAPI.

(**D**) Control immunostaining without primary antibody show no signal under the same experimental and image acquisition settings as in C. Cell nuclei were visualized with DAPI.

Scale bars: (**A**) 25 μm; (**B**) 100 μm; (**C**) 10 μm; (**D**) 25 μm.

Supplementary Figure 2

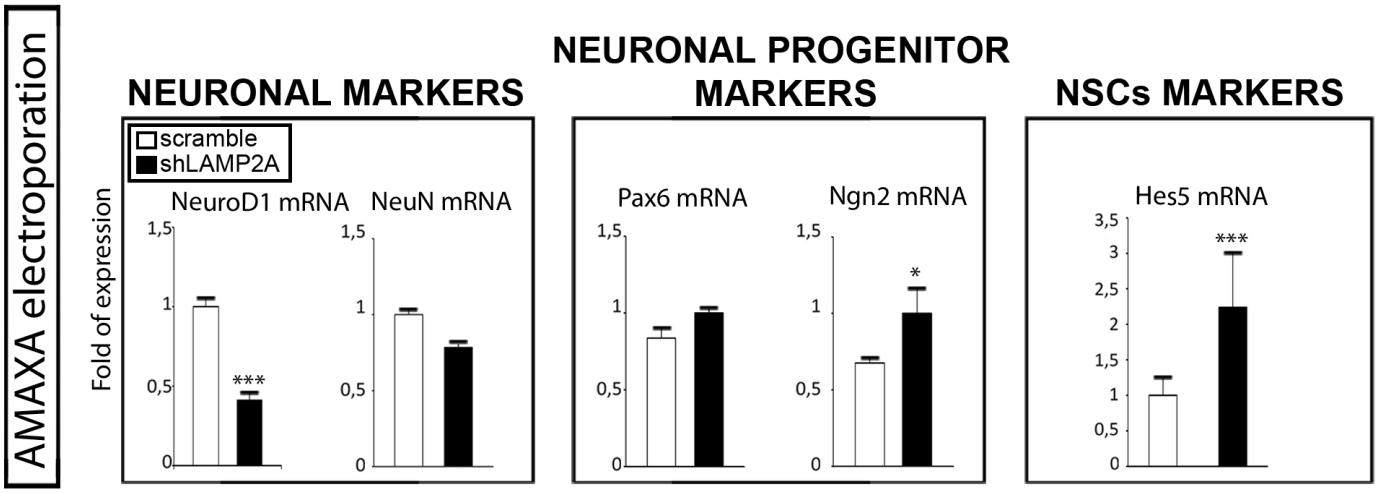

Supplementary Figure 2. shRNA-mediated knockdown of LAMP2A affects neuronal gene expression in NSCS.

Real time RT–qPCR analyses of expression levels of various genes (as indicated) after AMAXA electroporation of either control scramble shRNA vector or shRNA targeting Lamp2a. The results are shown as mean ± SD, * $P<0.05$, *** $P<0.001$ (Student's *t*-test).

Supplementary Figure 3

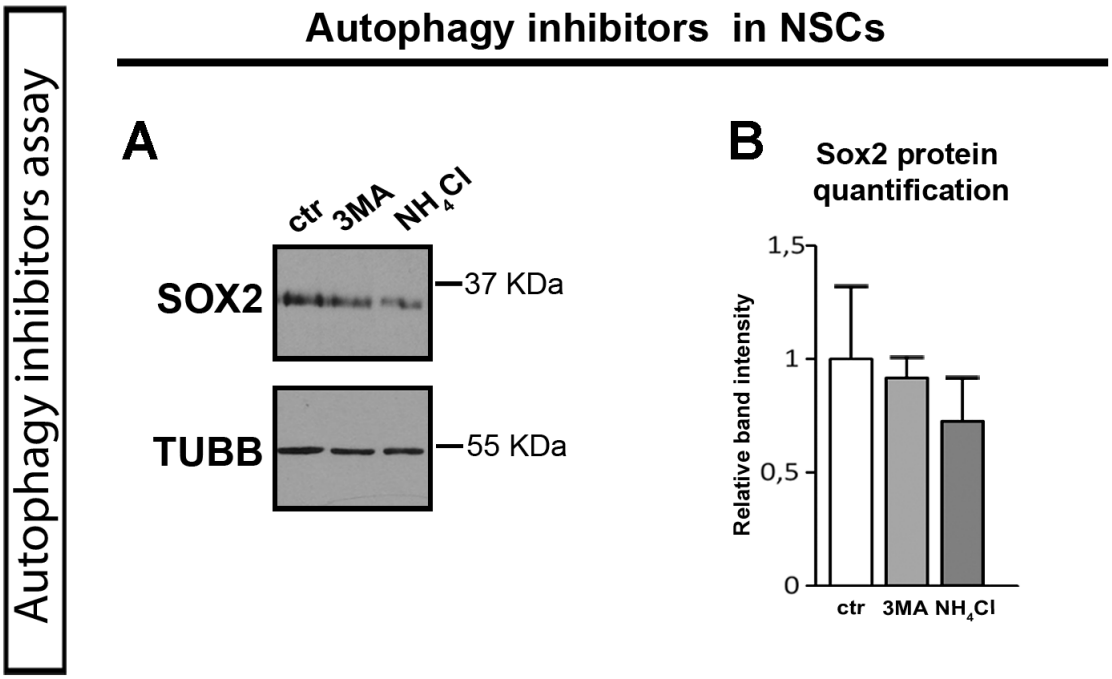

Supplementary Figure 3. Autophagy inhibitors do not affect SOX2 protein levels.

(**A**) Western blot analysis of NSCs treated with 10 mM 3MA, 20mM NH_4Cl or control untreated NSCs (ctr) (**H**).

(**B**) Quantification of SOX2 protein levels relative to TUBB reference protein levels, as indicated.

References

2013.08. *Molecular Operating Environment (MOE)* [Online]. 1010 Sherbooke St. West, Suite #910, Montreal, QC, Canada, H3A 2R7: Chemical Computing Group ULC. Available: https://www.chemcomp.com/Research-Citing_MOE.htm 2019].

Ahmed, S., Gan, H. T., Lam, C. S., Poonepalli, A., Ramasamy, S., Tay, Y., . .Yu, Y. H. 2009. Transcription factors and neural stem cell self-renewal, growth and differentiation. *Cell Adh Migr,* 3**,** 412-24.

Alfaro, I. E., Albornoz, A., Molina, A., Moreno, J., Cordero, K., Criollo, A. & Budini, M. 2018. Chaperone Mediated Autophagy in the Crosstalk of Neurodegenerative Diseases and Metabolic Disorders. *Front Endocrinol (Lausanne),* 9**,** 778.

Alvarez-Erviti, L., Rodriguez-Oroz, M. C., Cooper, J. M., Caballero, C., Ferrer, I., Obeso, J. A. & Schapira, A. H. 2010. Chaperone-mediated autophagy markers in Parkinson disease brains. *Arch Neurol,* 67**,** 1464-72.

Amador-Arjona, A., Cimadamore, F., Huang, C. T., Wright, R., Lewis, S., Gage, F. H. & Terskikh, A. V. 2015. SOX2 primes the epigenetic landscape in neural precursors enabling proper gene activation during hippocampal neurogenesis. *Proc Natl Acad Sci U S A,* 112**,** E1936-45.

Androutsellis-Theotokis, A., Leker, R. R., Soldner, F., Hoeppner, D. J., Ravin, R., Poser, S. W., . .Mckay, R. D. 2006. Notch signalling regulates stem cell numbers in vitro and in vivo. *Nature,* 442**,** 823-6.

Antoniou, D., Stergiopoulos, A. & Politis, P. K. 2014. Recent advances in the involvement of long non-coding RNAs in neural stem cell biology and brain pathophysiology. *Front Physiol,* 5**,** 155.

Artavanis-Tsakonas, S., Rand, M. D. & Lake, R. J. 1999. Notch signaling: cell fate control and signal integration in development. *Science,* 284**,** 770-6.

Aster, J. C., Pear, W. S. & Blacklow, S. C. 2017. The Varied Roles of Notch in Cancer. *Annu Rev Pathol,* 12**,** 245-275.

Bally-Cuif, L. & Hammerschmidt, M. 2003. Induction and patterning of neuronal development, and its connection to cell cycle control. *Curr Opin Neurobiol,* 13**,** 16-25.

Bandyopadhyay, U. & Cuervo, A. M. 2008. Entering the lysosome through a transient gate by chaperone-mediated autophagy. *Autophagy,* 4**,** 1101-3.

Bandyopadhyay, U., Kaushik, S., Varticovski, L. & Cuervo, A. M. 2008. The chaperone-mediated autophagy receptor organizes in dynamic protein complexes at the lysosomal membrane. *Mol Cell Biol,* 28**,** 5747-63.

Barth, J. M. & Kohler, K. 2014. How to take autophagy and endocytosis up a notch. *Biomed Res Int,* 2014**,** 960803.

Bauer, P. O., Goswami, A., Wong, H. K., Okuno, M., Kurosawa, M., Yamada, M., . .Nukina, N. 2010. Harnessing chaperone-mediated autophagy for the selective degradation of mutant huntingtin protein. *Nat Biotechnol,* 28**,** 256-63.

Biebl, M., Cooper, C. M., Winkler, J. & Kuhn, H. G. 2000. Analysis of neurogenesis and programmed cell death reveals a self-renewing capacity in the adult rat brain. *Neurosci Lett,* 291**,** 17-20.

Boyer, L. A., Lee, T. I., Cole, M. F., Johnstone, S. E., Levine, S. S., Zucker, J. P., . .Young, R. A. 2005. Core transcriptional regulatory circuitry in human embryonic stem cells. *Cell,* 122**,** 947-56.

Brekk, O. R., Makridakis, M., Mavroeidi, P., Vlahou, A., Xilouri, M. & Stefanis, L. 2018. Impairment of chaperone-mediated autophagy affects neuronal homeostasis through altered expression of DJ-1 and CRMP-2 proteins. *Mol Cell Neurosci,* 95**,** 1-12.

Brekk, O. R., Makridakis, M., Mavroeidi, P., Vlahou, A., Xilouri, M. & Stefanis, L. 2019. Impairment of chaperone-mediated autophagy affects neuronal homeostasis through altered expression of DJ-1 and CRMP-2 proteins. *Mol Cell Neurosci,* 95**,** 1-12.

Breunig, J. J., Silbereis, J., Vaccarino, F. M., Sestan, N. & Rakic, P. 2007. Notch regulates cell fate and dendrite morphology of newborn neurons in the postnatal dentate gyrus. *Proc Natl Acad Sci U S A,* 104**,** 20558-63.

Caballero, B., Wang, Y., Diaz, A., Tasset, I., Juste, Y. R., Stiller, B., . .Cuervo, A. M. 2018. Interplay of pathogenic forms of human tau with different autophagic pathways. *Aging Cell,* 17.

Campbell, P., Morris, H. & Schapira, A. 2018. Chaperone-mediated autophagy as a therapeutic target for Parkinson disease. *Expert Opin Ther Targets,* 22**,** 823-832.

Catarino, S., Pereira, P. & Girao, H. 2017. Molecular control of chaperone-mediated autophagy. *Essays Biochem,* 61**,** 663-674.

Cecconi, F. & Levine, B. 2008. The role of autophagy in mammalian development: cell makeover rather than cell death. *Dev Cell,* 15**,** 344-57.

Chevalier, S. & Blow, J. J. 1996. Cell cycle control of replication initiation in eukaryotes. *Curr Opin Cell Biol,* 8**,** 815-21.

Chiang, H. L., Terlecky, S. R., Plant, C. P. & Dice, J. F. 1989. A role for a 70-kilodalton heat shock protein in lysosomal degradation of intracellular proteins. *Science,* 246**,** 382-5.

Chung, K. M. & Yu, S. W. 2013. Interplay between autophagy and programmed cell death in mammalian neural stem cells. *BMB Rep,* 46**,** 383-90.

Corbin, J. G., Gaiano, N., Juliano, S. L., Poluch, S., Stancik, E. & Haydar, T. F. 2008. Regulation of neural progenitor cell development in the nervous system. *J Neurochem,* 106**,** 2272-87.

Cuervo, A. M. 2010. Chaperone-mediated autophagy: selectivity pays off. *Trends Endocrinol Metab,* 21**,** 142-50.

Cuervo, A. M. & Dice, J. F. 2000. Unique properties of lamp2a compared to other lamp2 isoforms. *J Cell Sci,* 113 Pt 24**,** 4441-50.

Cuervo, A. M., Dice, J. F. & Knecht, E. 1997. A population of rat liver lysosomes responsible for the selective uptake and degradation of cytosolic proteins. *J Biol Chem,* 272**,** 5606-15.

Cuervo, A. M., Stefanis, L., Fredenburg, R., Lansbury, P. T. & Sulzer, D. 2004. Impaired degradation of mutant alpha-synuclein by chaperone-mediated autophagy. *Science,* 305**,** 1292-5.

Dice, J. F. 1990. Peptide sequences that target cytosolic proteins for lysosomal proteolysis. *Trends Biochem Sci,* 15**,** 305-9.

Doe, C. Q. 2008. Neural stem cells: balancing self-renewal with differentiation. *Development,* 135**,** 1575-87.

Dohi, E., Tanaka, S., Seki, T., Miyagi, T., Hide, I., Takahashi, T., . .Sakai, N. 2012. Hypoxic stress activates chaperone-mediated autophagy and modulates neuronal cell survival. *Neurochem Int,* 60**,** 431-42.

Dunn, K. W., Kamocka, M. M. & Mcdonald, J. H. 2011. A practical guide to evaluating colocalization in biological microscopy. *Am J Physiol Cell Physiol,* 300**,** C723-42.

Dunn, W. A., Jr. 1990. Studies on the mechanisms of autophagy: maturation of the autophagic vacuole. *J Cell Biol,* 110**,** 1935-45.

Farkas, L. M. & Huttner, W. B. 2008. The cell biology of neural stem and progenitor cells and its significance for their proliferation versus differentiation during mammalian brain development. *Curr Opin Cell Biol,* 20**,** 707-15.

Favaro, R., Valotta, M., Ferri, A. L., Latorre, E., Mariani, J., Giachino, C., . .Nicolis, S. K. 2009. Hippocampal development and neural stem cell maintenance require Sox2-dependent regulation of Shh. *Nat Neurosci,* 12**,** 1248-56.

Feng, Y., He, D., Yao, Z. & Klionsky, D. J. 2014. The machinery of macroautophagy. *Cell Res,* 24**,** 24-41.

Fimia, G. M., Stoykova, A., Romagnoli, A., Giunta, L., Di Bartolomeo, S., Nardacci, R., . .Cecconi, F. 2007. Ambra1 regulates autophagy and development of the nervous system. *Nature,* 447**,** 1121-5.

Finn, P. F. & Dice, J. F. 2005. Ketone bodies stimulate chaperone-mediated autophagy. *J Biol Chem,* 280**,** 25864-70.

Foskolou, I. P., Stellas, D., Rozani, I., Lavigne, M. D. & Politis, P. K. 2013. Prox1 suppresses the proliferation of neuroblastoma cells via a dual action in p27-Kip1 and Cdc25A. *Oncogene,* 32**,** 947-60.

Gaiano, N., Nye, J. S. & Fishell, G. 2000. Radial glial identity is promoted by Notch1 signaling in the murine forebrain. *Neuron,* 26**,** 395-404.

Garg, V., Muth, A. N., Ransom, J. F., Schluterman, M. K., Barnes, R., King, I. N., . .Srivastava, D. 2005. Mutations in NOTCH1 cause aortic valve disease. *Nature,* 437**,** 270-4.

Ghavami, S., Shojaei, S., Yeganeh, B., Ande, S. R., Jangamreddy, J. R., Mehrpour, M., . .Los, M. J. 2014. Autophagy and apoptosis dysfunction in neurodegenerative disorders. *Prog Neurobiol,* 112**,** 24-49.

Gotz, M. & Huttner, W. B. 2005. The cell biology of neurogenesis. *Nat Rev Mol Cell Biol,* 6**,** 777-88.

Gridley, T. 2003. Notch signaling and inherited disease syndromes. *Hum Mol Genet,* 12 Spec No 1**,** R9-13.

Guerout, N., Li, X. & Barnabe-Heider, F. 2014. Cell fate control in the developing central nervous system. *Exp Cell Res,* 321**,** 77-83.

Han, Q., Deng, Y., Chen, S., Chen, R., Yang, M., Zhang, Z., . .Li, S. 2017. Downregulation of ATG5-dependent macroautophagy by chaperone-mediated autophagy promotes breast cancer cell metastasis. *Sci Rep,* 7**,** 4759.

Hao, Y., Kacal, M., Ouchida, A. T., Zhang, B., Norberg, E. & Vakifahmetoglu-Norberg, H. 2019. Targetome analysis of chaperone-mediated autophagy in cancer cells. *Autophagy***,** 1-14.

Hatakeyama, J., Bessho, Y., Katoh, K., Ookawara, S., Fujioka, M., Guillemot, F. & Kageyama, R. 2004. Hes genes regulate size, shape and histogenesis of the nervous system by control of the timing of neural stem cell differentiation. *Development,* 131**,** 5539-50.

Haubensak, W., Attardo, A., Denk, W. & Huttner, W. B. 2004. Neurons arise in the basal neuroepithelium of the early mammalian telencephalon: a major site of neurogenesis. *Proc Natl Acad Sci U S A,* 101**,** 3196-201.

Hitoshi, S., Alexson, T., Tropepe, V., Donoviel, D., Elia, A. J., Nye, J. S., . .Van Der Kooy, D. 2002. Notch pathway molecules are essential for the maintenance, but not the generation, of mammalian neural stem cells. *Genes Dev,* 16**,** 846-58.

Huang, C. C., Bose, J. K., Majumder, P., Lee, K. H., Huang, J. T., Huang, J. K. & Shen, C. K. 2014. Metabolism and mis-metabolism of the neuropathological signature protein TDP-43. *J Cell Sci,* 127**,** 3024-38.

Hubbi, M. E., Hu, H., Kshitiz, Ahmed, I., Levchenko, A. & Semenza, G. L. 2013. Chaperone-mediated autophagy targets hypoxia-inducible factor-1alpha (HIF-1alpha) for lysosomal degradation. *J Biol Chem,* 288**,** 10703-14.

Imayoshi, I. & Kageyama, R. 2011. The role of Notch signaling in adult neurogenesis. *Mol Neurobiol,* 44**,** 7-12.

Isenman, L. D. & Dice, J. F. 1989. Secretion of intact proteins and peptide fragments by lysosomal pathways of protein degradation. *J Biol Chem,* 264**,** 21591-6.

Issa, A. R., Sun, J., Petitgas, C., Mesquita, A., Dulac, A., Robin, M., . .Birman, S. 2018. The lysosomal membrane protein LAMP2A promotes autophagic flux and prevents SNCA-induced Parkinson disease-like symptoms in the Drosophila brain. *Autophagy,* 14**,** 1898-1910.

Jacob, J. A., Salmani, J. M. M., Jiang, Z., Feng, L., Song, J., Jia, X. & Chen, B. 2017. Autophagy: An overview and its roles in cancer and obesity. *Clin Chim Acta,* 468**,** 85-89.

Juste, Y. R. & Cuervo, A. M. 2019. Analysis of Chaperone-Mediated Autophagy. *Methods Mol Biol,* 1880**,** 703-727.

Kageyama, R., Ohtsuka, T., Shimojo, H. & Imayoshi, I. 2008. Dynamic Notch signaling in neural progenitor cells and a revised view of lateral inhibition. *Nat Neurosci,* 11**,** 1247-51.

Kaltezioti, V., Antoniou, D., Stergiopoulos, A., Rozani, I., Rohrer, H. & Politis, P. K. 2014. Prox1 regulates Olig2 expression to modulate binary fate decisions in spinal cord neurons. *J Neurosci,* 34**,** 15816-31.

Kaltezioti, V., Kouroupi, G., Oikonomaki, M., Mantouvalou, E., Stergiopoulos, A., Charonis, A., . .Politis, P. K. 2010. Prox1 regulates the notch1-mediated inhibition of neurogenesis. *PLoS Biol,* 8**,** e1000565.

Kaushik, S., Bandyopadhyay, U., Sridhar, S., Kiffin, R., Martinez-Vicente, M., Kon, M., . .Cuervo, A. M. 2011. Chaperone-mediated autophagy at a glance. *J Cell Sci,* 124**,** 495-9.

Kaushik, S. & Cuervo, A. M. 2009. Methods to monitor chaperone-mediated autophagy. *Methods Enzymol,* 452**,** 297-324.

Kaushik, S. & Cuervo, A. M. 2012. Chaperone-mediated autophagy: a unique way to enter the lysosome world. *Trends Cell Biol,* 22**,** 407-17.

Kiffin, R., Christian, C., Knecht, E. & Cuervo, A. M. 2004. Activation of chaperone-mediated autophagy during oxidative stress. *Mol Biol Cell,* 15**,** 4829-40.

Kim, J., Chu, J., Shen, X., Wang, J. & Orkin, S. H. 2008. An extended transcriptional network for pluripotency of embryonic stem cells. *Cell,* 132**,** 1049-61.

Klionsky, D. J., Abdelmohsen, K., Abe, A., Abedin, M. J., Abeliovich, H., Acevedo Arozena, A., . .Zughaier, S. M. 2016. Guidelines for the use and interpretation of assays for monitoring autophagy (3rd edition). *Autophagy,* 12**,** 1-222.

Koga, H., Martinez-Vicente, M., Arias, E., Kaushik, S., Sulzer, D. & Cuervo, A. M. 2011a. Constitutive upregulation of chaperone-mediated autophagy in Huntington's disease. *J Neurosci,* 31**,** 18492-505.

Koga, H., Martinez-Vicente, M., Macian, F., Verkhusha, V. V. & Cuervo, A. M. 2011b. A photoconvertible fluorescent reporter to track chaperone-mediated autophagy. *Nat Commun,* 2**,** 386.

Kopan, R. & Ilagan, M. X. 2009. The canonical Notch signaling pathway: unfolding the activation mechanism. *Cell,* 137**,** 216-33.

Kyrousi, C., Arbi, M., Pilz, G. A., Pefani, D. E., Lalioti, M. E., Ninkovic, J., . .Taraviras, S. 2015. Mcidas and GemC1 are key regulators for the generation of multiciliated ependymal cells in the adult neurogenic niche. *Development,* 142**,** 3661-74.

Lathia, J. D., Mattson, M. P. & Cheng, A. 2008. Notch: from neural development to neurological disorders. *J Neurochem,* 107**,** 1471-81.

Lavado, A. & Oliver, G. 2014. Jagged1 is necessary for postnatal and adult neurogenesis in the dentate gyrus. *Dev Biol,* 388**,** 11-21.

Lee, H. J., Kim, M. Y. & Park, H. S. 2015. Phosphorylation-dependent regulation of Notch1 signaling: the fulcrum of Notch1 signaling. *BMB Rep,* 48**,** 431-7.

Lee, K. M., Hwang, S. K. & Lee, J. A. 2013. Neuronal autophagy and neurodevelopmental disorders. *Exp Neurobiol,* 22**,** 133-42.

Liu, H., Wang, P., Song, W. & Sun, X. 2009. Degradation of regulator of calcineurin 1 (RCAN1) is mediated by both chaperone-mediated autophagy and ubiquitin proteasome pathways. *FASEB J,* 23**,** 3383-92.

Louvi, A. & Artavanis-Tsakonas, S. 2006. Notch signalling in vertebrate neural development. *Nat Rev Neurosci,* 7**,** 93-102.

Lv, X., Jiang, H., Li, B., Liang, Q., Wang, S., Zhao, Q. & Jiao, J. 2014. The crucial role of Atg5 in cortical neurogenesis during early brain development. *Sci Rep,* 4**,** 6010.

Majer, F., Pelak, O., Kalina, T., Vlaskova, H., Dvorakova, L., Honzik, T., . .Sikora, J. 2014. Mosaic tissue distribution of the tandem duplication of LAMP2 exons 4 and 5 demonstrates the limits of Danon disease cellular and molecular diagnostics. *J Inherit Metab Dis,* 37**,** 117-24.

Mak, S. K., Mccormack, A. L., Manning-Bog, A. B., Cuervo, A. M. & Di Monte, D. A. 2010. Lysosomal degradation of alpha-synuclein in vivo. *J Biol Chem,* 285**,** 13621-9.

Martinez-Vicente, M., Talloczy, Z., Kaushik, S., Massey, A. C., Mazzulli, J., Mosharov, E. V., . .Cuervo, A. M. 2008. Dopamine-modified alpha-synuclein blocks chaperone-mediated autophagy. *J Clin Invest,* 118**,** 777-88.

Martynoga, B., Drechsel, D. & Guillemot, F. 2012. Molecular control of neurogenesis: a view from the mammalian cerebral cortex. *Cold Spring Harb Perspect Biol,* 4.

Mason, H. A., Rakowiecki, S. M., Raftopoulou, M., Nery, S., Huang, Y., Gridley, T. & Fishell, G. 2005. Notch signaling coordinates the patterning of striatal compartments. *Development,* 132**,** 4247-58.

Massey, A. C., Kaushik, S., Sovak, G., Kiffin, R. & Cuervo, A. M. 2006. Consequences of the selective blockage of chaperone-mediated autophagy. *Proc Natl Acad Sci U S A,* 103**,** 5805-10.

Mizushima, N. & Levine, B. 2010. Autophagy in mammalian development and differentiation. *Nat Cell Biol,* 12**,** 823-30.

Mizutani, K., Yoon, K., Dang, L., Tokunaga, A. & Gaiano, N. 2007. Differential Notch signalling distinguishes neural stem cells from intermediate progenitors. *Nature,* 449**,** 351-5.

Nimchinsky, E. A., Oberlander, A. M. & Svoboda, K. 2001. Abnormal development of dendritic spines in FMR1 knock-out mice. *J Neurosci,* 21**,** 5139-46.

Noctor, S. C., Martinez-Cerdeno, V., Ivic, L. & Kriegstein, A. R. 2004. Cortical neurons arise in symmetric and asymmetric division zones and migrate through specific phases. *Nat Neurosci,* 7**,** 136-44.

Ohtsuka, T., Ishibashi, M., Gradwohl, G., Nakanishi, S., Guillemot, F. & Kageyama, R. 1999. Hes1 and Hes5 as notch effectors in mammalian neuronal differentiation. *EMBO J,* 18**,** 2196-207.

Orenstein, S. J., Kuo, S. H., Tasset, I., Arias, E., Koga, H., Fernandez-Carasa, I., . .Cuervo, A. M. 2013. Interplay of LRRK2 with chaperone-mediated autophagy. *Nat Neurosci,* 16**,** 394-406.

Packard, A. I., Lin, B. & Schwob, J. E. 2016. Sox2 and Pax6 Play Counteracting Roles in Regulating Neurogenesis within the Murine Olfactory Epithelium. *PLoS One,* 11**,** e0155167.

Park, C., Suh, Y. & Cuervo, A. M. 2015. Regulated degradation of Chk1 by chaperone-mediated autophagy in response to DNA damage. *Nat Commun,* 6**,** 6823.

Park, J. S., Kim, D. H. & Yoon, S. Y. 2016. Regulation of amyloid precursor protein processing by its KFERQ motif. *BMB Rep,* 49**,** 337-42.

Patel, B. & Cuervo, A. M. 2015. Methods to study chaperone-mediated autophagy. *Methods,* 75**,** 133-40.

Piton, A., Redin, C. & Mandel, J. L. 2013. XLID-causing mutations and associated genes challenged in light of data from large-scale human exome sequencing. *Am J Hum Genet,* 93**,** 368-83.

Politis, P. K., Akrivou, S., Hurel, C., Papadodima, O. & Matsas, R. 2008. BM88/Cend1 is involved in histone deacetylase inhibition-mediated growth arrest and differentiation of neuroblastoma cells. *FEBS Lett,* 582**,** 741-8.

Politis, P. K., Rohrer, H. & Matsas, R. 2007. Expression pattern of BM88 in the developing nervous system of the chick and mouse embryo. *Gene Expr Patterns,* 7**,** 165-77.

Qi, L., Zhang, X. D., Wu, J. C., Lin, F., Wang, J., Difiglia, M. & Qin, Z. H. 2012. The role of chaperone-mediated autophagy in huntingtin degradation. *PLoS One,* 7**,** e46834.

Reinstein, E. & Ciechanover, A. 2006. Narrative review: protein degradation and human diseases: the ubiquitin connection. *Ann Intern Med,* 145**,** 676-84.

Rothaug, M., Stroobants, S., Schweizer, M., Peters, J., Zunke, F., Allerding, M., . .Blanz, J. 2015. LAMP-2 deficiency leads to hippocampal dysfunction but normal clearance of neuronal substrates of chaperone-mediated autophagy in a mouse model for Danon disease. *Acta Neuropathol Commun,* 3**,** 6.

Rout, A. K., Strub, M. P., Piszczek, G. & Tjandra, N. 2014. Structure of transmembrane domain of lysosome-associated membrane protein type 2a (LAMP-2A) reveals key features for substrate specificity in chaperone-mediated autophagy. *J Biol Chem,* 289**,** 35111-23.

Rowitch, D. H. & Kriegstein, A. R. 2010. Developmental genetics of vertebrate glial-cell specification. *Nature,* 468**,** 214-22.

Saha, T. 2012. LAMP2A overexpression in breast tumors promotes cancer cell survival via chaperone-mediated autophagy. *Autophagy,* 8**,** 1643-56.

Sala, G., Marinig, D., Arosio, A. & Ferrarese, C. 2016. Role of Chaperone-Mediated Autophagy Dysfunctions in the Pathogenesis of Parkinson's Disease. *Front Mol Neurosci,* 9**,** 157.

Seglen, P. O. & Gordon, P. B. 1982. 3-Methyladenine: specific inhibitor of autophagic/lysosomal protein degradation in isolated rat hepatocytes. *Proc Natl Acad Sci U S A,* 79**,** 1889-92.

Shimojo, H., Ohtsuka, T. & Kageyama, R. 2008. Oscillations in notch signaling regulate maintenance of neural progenitors. *Neuron,* 58**,** 52-64.

Shimojo, H., Ohtsuka, T. & Kageyama, R. 2011. Dynamic expression of notch signaling genes in neural stem/progenitor cells. *Front Neurosci,* 5**,** 78.

Srivastava, D. P., Woolfrey, K. M., Jones, K. A., Anderson, C. T., Smith, K. R., Russell, T. A., . .Penzes, P. 2012. An autism-associated variant of Epac2 reveals a role for Ras/Epac2 signaling in controlling basal dendrite maintenance in mice. *PLoS Biol,* 10**,** e1001350.

Stergiopoulos, A. & Politis, P. K. 2016. Nuclear receptor NR5A2 controls neural stem cell fate decisions during development. *Nat Commun,* 7**,** 12230.

Storrie, B. & Madden, E. A. 1990. Isolation of subcellular organelles. *Methods Enzymol,* 182**,** 203-25.

Tamaki, Y., Shodai, A., Morimura, T., Hikiami, R., Minamiyama, S., Ayaki, T., . .Urushitani, M. 2018. Elimination of TDP-43 inclusions linked to amyotrophic lateral sclerosis by a misfolding-specific intrabody with dual proteolytic signals. *Sci Rep,* 8**,** 6030.

Tang, Y., Wang, X. W., Liu, Z. H., Sun, Y. M., Tang, Y. X. & Zhou, D. H. 2017. Chaperone-mediated autophagy substrate proteins in cancer. *Oncotarget,* 8**,** 51970-51985.

Tekirdag, K. & Cuervo, A. M. 2018. Chaperone-mediated autophagy and endosomal microautophagy: Joint by a chaperone. *J Biol Chem,* 293**,** 5414-5424.

Thorburn, A. & Debnath, J. 2011. Targeting chaperone-mediated autophagy in cancer. *Sci Transl Med,* 3**,** 109ps45.

Urban, N. & Guillemot, F. 2014. Neurogenesis in the embryonic and adult brain: same regulators, different roles. *Front Cell Neurosci,* 8**,** 396.

Uttenweiler, A., Schwarz, H., Neumann, H. & Mayer, A. 2007. The vacuolar transporter chaperone (VTC) complex is required for microautophagy. *Mol Biol Cell,* 18**,** 166-75.

Vogiatzi, T., Xilouri, M., Vekrellis, K. & Stefanis, L. 2008. Wild type alpha-synuclein is degraded by chaperone-mediated autophagy and macroautophagy in neuronal cells. *J Biol Chem,* 283**,** 23542-56.

Wang, B., Cai, Z., Tao, K., Zeng, W., Lu, F., Yang, R., . .Yang, Q. 2016. Essential control of mitochondrial morphology and function by chaperone-mediated autophagy through degradation of PARK7. *Autophagy,* 12**,** 1215-28.

Wang, G. & Mao, Z. 2014. Chaperone-mediated autophagy: roles in neurodegeneration. *Transl Neurodegener,* 3**,** 20.

Wang, X., Mao, X., Xie, L., Greenberg, D. A. & Jin, K. 2009a. Involvement of Notch1 signaling in neurogenesis in the subventricular zone of normal and ischemic rat brain in vivo. *J Cereb Blood Flow Metab,* 29**,** 1644-54.

Wang, Y., Martinez-Vicente, M., Kruger, U., Kaushik, S., Wong, E., Mandelkow, E. M., . .Mandelkow, E. 2009b. Tau fragmentation, aggregation and clearance: the dual role of lysosomal processing. *Hum Mol Genet,* 18**,** 4153-70.

Wang, Y., Martinez-Vicente, M., Kruger, U., Kaushik, S., Wong, E., Mandelkow, E. M., . .Mandelkow, E. 2010. Synergy and antagonism of macroautophagy and chaperone-mediated autophagy in a cell model of pathological tau aggregation. *Autophagy,* 6**,** 182-3.

Weng, A. P., Ferrando, A. A., Lee, W., Morris, J. P. T., Silverman, L. B., Sanchez-Irizarry, C., . .Aster, J. C. 2004. Activating mutations of NOTCH1 in human T cell acute lymphoblastic leukemia. *Science,* 306**,** 269-71.

Wing, S. S., Chiang, H. L., Goldberg, A. L. & Dice, J. F. 1991. Proteins containing peptide sequences related to Lys-Phe-Glu-Arg-Gln are selectively depleted in liver and heart, but not skeletal muscle, of fasted rats. *Biochem J,* 275 (Pt 1)**,** 165-9.

Wu, X., Fleming, A., Ricketts, T., Pavel, M., Virgin, H., Menzies, F. M. & Rubinsztein, D. C. 2016. Autophagy regulates Notch degradation and modulates stem cell development and neurogenesis. *Nat Commun,* 7**,** 10533.

Xilouri, M., Brekk, O. R., Landeck, N., Pitychoutis, P. M., Papasilekas, T., Papadopoulou-Daifoti, Z., . .Stefanis, L. 2013. Boosting chaperone-mediated autophagy in vivo mitigates alpha-synuclein-induced neurodegeneration. *Brain,* 136**,** 2130-46.

Xilouri, M., Brekk, O. R., Polissidis, A., Chrysanthou-Piterou, M., Kloukina, I. & Stefanis, L. 2016a. Impairment of chaperone-mediated autophagy induces dopaminergic neurodegeneration in rats. *Autophagy,* 12**,** 2230-2247.

Xilouri, M., Brekk, O. R. & Stefanis, L. 2016b. Autophagy and Alpha-Synuclein: Relevance to Parkinson's Disease and Related Synucleopathies. *Mov Disord,* 31**,** 178-92.

Xilouri, M. & Stefanis, L. 2011. Autophagic pathways in Parkinson disease and related disorders. *Expert Rev Mol Med,* 13**,** e8.

Xilouri, M. & Stefanis, L. 2015. Chaperone mediated autophagy to the rescue: A new-fangled target for the treatment of neurodegenerative diseases. *Mol Cell Neurosci,* 66**,** 29-36.

Xilouri, M. & Stefanis, L. 2016. Chaperone mediated autophagy in aging: Starve to prosper. *Ageing Res Rev,* 32**,** 13-21.

Xilouri, M., Vogiatzi, T., Vekrellis, K., Park, D. & Stefanis, L. 2009. Abberant alpha-synuclein confers toxicity to neurons in part through inhibition of chaperone-mediated autophagy. *PLoS One,* 4**,** e5515.

Yan, B., Neilson, K. M. & Moody, S. A. 2009. Notch signaling downstream of foxD5 promotes neural ectodermal transcription factors that inhibit neural differentiation. *Dev Dyn,* 238**,** 1358-65.

Yang, Q., She, H., Gearing, M., Colla, E., Lee, M., Shacka, J. J. & Mao, Z. 2009. Regulation of neuronal survival factor MEF2D by chaperone-mediated autophagy. *Science,* 323**,** 124-7.

Yang, Z., Funke, B. H., Cripe, L. H., Vick, G. W., 3rd, Mancini-Dinardo, D., Pena, L. S., . .Vatta, M. 2010. LAMP2 microdeletions in patients with Danon disease. *Circ Cardiovasc Genet,* 3**,** 129-37.

Yoon, K. & Gaiano, N. 2005. Notch signaling in the mammalian central nervous system: insights from mouse mutants. *Nat Neurosci,* 8**,** 709-15.

Yoon, K., Nery, S., Rutlin, M. L., Radtke, F., Fishell, G. & Gaiano, N. 2004. Fibroblast growth factor receptor signaling promotes radial glial identity and interacts with Notch1 signaling in telencephalic progenitors. *J Neurosci,* 24**,** 9497-506.

Zhang, S. J., Yang, W., Wang, C., He, W. S., Deng, H. Y., Yan, Y. G., . .Wang, W. J. 2016. Autophagy: A double-edged sword in intervertebral disk degeneration. *Clin Chim Acta,* 457**,** 27-35.

Zhang, Y., Argaw, A. T., Gurfein, B. T., Zameer, A., Snyder, B. J., Ge, C., . .John, G. R. 2009. Notch1 signaling plays a role in regulating precursor differentiation during CNS remyelination. *Proc Natl Acad Sci U S A,* 106**,** 19162-7.